Spring 5-15-2019

Sufficient Conditions for Optimal Control Problems with Terminal Constraints and Free Terminal Times with Applications to Aerospace

Sankalp Kishan Bhan
Washington University in St. Louis

Washington University in St. Louis

McKelvey School of Engineering

Department of Electrical and Systems Engineering

Dissertation Examination Committee:
Heinz Schättler, Chair
Hiro Mukai
ShiNung Ching
Jr-Shin Li
Ramesh Agarwal
Ron Cytron

Sufficient Conditions for Optimal Control Problems with Terminal Constraints and Free Terminal Times with Applications to Aerospace

by

Sankalp Kishan Bhan

A dissertation presented to the McKelvey School of Engineering
of Washington University in partial fulfillment of the
requirements for the degree of

Doctor of Science

May 2019
Saint Louis, Missouri

Contents

List of Figures

Acknowledgments

According to geometric optics, light travels like the Brachistochrone. It bends along shortest-time extremal paths through one medium into another, satisfying Snell's law by refracting at entry and exit. Certainly, I did not take the time-optimal path through Washington University in St. Louis. I think I am on the path towards maximal gratitude. I travelled through several institutions: first, Shell Oil Company, then, the Boeing Company, and, somehow again, I returned to Washington University in parallel. On the way to this acknowledgement, many provided more than a gentle nudge (rather, a dramatic bang) to my maturity and understanding.

At Washington University, I have the honor to work with my advisor. Professor Schättler, you will always be someone I aspire to emulate–a true teacher. You pass along timely wisdom (understanding is, in fact, dimensional and measured in units of hours-per-page), infect your students with curiosity, lead by example. Most of all, you inspire. You coached me to this finish-line with only positivity, encouragement, and enthusiasm. This work would be impossible without you. I hope that we will wrap up path constraints and venture into games before you leave an infinite void in our department.

I thank the members of my committee. It is no secret that it is full of my favorite teachers. Professor Mukai, you are a mythic, joyful figure who rescued me to the ESE department from a badly mangled education and introduced me to the simplicity and superiority of mathematics. Professor Li, you treated me as if I was one of your students. You allowed me into your lab and provided me a sense of community. Professor Ching, I am so excited that you suggested me for a teaching opportunity. I sincerely hope to build something incredible with you, Professor Zeng, and Professor Trobaugh. Professor Agarwal, you introduced me to the beauty of aerodynamics and provided feedback on the aspects of this dissertation related to flight. Professor Cytron, thank you for volunteering to join my comittee.

Professor Cytron, Professor Joan Brockmann, and Professor Kevin Wise: you are all especially refractive teachers. You all recommended me for this degree. Much like Professor Schättler, Professor Cytron, you are an ever-helpful soul, with giant intelligence, who gave me my first opportunity to pursue undergraduate research: optimal tablature and Alex's

guitar-hero playing robot. Professor Brockmann, you taught me small things. You also taught me big things: the ability to listen and empathize; to argue and present. Professor Wise, you pulled me into Boeing and gave me my first "first flight" (the opportunity to design Dominator's air-launch). You demonstrate to me that control theory is more than just theory.

To my manger at Boeing, Matt Masalskis thank you for supporting my graduate study and pushing me to find new applications of control theory on the F-15X. I thank my official and unofficial "TLE's" Jeremy Clark, Dr. Jeff Barker, Dr. Ross Gadient, Dr. Ryan Ratliff, Dr. James Ramsey, Dr. Eugene Lavretsky, Bobby Cartmill, Jon Gettinger, Larry Arnold, Dr. Dale Hiltner, Craig Pulley, Dave Klein, Al Dietz, Dr. Mark Hreha, Wes Sawhill, Ken Catalano, Paul Dobberstein, Brad Hopping, Mark Witten, and Will Stieglitz for teaching me to be a better flight engineer. Dr. Philip Freeman and Dr. Ross Gadient provided advice at every step of the way. To Steve Sherman, thank you for allowing me the leeway to finish this degree. To Rick Martin, thank you for reading and approving my dissertation and our paper. To my many teammates on the Dominator team, F-15SA team, and the MQ-25 teams, thank you for supporting me throughout this pursuit.

At Shell, I thank Ralph Faxel, John Williamson, Dr. Bob Brown, Dr. Pierre Carrette, Dr. Chris Seppalla, Dr. Rishi Armit, Dr. Janet Fox, and Dr. Carlos Garcia. You all showed me control theory done right.

Lastly, no one manages a full-time job and finishes a doctorate without a scaffolding that supports their life. In my student life, I thank Dr. Li's students, Wei Zhang, Dr. Shuo Wang, Pierre Ursinga, and Dr. Walter Bomela. In my workplace, I thank my friends, Ryan Endres, Dan Donahue, Nathan and Elena Selling, Shannon Meyer, Steve Ampleman, Anne Kitzmiller, Dr. Brian Roberts, and Juan Cajigas.

To those who are closest to me: my family and Cat, Sam and Diana, Alex, Michelle, Will, Emily, Mark, Adrian, Gab, Emery, Juliana, Justin, Brianna, and Patty. Through carbon monoxide poisoning, hospitalizations, car accidents, and more, you remained steadfast. Thank you so much for helping me overcome them. I know what path I took. It's the one that maximizes the length of my acknowledgment.

Sankalp Kishan Bhan

Washington University in Saint Louis
May 2019

Dedicated to my parents, Sushma and Opinder, my brother, Nischay, and my Nana Ji.

I cannot think of anyone with more luck than me. Not only because I, like Ganesh, won the race around the World (my perfect parents, who selflessly give me every opportunity and no setbacks); not just because my brother is gifted beyond belief, with an enormous capacity for good and affection; but also because I have a grandfather, who blesses my life with joy and laughter. To my devoted family, who sprout tears of gratitude in my eyes: I am effusively thankful for you. I succeed due to you. I love you all.

ABSTRACT OF THE DISSERTATION

Sufficient Conditions for Optimal Control Problems with Terminal Constraints and Free Terminal Times with Applications to Aerospace

by

Sankalp Kishan Bhan

Doctor of Science in System Science and Mathematics

Washington University in St. Louis, May 2019

Research Advisor: Professor Heinz Schättler

Motivated by the flight control problem of designing control laws for a Ground Collision Avoidance System (GCAS), this thesis formulates sufficient conditions for a strong local minimum for a terminally constrained optimal control problem with a free-terminal time. The conditions develop within the framework of a construction of a field of extremals by means of the method of characteristics, a procedure for the solution of first-order linear partial differential equations, but modified to apply to the Hamilton-Jacobi-Bellman equation of optimal control. Additionally, the thesis constructs these sufficient conditions for optimality with a mathematically rigorous development. The proof uses an approach which generalizes and differs significantly from procedures outlined in the classical literature on control engineering, where similar formulas are derived, but only in a cursory, formal and sometimes incomplete way. Additionally, the thesis gives new arrangements of the relevant expressions arising in the formulation of sufficient conditions for optimality that lead to more concise formulas for the resulting perturbation feedback control schemes.

These results are applied to an emergency perturbation-feedback guidance scheme which recovers an aircraft from a dangerous flight-path angle to a safe one. Discussion of required background material contrasts nonlinear and linear optimal control theory are contrasted in the context of aerospace applications. A simplified version of the classical model for an F-16 fighter aircraft is used in numerical computation to very, by example, that the sufficient conditions for optimality developed in this thesis can be used off-line to detect possible failures in perturbation feedback control schemes, which arise if such methods are applied along extremal controlled trajectories and which only satisfy the necessary conditions for optimality without being locally optimal. The sufficient conditions for optimality developed in this thesis, on the other hand, guarantee the local validity of such perturbation feedback control schemes. This thesis presents various graphs that compare the neighboring extremals which were derived from the perturbation feedback control scheme with optimal ones that start from the same initial condition.

Future directions for this work include extending the perturbation feedback control schemes to optimization problems that are further constrained, possibly through control constraints, state-space constraints or mixed state-control constraints.

Nomenclature

Adjoint Vector	$\lambda(t)$	Drag Coefficient	C_D
Air Density	ρ	Dual Space of $(\cdot)$	$(\cdot)^*$
Air Speed	V	Dynamic Axial Force Coefficient	C_{X_q}
Air Speed	V	Dynamic Moment Coefficient	C_{M_q}
Altitude	h	Dynamic Normal Force Coeff.	C_{N_q}
Angle of Attack (AOA)	α	Dynamic Pressure	$\bar{q}$
Angle of Sideslip (AOS)	β	Error	e
Angular Velocity	Ω	Euler Pitch Angle	θ
Axial Force	A	Final Time	T
Axial Force Coefficient	C_X	Flight Path Angle	γ
Block of Riccati Matrices	$\mathcal{Q}$, $\mathcal{R}$	Flight Path Angle Dynamics	f
Center of Gravity	x	Flow of Trajectories	F
class of admissible controls	$\mathcal{U}$	Force	F
Clock Constraint	Ω	Force in the x axis in body axis	F_x
Control	u	Force in the z axis in body axis	F_Z
Control Parameter	ν	Gross Weight	W
Control Parameters	ν	Hamiltonian	H
Control Set	U	Initial Parameter for State	ξ
Ordinary derivative in time	$\dot{(\cdot)}$	Initial Time	t_0
Drag	D	Lagrangian	L
Lagrangian	L	Riccati Scalar	a
Lift Coefficient	C_L	Riccati Vector	q, r
Linear Control Matrix	$B(t)$	Smooth manifold	M
Linear State Matrix	$A(t)$	State	x
Linear Feedback Gain	$K(t)$	Terminal Constraint	Ψ
Linear Feedforward Gain	$F(t)$	Terminal Manifold	N
Mean Aerodynamic Chord	$\bar{c}$	Terminal Penalty	ϕ
Moment	M	Thrust	T
Pitch Inertia	I	Time	t

Table 1: Nomenclature

Net Propulsive Thrust	F_{NP}	Total Derivative of $\cdot$ in t	$\frac{\mathrm{d}\cdot}{\mathrm{d}t}$
Normal Force	N	Total Terminal Constraint	Υ
Normal Force Coefficient	C_N	Transition matrix , t to t_0	$\Psi(t, t_0)$
Performance Criterion	$\mathcal{J}$	Transpose of $(\cdot)$	$(\cdot)^T$
Perturbation in $(\cdot)$	$\delta(\cdot)$	Value Function	V
Pitch Rate	q	Velocity	V
Pitching Moment Coefficient	C_m	Weighting on Control Inputs	$D(t)$
Planform of the Wings	$\bar{S}$	Weighting on States	$C(t)$
Real Numbers	$\mathbb{R}$	Wing Span	S
Riccati Matrix	S, Q, R	Wing Span	$\bar{b}$

Table 2: Nomenclature (cont.)

Chapter 1

Introduction

Controlled flight into terrain or other obstacles presents an innocuous danger to any piloted aircraft. This situation is typically referred to in the aerospace industry as CFIT, and it presents a significant problem for aircraft of all types, from civilian to commercial. A CFIT accident occurs "when an airworthy aircraft under the control of a pilot is flown (unintentionally) into terrain, water, or obstacles with inadequate awareness on the part of the pilot (crew) of the impending collision" [2], [60].

While there are varying definitions about how the incidents of CFIT should be categorized, [1] estimates that 17% of all general aviation accidents occur as a result of CFIT. Almost assuredly, since the vehicle is traveling at flight speeds, these are fatal incidents for all involved. For commercial aircraft, CFIT is by far the most dangerous category of flight incidents with more than 55% of worldwide incidents stemming from commercial incidents starting (circa 2005) [22]. For other types of aviation, for example, military aviation, estimates suggest that controlled flight of military helicopters into terrain has cost the army 308 million dollars and 78 lives [13]. For fighter aircraft, one in four fighter crashes result from CFIT [20].

The causes for controlled flight into terrain are documented in [16],[27] as errors in air traffic control system, weather, navigation errors, and spatial disorientation. According to [27], spatial disorientation contributes to nearly 33% of CFIT incidents with 100% fatality rate. Spatial disorientation contributes exceedingly to military incidents when compared to other types of aviation. Spatial disorientation may also be a cause of loss of control, inadvertent flight into weather, and loss of situational awareness.

The current method of prevention for CFIT are [16] air traffic control systems, onboard proximity and warning sensors or Ground Proximity Warning, and "Ground Collision Avoidance Systems" (GCAS).

The stability and control of an aircraft in flight is one of the major challenges for the design of any flying vehicle. There are traditionally three branches that must work in synchrony for a vehicle to fly, and some of these functions are entirely subsumed by a pilot or a computer. Control is the change to an aircraft's surfaces or motors that provide desired changes in forces and moments. Guidance is the process of determining the required changes in forces and moments on an aircraft to travel along a starting point to a final point. Navigation is the process of determining where the vehicle, this starting point, and this final point are in space.

When an imminent crash is occurring, a flight control system can attempt to make recovery actions to change the flight path of a vehicle. Emergency corrections include changes to throttle settings, changes to control surface inputs, and changes to flight control system gains. Automatic collsion avoidance operates with any of the following: aural warning systems, visual indication systems, detection systems, switching systems, automatic flight control systems, sensor systems, and databases of terrains. For practical reasons, these systems need to be fused with the existing guidance, navigation, and control systems of the aircraft.

An example of a successful fusion of a GCAS systems into an existing aircraft is the F-16 Analog Auto GCAS [20], which automatically recovers the F-16 aircraft to a safe trajectory and notifies a pilot when an emergency is detected. According to [20], the fundamental parts of the algorithm are a predictor for the aircraft's trajectory, a terrain database scanning algorithm, a collision avoidance estimation routine, and a coupler into the flight control system. The algorithm commands into the existing terrain following the architecture of the aircraft and activates the existing pathways for a "fly-up."

Almost all of the current approaches to GCAS systems employ prediction and a terrain avoidance maneuver. Some of these methods generate trajectories through information from all of the aircraft's sensor inputs, while others only use a fixed set of recovery inputs to save an aircraft. All of these systems balance the capability of giving pilots the margin to fly the

aircraft, usually while still providing the capability to warn or take-over when an emergency occurs.

Many aircraft exist with limitations on their designs that prevent straight forward applications of automatic flight control systems. For example, some aircraft have purely mechanically controlled systems and do not fly with a fly-by-wire system. Furthermore, even if a digital flight control system exists, there may not be a digital throttle-by-wire system that electronically controls the engine. As a result, the design of automatic recovery flight control systems cannot replace the functions of the pilot.

Additionally, these are emergencies and, while the probability may be low, other components on an aircraft may fail. For example, if during one of these emergencies, an air data system has failed and the aircraft is unable to assess its flight condition, what capabilities exist to recover the aircraft?

There are a multitude of patents on GCAS systems using a variety of techniques [57, 25, 11, 23, 9]. Some GCAS techniques use adaptive control to take in measurements from all of the aircraft sensors and dynamically compute a ground collision avoidance trajectory [58]. Other techniques, such as the IGCAS (improved GCAS) of NASA, utilize image processing software to determine when and how to recover the aircraft dynamically [51].

While it would seem obvious to try to pad as much margin into these systems as possible, [30] doing so leads to pilots turning off these safety systems. A late recovery is deadly, but assuredly, no recovery is also deadly. Mathematically, this raises the following question from a fundamental scientific perspective: "What are the extremes for a recovery trajectory?" Given the failures, components, available inputs, and available outputs, the desire is to alter a system in such a way to maximize the probability of survival. Basic questions one might need to answer for a GCAS system are: what energy must remain? How long must recovery take? How much altitude must be lost?

We seek to optimize designs for superlative performance–quickest, highest, fastest; yet, we are also restricted to maintain costs, schedules, and operational margins. Optimization is the mathematical theory to design to these competing objectives. In particular, for mobile autonomous systems, like an aircraft in flight, dynamic selections of the inputs required to fly an aircraft present an optimization problem, constrained by differential equations. The

calculus of variations and optimal control theory solve this type of optimization problem. This branch of mathematics has had impacts on the field of aerospace [53] dating from the accidental design of a hypersonic ship hull in 1686 by Newton ([33]) to the launch of the Soviet satellite Sputnik ([50], pg v). Optimal control theory provides an excellent framework to consider questions of possibilities in the design and construction of aircraft recovery systems to rectify an imminently dangerous situation.

Optimal control theory not only provides a method to answer what is possible but also gives the tools to achieve these possibilities. The systematic solution of a dynamical flight problem starting from arbitrary initial conditions to some desired safe, terminal condition can be posed as an optimization problem, and we have an interest in automatic controllers that can rectify such a situation and bring the plane back into horizontal or slightly elevated flight. This is a typical situation of an optimal control problem with terminal constraints and free terminal time. It was this practical scenario that led us to try and understand the geometric features of perturbation feedback. While it lies well beyond the scope of this dissertation to describe this practically relevant application, in this dissertation a rigorous theoretical foundation is laid that has the potential to become the basis for such a framework. This is accomplished by developing necessary and sufficient conditions for a strong local minimum for optimal control problems with terminal constraints that involve free terminal times, establishing the precise relations with the classical engineering perturbation feedback control design schemes.

Perturbation feedback control schemes are well-known in engineering and go back to the literature connected with the space program [15, 14, 34, 41]. While these procedures are relatively straightforward, and trace in principle to Legendre and the classical calculus of variations for unconstrained problems with fixed terminal times, they complicate when terminal constraints are imposed. In this case, desingularizations near the terminal manifold are needed. These generate singularities in the resulting control laws. In the literature, this problem has been fully solved for the case of a fixed terminal time. However, only cursory, formal and incomplete results exist for problem with fixed terminal time.

Essentially, these are simply conditions which reduce the problem to one with free terminal time and thus make unnecessary assumptions and sometimes even give incorrect formulations

of necessary conditions for optimality. These in turn are only the conditions sufficient to reduce the problem to one with fixed terminal times.

In this dissertation, the method of characteristics for solving first-order partial differential equations (in a modified version that is applicable to solve the Hamilton-Jacobi-Bellman equation of optimal control theory) is used to construct a field of extremals. This dissertation gives a mathematically rigorous development of these constructions which lead to the sufficient conditions for optimality. It briefly mentions the resulting necessary conditions because sufficient conditions enable a perturbation feedback control scheme. This dissertation's approach differs significantly from the formal procedures of the classical literature on control engineering, and it generalizes these results. Its formulations clarify the role of the terminal conditions without requiring one to reduce the problem to one with a fixed terminal time. They also provide new arrangements of the relevant expressions which arise in the formulation of sufficient conditions for optimality. This leads to more concise formulas and controllability interpretations for the resulting perturbation feedback control schemes.

As a proof of concept verification, these results are applied to an emergency perturbation-feedback guidance scheme, which recovers an aircraft from a dangerous flight-path angle to a safe one. It employs a simplified version of the classical model for an F-16 fighter aircraft in its numerical computations. These calculations are verified by means of an example, i.e., the sufficient conditions for optimality developed in this dissertation are useful to detect possible failures in perturbation feedback control schemes off-line. These failures arise if the methods are applied along extremal controlled trajectories which only satisfy the necessary conditions for optimality, without being locally optimal. The sufficient conditions for optimality developed in this dissertation, on the other hand, guarantee the local validity of such perturbation feedback control schemes. To this end, this dissertation presents various graphs comparing the neighboring extremals, which were derived from the perturbation feedback control scheme, with optimal ones starting from the same initial condition.

A brief outline of the dissertation follows. Chapter 2 gives a brief review of principal results from optimal control theory that are used in the dissertation within the context of flight control systems. This discussion of required background material contrasts nonlinear and linear optimal control theory in the context of aerospace applications. Chapter 3, after a brief discussion of the method of characteristics in optimal control, constructs a field of

extremals for a terminally constrained optimal control problem with free terminal time and develops various formulations of associated sufficient conditions for strong local optimality. This chapter contains the main theoretical contributions of the dissertation. Chapter 4 briefly discusses flight control dynamics, after which Chapter 5 applies these equations of motion to set up a perturbation control scheme using a simplified version of the classical model for an F-16 fighter aircraft in numerical computations. Chapter 6 indicates future directions and possible extensions of this work, which include extensions of perturbation feedback control schemes to optimization problems that are further constrained, possibly by control constraints, state-space constraints or mixed state-control constraints.

Chapter 2

Optimal Control Theory: A Review of Necessary and Sufficient Conditions for Optimality within the Context of Flight Control Systems

This chapter reviews results from optimal control theory. It gives a practical viewpoint on why a mathematical approach to engineering design can save both time and cost, and it explains why the practitioner should choose optimal design approaches over *ad-hoc* design approaches. It provides background on linearization and linear systems, particularly, the minimum energy control and the linear quadratic regulator (LQR). The chapter indicates practical reasons to look beyond linear quadratic control and towards perturbation feedback control (an optimal control technique that does not require the assumption of linear dynamics). Finally, it states the necessary conditions for optimality of the Pontryagin Maximum principle [48] and explains the dynamic programming approach to sufficient conditions for optimality (Hamilton-Jacobi-Bellman equation) [7].

2.1 Linearization as a Means to Regulate Nonlinear Systems

2.1.1 Design by Linearization: A Discussion

In aerospace applications, control systems regulate the subsystems required for flight, ranging from an aircraft's digital engine control to its environmental control system. Although each of these subsystems are complicated nonlinear interconnected systems, they can be regulated as a linear system, via linearization of their dynamics, about a reference operating point or a reference time-history. In this section, this section discusses this principle to both explain notation used throughout this dissertation and to review the fundamentals of optimal control theory.

Consider a pilot in flight aided by an autopilot, a control system which combines electrical, mechanical, and software components to reduce the pilot's workload during simple tasks. For example, an autopilot Flight Path Angle Hold (FPAH) regulates a constant angle of climb or descent relative to the horizon.

Figure 2.1 illustrates a closed-loop system for an autopilot. Each component represents significant non-linearity. The aircraft is ideally a 9 dimensional system governed by Newton's laws, geometry, and the aerodynamics of airflow and wind slipping past its shape. The lines in the diagram represent a number of electronic, mechanical, and physiological systems which function as sensation and actuation pathways. Lastly, the pilot—the most nonlinear element in the loop—controls the entire operation with the control stick, and ultimately determines whether it performs satisfactorily.

The FPAH exemplifies a system that can be controlled via linearization of nonlinear dynamics. During the FPAH operation, the expected deviations from a nominal trajectory are considered minor, and the language of linear systems effectively describes these deviations from a constant flight path angle. In Figure 2.2, the FPAH regulates the vector V relative to axis 2, the horizon line.

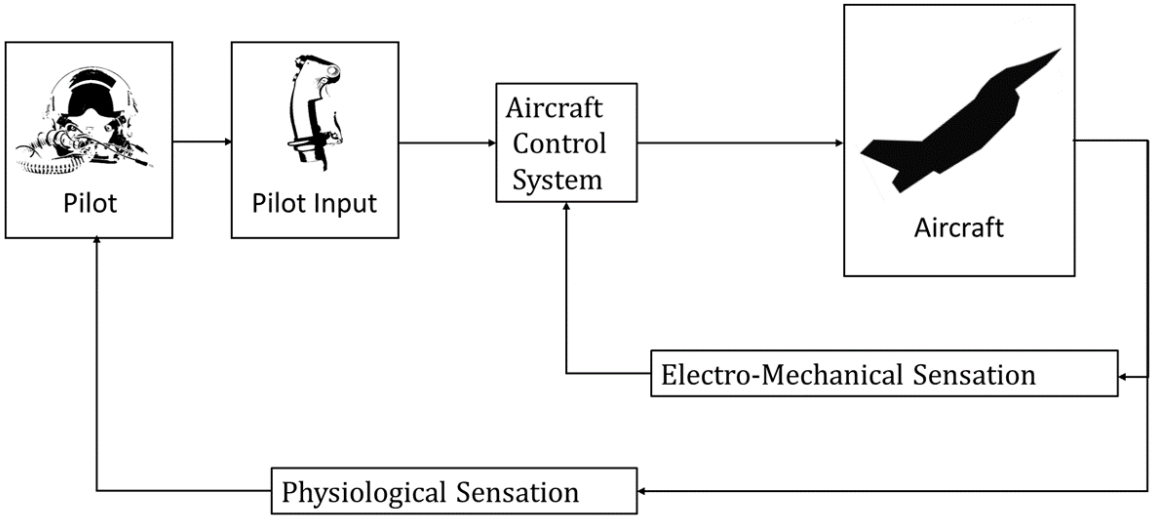

Figure 2.1: A closed-loop nonlinear system.

Considered in isolation from other states, a change in certain states δx of the control system is required to track a command $\delta\psi$. According to Figure 2.2, δx could represent the angles α and θ, which are the aircraft's angle of attack and pitch angle, respectively. Another suitable choice of states is their difference, $\theta - \alpha$. The salient requirement is that knowledge of the state δx sufficiently informs predictions of future behavior of the system.

In our idealization, the state space M is the set of all possible states of the linear system. Since the state δx takes values in the real numbers, we set $M = \mathbb{R}^n$. The commands $\delta\psi$ also belongs to a small subset of $\mathbb{R}^n$, meaning we intentionally command small values to ignore constraints on the state space. Angles, measurements, and currents cannot be arbitrarily large, but if the commands take small values and the states regulate successfully around the command, we can safely ignore the realities of physical constraints.

To effectively operate under these assumptions, an engineer should carefully carve a region of commands in M where the FPAH operates. If the FPAH operates within the bounds of expected errors $e = \delta\psi - \delta x$, then the states should remain within the operating region. If errors operate outside these bounds, it warns the pilot to abandon the task.

In this hypothetical mathematical model, the states will then evolve according to linear dynamics, driven by linear changes in the control inputs δu. We define the control set, U, as the set of all possible control inputs, such that $U = \mathbb{R}^m$. We ignore the idea that the controls for any physical system must be bounded. Rather, we choose $\delta\psi$ to be bounded and design the system to ensure that the resulting control inputs remain away from their physical constraints.

Since the dynamics are linear, we presume that an ordinary differential equation (ODE) of the following form describes the FPAH:

$$\delta\dot{x}(t) = A(t)\delta x(t) + B(t)\delta u(t). \tag{2.1}$$

Additionally, we set rules for what constitutes an acceptable control input, δu, in the system. The set of admissible controls, $\mathcal{U}$, defines the permissible functions, δu, in any time interval with start time, t_0, and stop time, T. Since we expect a nominal flight to experience a level of random fluctuation or turbulence, then we may take the admissible controls, $\mathcal{U}$, to be $\mathcal{L}_2[t_0, T]$, the space of Lebesgue measurable functions with a 2-norm over the time interval $[t_0, T]$. But many other specifications are feasible as well, such as functions from $\mathcal{C}[t_0, T]$, the set of continuous functions on t_0 to T (equipped with a supremum norm).

Furthermore, the admissible controls transfer the aircraft's initial state, δx_0, to other states over the entire interval. In essence, the admissible controls yield solutions to the linear

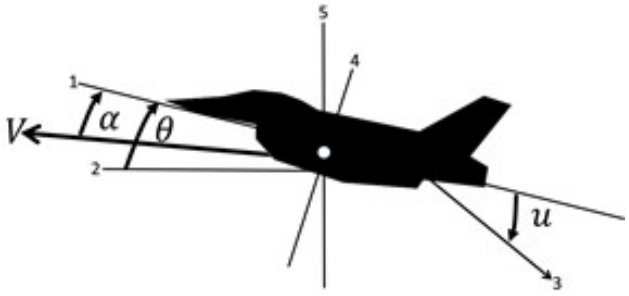

Figure 2.2: A depiction of an aircraft in FPAH. The angle of attack, α is the angle of the nose with respect to the airflow around the aircraft. The pitch angle, θ, is the angle of the nose with respect to the horizon.

dynamical Initial Value Problem (IVP):

$$\delta\dot{x}(t) = A(t)\delta x(t) + B(t)\delta u(t), \quad \delta(x(t_0)) = \delta x_0. \tag{2.2}$$

An engineer tasked with the design of an FPAH can leverage numerous techniques to design the system. Efficient control design generally mixes "cookbook techniques", leverages past experience, and employs some level of creativity and specificity. In essence, a suitable control system must compromise between open loop control inputs and closed-loop control inputs.

An open loop control input, δu, is an explicit function of the independent variable which is usually time, t. The open loop control moves the system according to a priori assumptions about the behavior of the airplane, pilot, and environment. For example, flaps may retract deterministically as a function of time after certain atmospheric conditions occur or the engines may spool down or up when the aircraft changes to a lower or higher flight path angle.

In contrast, a closed loop control input is an implicit function of time and an explicit function of other states, *i.e.,* $\delta u = \delta u(t, \delta x(t))$. When the control input is a function of the error between the commanded state and its estimated value, it is a feedback control. When the control is not a function of the error, it is a linear function $F(t)$ called a feed-forward gain of the command, δx_{cmd}, known as a linear feed-forward.

A linear control is a non-complicated and effective tool to control a system. A linear control composed of some combination of feedback and feed-forward control should be pursued whenever practical. The ideal input is then a linear function with a feedback gain, $K(t)$, of the state, δx, in combination with a feed-forward gain, $F(t)$, of the command, δx_{cmd}.

The open loop control allows performance to be maximized based on an assumption of the system's future trajectory. The closed loop control maximizes the robustness of the system to reject unforeseeable effects which can alter the trajectory of a system. The interchange between open-loop and closed-loop controls is non-trivial. For example, one significant drawback of closed-loop control is instability, *i.e.*, poor design can cause the errors in the system e to asymptotically increase.

While we as engineers can evaluate the performance of a control system in myriad ways, we must nonetheless agree on what constitutes effective design. The preface of *Optimal Control* [4] articulates an optimum approach to design, which contrasts with ad-hoc design approaches.

The ad-hoc approach designs commands, open-loop controls and closed-loop controls, using whichever approach intuitively mitigates problems and causes the system to perform as desired.

After design, system performance is evaluated against design-metrics, for example, time-domain performance or frequency-domain performance. Simulation and testing help identify problems in the design. The processes repeat as designs change, and eventually, after successive iterations, performance improves.

On the other hand, the optimal approach uses mathematical optimization of performance metrics to effectuate design. These performance metrics evolve along trajectories with the dynamics of the system. Metric optimization determines the optimal control to input into the system, and selects the "best" solution.

Of course, performance is dependent on the chosen design criterion. Resultantly, engineering design becomes the search for a proper design metric, which successfully captures the trade-offs between performance and cost.

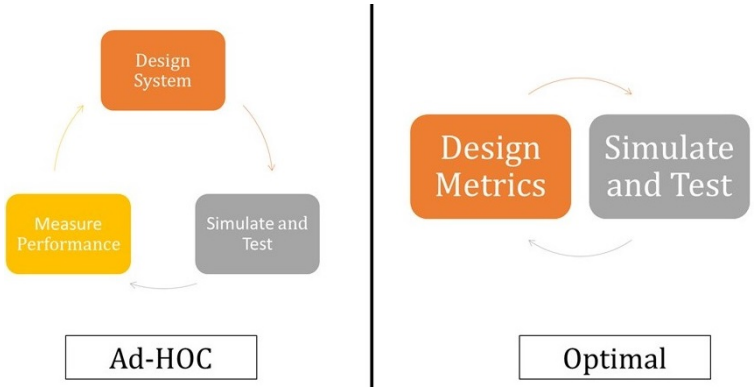

Figure 2.3: The ad hoc versus the optimal approach to control design.

The classical and pervasive engineering design metric, used across many industries, is the quadratic performance index, J, which penalizes large errors in the states and large effort in

the controls:

$$\mathcal{J} = \int_{t_0}^{T} \left(\delta x^T(t) C(t) \delta x(T) + \delta u^T(t) D(t) \delta u(t) \right) \mathrm{d}t, \tag{2.3}$$

where C and D are positive-definite matrices chosen to influence the performance index. For small errors or inputs, a quadratic performance index grows gradually. For large errors or inputs, a quadratic performance index grows dramatically.

Linear systems, which minimize quadratic performance indices, have excellent stability properties. An effective design approach for a linear system is to select $C(t)$ and $D(t)$ to meet time-domain criteria, while simultaneously minimizing a quadratic performance index. Furthermore, linear quadratic optimum controls fit within a framework of proportion, integral, and derivative (PID) controls, which are linear feedforward and feedback gains that are, respectively, functions of the present, past, and future errors of a system. PID controls are the most common approach to control systems design.

The FPAH example constitutes the optimal approach to the design of a linear system. The diagram in Figure 2.4 illustrates some of the points above, which are summarized as follows:

1. We desire to maneuver a system from some fixed initial condition, δx_0, to the command, $\delta \psi$, over a prescribed interval, $t_0 \leq t \leq T$.

2. The system is modeled by the dynamics and is driven by a linear system:

$$\delta \dot{x} = A(t) \delta x(t) + B(t) \delta u(t). \tag{2.4}$$

3. Along its maneuver, the controlled trajectory of the system along with the control should minimize a cost functional of the form:

$$\mathcal{J} = \int_{t_0}^{T} \left(\delta x^T(t) C(t) \delta x(t) + \delta u^T(t) D(t) \delta u(t) \right) \mathrm{d}t, \tag{2.5}$$

   over all admissible controls, $u \in U$.

4. The system can be controlled by some combination of open-loop control, $\delta u_0(t)$, and feedback and feedforward gains, *i.e.*,

$$\delta u(t) = \delta u_0(t) + K(t)\left(\delta\psi - \delta x\right) + F(t)\delta\psi. \tag{2.6}$$

5. The engineer derives functions, δu, from the choice of the cost functional (2.5), and δu combines an open-loop control, $u_0(t)$, with feed-forward and feedback gains that linearly scale the commands and the errors.

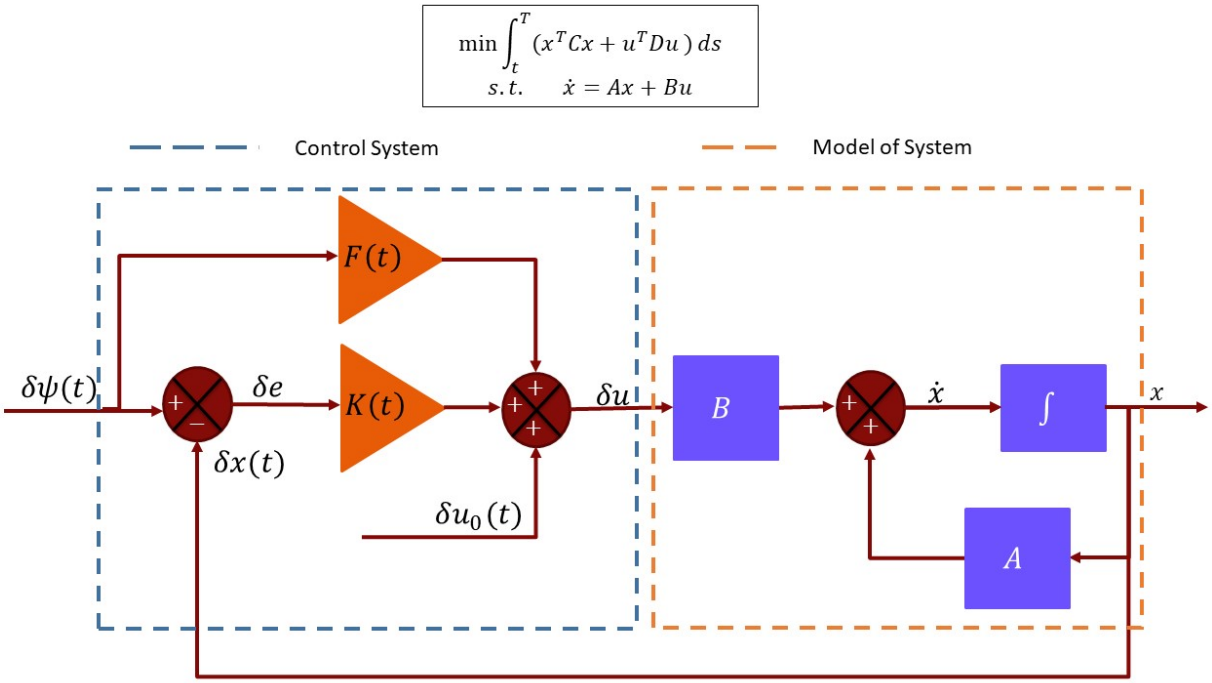

Figure 2.4: Linear Optimal Control Design

2.1.2 Some Concepts from Linear Systems

The following discussion is based on [59]. Consider a linear dynamical system which is linear in the state, $x(t)$, and the control, $u(t)$:

$$\Sigma: \quad \dot{x}(t) = A(t)x(t) + B(t)u(t). \tag{2.7}$$

For simplicity, assume that the entries of the matrices, A and B, are continuous functions. Furthermore, since we are considering quadratic objectives, we select $\mathcal{L}_2$, the space of square integrable functions, as the class of admissible controls, for the sake of convenience.

Another important concept for our work later-on is the notion of the adjoint equation, which we shall write in terms of a row vector.

The adjoint differential equation for Σ is

$$\dot{\lambda}(t) = -\lambda(t)A(t) \tag{2.8}$$

where λ is a row vector in $(\mathbb{R}^n)^*$. We denote the space of n-dimensional column vectors by $\mathbb{R}^n$ and the dual space to $\mathbb{R}^n$, *i.e.* the space of all linear functionals, which we write as row vectors, as $(\mathbb{R}^n)^*$.

Note that:

$$\frac{\mathrm{d}}{\mathrm{d}t}\left(\lambda(t)x(t)\right) = \dot{\lambda}(t)x(t) + \lambda(t)A(t)x(t) + \lambda(t)B(t)u(t) = \lambda(t)B(t)u(t), \tag{2.9}$$

so that the adjoint annihilates the drift from Ax in the dynamics. From Equation (2.9) it can also be seen that when choosing the trivial control, the inner product, λx, is constant.

For the linear system, Σ, the solution is given in terms of the state transition matrix $\Phi_\Sigma(t, t_0)$. The state transition matrix satisfies the differential equation for the drift vector field, Ax :

$$\dot{\Phi}(t, t_0) = A(t)\Phi(t, t_0), \tag{2.10}$$

with the initial condition $\Phi(t_0, t_0) = I$, and the solution to the equation (2.7) is given by (2.11).

$$x(t) = \Phi(t, t_0)x(t_0) + \int_{t_0}^{t} \Phi(t, s)B(s)u(s)\mathrm{d}s. \tag{2.11}$$

The fundamental matrix, Ψ, for the adjoint equation is the solution to

$$\dot{\Psi}(t_0, t) = -\Psi(t_0, t)A(t), \qquad \Psi(t_0, t_0) = I. \tag{2.12}$$

Hence,

$$\frac{\mathrm{d}}{\mathrm{d}t}\left(\Psi(t_0,t)\Phi(t,t_0)\right) = \dot{\Psi}(t_0,t)\Phi(t,t_0) + \Psi(t_0,t)\dot{\Phi}(t,t_0), \tag{2.13}$$

$$= -\Psi(t_0,t)A(t)\Phi(t,t_0) + \Psi(t_0,t)A(t)\Phi(t,t_0) \equiv 0. \tag{2.14}$$

Thus $\Psi(t_0,t)\Phi(t,t_0)$ is constant and since this value is the identity matrix for $t = t_0$, it follows that

$$\Psi(t_0,t) = \Phi(t,t_0)^{-1} = \Phi(t_0,t). \tag{2.15}$$

These matrices are essentially identical, with the difference being that Φ moves vectors forward from time t_0 to time t, while Ψ moves a covector backward from time t to time t_0. See their depiction in Figure 2.5.

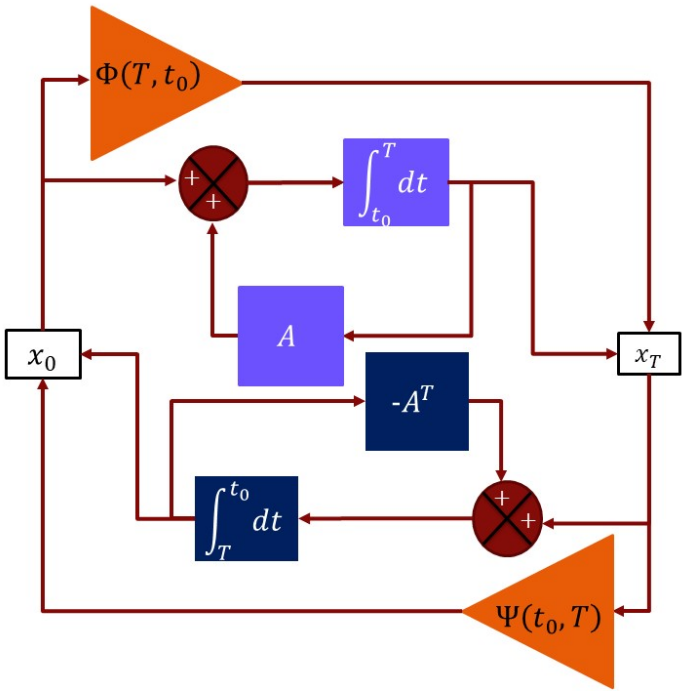

Figure 2.5: The relationship between the state transition matrix and the adjoint

2.1.3 Linear Quadratic Control

Engineers practicing the science of control theory primarily design feedback controls for linear systems. An optimization problem for a linear system can be constructed as state feedback solution. For simplicity, consider the following quadratic costs:

- Quadratic Functional of the state:

$$\mathcal{J} = \int_{t_0}^{T} x^T(t)C(t)x(t)\mathrm{d}t. \tag{2.16}$$

- Quadratic Functional of the control:

$$\mathcal{J} = \int_{t_0}^{T} u^T(t)D(t)u(t)\mathrm{d}t. \tag{2.17}$$

Both quadratic functions yield a highly intuitive methodology for control design. They offer the designer the opportunity to compromise between performance and stability. For example, if the state, x, represents the error in the system states, then a quadratic cost function penalizes large errors more severely than it penalizes small ones. Analogously, the cost function prefers small control deviations to large ones.

With this incentive in mind, we pose the following classical problem: find the minimum energy control, u, in state feedback form,

$$u(t) = K(t)x(t). \tag{2.18}$$

The minimum energy control problem for the system Σ is to determine the control of the form in Equation (2.18), which transfers the state from x_0 to x_T for which (2.17) is minimized.

2.1.4 Minimum Energy Control

Using a change of coordinates we can eliminate the dependence of the solution on x_0 or, without loss of generality, assume that $x_0 = 0$. Then the solution takes the form

$$x(T) = \int_{t_0}^{T} \Phi(T, s)B(s)u(s)\mathrm{d}s. \tag{2.19}$$

This corresponds to an operator, L, that maps controls to the state and is given by

$$L : L_2([t_0, T]) \to \mathbb{R}^n, \quad u \mapsto L(u) = \int_{t_0}^{T} \Phi(T, s)B(s)u(s)\mathrm{d}s. \tag{2.20}$$

The adjoint operator, L^*, maps $\mathbb{R}^n$ to control functions and the equation,

$$\left\langle x, L(u) \right\rangle = \left\langle L^*(x), u \right\rangle, \qquad \text{holds for all } x \in \mathbb{R}^n, u \in C([t_0, T]). \tag{2.21}$$

We have

$$\left\langle x, L(u) \right\rangle = x^T \int_{t_0}^{T} \Phi(T, s)B(s)u(s)\mathrm{d}s \tag{2.22}$$

$$= \int_{t_0}^{T} \left(B(s)^T \Phi^T(T, s)x\right)^T \cdot u(s)\mathrm{d}s \tag{2.23}$$

and thus,

$$L^\star : \mathbb{R}^n \to L_2([t_0, T]), \qquad x \mapsto L^*(x)(s) = B(s)^T \Phi(T, s)x. \tag{2.24}$$

The operator LL^* maps $\mathbb{R}^n$ into $\mathbb{R}^n$ and is therefore given by

$$\left(LL^*\right)(z) = \left(\int_{t_0}^{T} \Phi(T, s)B(s) \cdot B(s)^T \Phi^T(T, s)\mathrm{d}s\right) x. \tag{2.25}$$

For a linear vector space, the method of least squares [18] says that for minimizing

$$\left\langle u, u \right\rangle_{L_2[a,b]} \tag{2.26}$$

subject to the constraint, $\delta z = Lu$, the optimum solution is given by the pseudoinverse:

$$u = L\left(LL^*\right)^{-1}\delta z. \tag{2.27}$$

Resultantly, the optimum control for $u^T u$ is given by

$$u = \Phi^T(t,s)B^T(s)\left(\int_{t_0}^{T}\Phi(t,s)B(s)B^T(s)\Phi^T(t,s)u(s)\mathrm{d}s\right)^{-1}\left(z_T - z_{t_0}\right). \tag{2.28}$$

Thus, the minimum energy control is given by a feedback law,

$$u(s) = K(s)\delta z, \tag{2.29}$$

with gain

$$K(s) = B^T(s)\phi^T(T,s)\cdot\left(\int_{t_0}^{T}\Phi(T,r)B(r)B^T(r)\Phi^T(T,r)\mathrm{d}r\right)^{-1}. \tag{2.30}$$

The matrix inverse is of special significance as its existence determines whether a control for the problem exists.

For, if $\delta z = Lu$, then it must be that $\delta z \in \mathcal{R}\left(L\right)$, meaning that $\delta_z \in \mathcal{R}\left(LL^*\right)$. This will only be possible when the matrix:

$$\int_{t_0}^{T}\Phi(t,s)B(s)B^T(s)\Phi^T(t,s)u(s)\mathrm{d}s, \tag{2.31}$$

which is called the controllability Grammian, is non-singular. To generalize this result to our cost function $u^T Du$ we substitute, $\bar{u} = \sqrt{D}u$, and $\bar{B} = B\sqrt{D}$, so that

$$u = D(s)B(s)^T\Phi^T(t,s)\left(\int_{t_0}^{T}\Phi(t,s)B(s)DB^T(s)\Phi^T(t,s)\mathrm{d}s\right)^{-1}(z_T - z_{t_0})\,. \tag{2.32}$$

The importance of this result cannot be overemphasized. When the matrix is evaluated at the final time, the matrix is singular. As a result, we see that even in the most basic optimization problem, singularity arises in the natural framework at the terminal time. A feedback control system which implements the solution is given in the Figure 2.6.

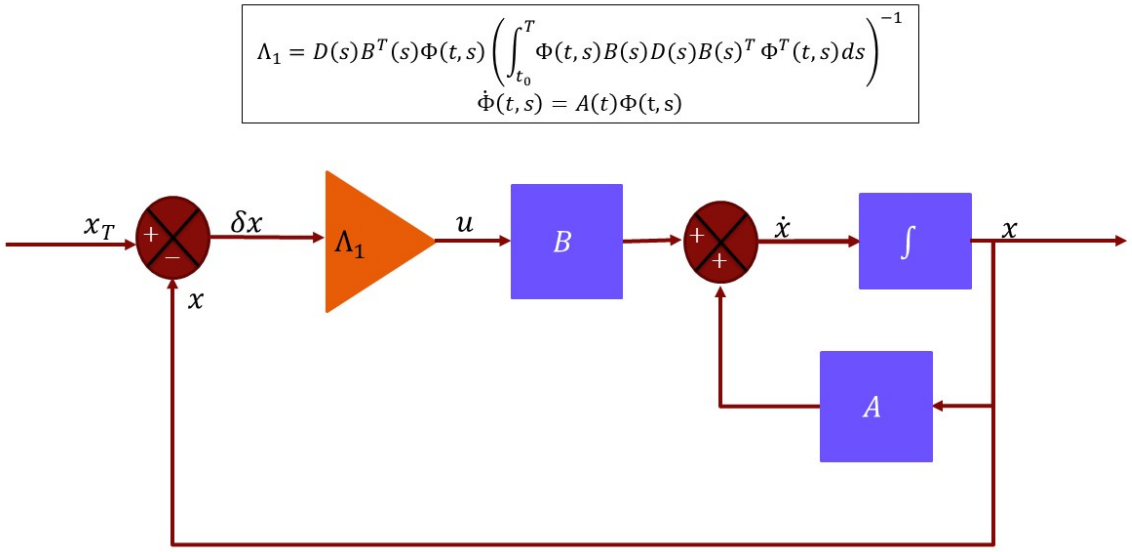

Figure 2.6: The minimum energy feedback control system.

2.1.5 Linear Quadratic Regulator

The celebrated linear quadratic regulator combines a minimum energy control with another control that minimizes a quadratic error in the states of a control system. The cost functional for this problem combines (2.16) with (2.17), and attempts to find a control that solves a

dilemma: how to maximize the performance of a system by minimizing the output error, while simultaneously using as little control as possible. The dilemma is resolved by applying a weighting to the cost matrix for the functions (2.16) and (2.17). Optimal control theory provides the functions which solve the optimization problem.

Formally, the linear quadratic regulator problem seeks the control functions amongst all the admissible controls, which for a linear system transfer the state from some initial condition, x_0, over a prescribed horizon $[0, T]$ while minimizing the functional,

$$\mathcal{J} = \int_{t_0}^{T} \left(x^T(s) Q(s) x(s) + u^T(s) u(s) \right) \mathrm{d}s. \tag{2.33}$$

It is convenient at this point to introduce the Schur complement, which is often used with block matrices to find their inverse. The result will be used later in the text. Given a block matrix, V,

$$V = \begin{bmatrix} W & X \\ Y & Z \end{bmatrix}, \tag{2.34}$$

where the matrix Z is nonsingular, the matrix.

$$W - XZ^{-1}Y, \tag{2.35}$$

is called the Schur complement of W. Analogously, there is another Schur complement, the Schur complement of Z, assuming W is nonsingular,

$$Z - YW^{-1}X. \tag{2.36}$$

For a symmetric block matrix, V, the Schur complement arises in a UDL block factorization.

$$\begin{bmatrix} W & X \\ X^T & Z \end{bmatrix} = \begin{bmatrix} I & XZ^{-1} \\ 0 & I \end{bmatrix} \begin{bmatrix} W - XZ^{-1}X^T & 0 \\ 0 & Z \end{bmatrix} \begin{bmatrix} I & 0 \\ Z^{-1}X^T & I \end{bmatrix} \tag{2.37}$$

Consider the quadratic form, Q, in the matrix, V, with the block, Z, set to identity

$$Q = z^T V z, \qquad \text{and} \qquad z = \begin{bmatrix} x \\ u \end{bmatrix}. \tag{2.38}$$

If $Z = I$, and the Schur complement of Z is zero, we can transform a quadratic form to a simplified form using the LDU factorization,

$$Q = z^T \begin{bmatrix} W & X \\ X^T & I \end{bmatrix} z = z^T \begin{bmatrix} XX^T & X \\ X^T & I \end{bmatrix} z = \left(X^T x + u\right)^T \left(X^T x + u\right). \tag{2.39}$$

We use the result for a quadratic cost functional. Suppose we wish to transfer the state from x_0 to time, $t = T$, so that it minimizes the quadratic cost functional,

$$\mathcal{J} = \int_{t_0}^{T} \begin{bmatrix} x^T & u^T \end{bmatrix} \begin{bmatrix} Q & 0 \\ 0 & I \end{bmatrix} \begin{bmatrix} x \\ u \end{bmatrix} \mathrm{d}t, \tag{2.40}$$

over the interval $[t_0, T]$.

We consider how a quadratic symmetric state functional changes with time for a linear system,

$$\frac{\mathrm{d}}{\mathrm{d}t} \int_{t_0}^{T} \left(\begin{bmatrix} x^T & u^T \end{bmatrix} \begin{bmatrix} S & 0 \\ 0 & 0 \end{bmatrix} \begin{bmatrix} x \\ u \end{bmatrix} \right) \mathrm{d}t = \int_{t_0}^{T} \begin{bmatrix} x^T & u^T \end{bmatrix} \begin{bmatrix} \dot{S} + SA + A^T S & SB \\ B^T S & 0 \end{bmatrix} \begin{bmatrix} x \\ u \end{bmatrix} \mathrm{d}t. \tag{2.41}$$

If we add this quantity as an identity to the original cost functional, we have

$$x(0)^T S(0) x(0) - x^T(T) S(T) x(T) + \int_{t_0}^{T} \begin{bmatrix} x^T & u^T \end{bmatrix} \begin{bmatrix} Q + \dot{S} + SA + A^T S & SB \\ B^T S & I \end{bmatrix} \begin{bmatrix} x \\ u \end{bmatrix} \mathrm{d}t. \tag{2.42}$$

We can select the Schur complement to be identically zero if there exists for all time $t \in [t_0, T]$ a matrix, S, satisfying the differential equation

$$Q + \dot{S} + SA + A^T S - SBB^T S = 0, \qquad \text{and} \qquad S(T) = 0, \tag{2.43}$$

so that in view of (2.39), $\mathcal{J}$ is simplified to:

$$\mathcal{J} = \int_{t_0}^{T} \left(u + B^T S x\right)^T \left(u + B^T S x\right) \mathrm{d}t. \tag{2.44}$$

Identifying $v = u + B^T S x$ as the control the system under state feedback

$$\dot{x} = \left(A - BB^T S\right) x + Bv = \bar{A}x + Bv, \tag{2.45}$$

we can reuse the result from earlier to minimize $\mathcal{J}$ by selecting v to satisfy the minimum energy control for the cost functional,

$$\mathcal{J} = \int_{t_0}^{T} v^T v \mathrm{d}t, \tag{2.46}$$

under the assumption that the solution, S, to the Riccati equation (2.43) exists over $[t_0, T]$. It can be shown that this is the case if the matrix Q is positive semi-definite. More generally, if we would use a term like $u^T R u$ instead of the identity weighting on the control, $u^T I u$, then R also needs to be positive definite.

2.2 Optimal Control Theory

2.2.1 Nonlinearity: A Discussion

In the previous section, we summarized some results of linear optimal control problems for fixed horizon problems. Now, to pursue a more general theory for control of dynamic systems, we contrast two trajectories of the same nonlinear system. One maneuver is easily captured by linear theory, and the other is not.

Consider, for example, Figure 2.8, where we depict two maneuvers. In the top half of Figure 2.8, the aircraft changes its attitude. During the maneuver, the dynamics are presumed to be linear. This situation corresponds to the discussion of linearization at the start of this chapter.

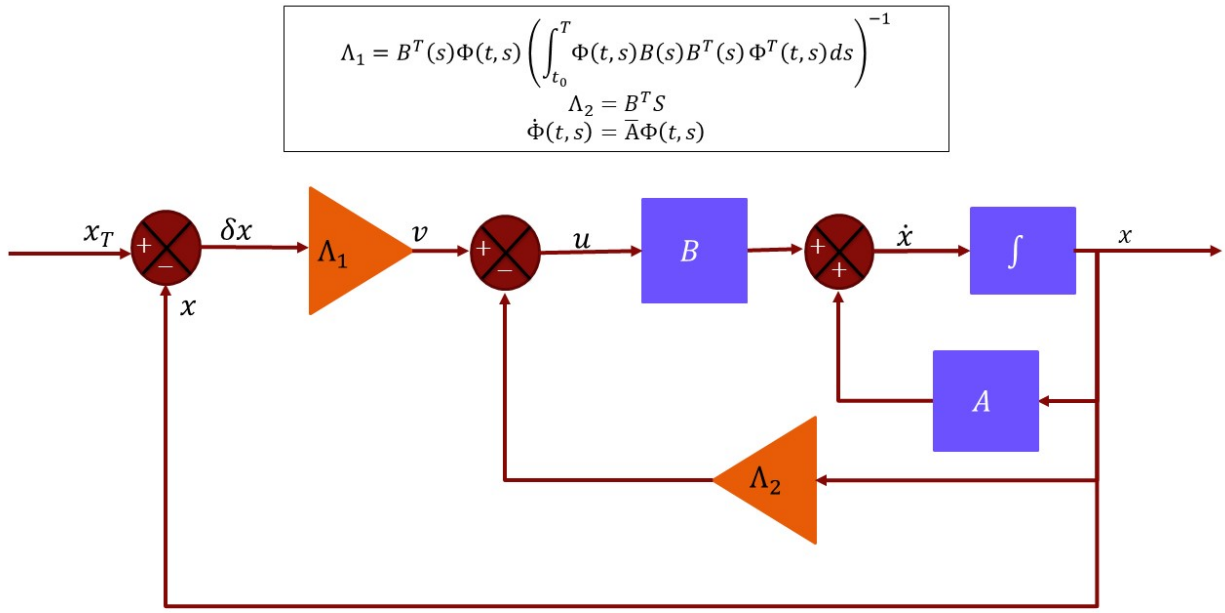

Figure 2.7: The Riccati matrix eliminates a quadratic state cost.

The bottom half of Figure 2.8 depicts an aircraft evading a missile to maximize the pilot's chance for survival. In this situation, the presumption of linearity throughout the maneuver does not hold. The aircraft rotates along multiple axes with extreme changes in speed and orientation. The commands, controls, and states for the system are likely constrained. Nevertheless, the system must stay within its structural and control limitations. Evasion could hardly be possible if the wings fall apart or the control effectors fail in a high-stress scenario.

We wish to extend the linear feedback control theory to situations where linearity of the dynamics cannot be presumed. This leads to our interest in perturbation feedback control. For the moment, let us assess the assumptions of linear control which may prove problematic for a general problem.

1. The system might behave non-linearly even in approximation.
2. The state space differs significantly from the friendly $\mathbb{R}^N$.
3. The system could be constrained in the following:

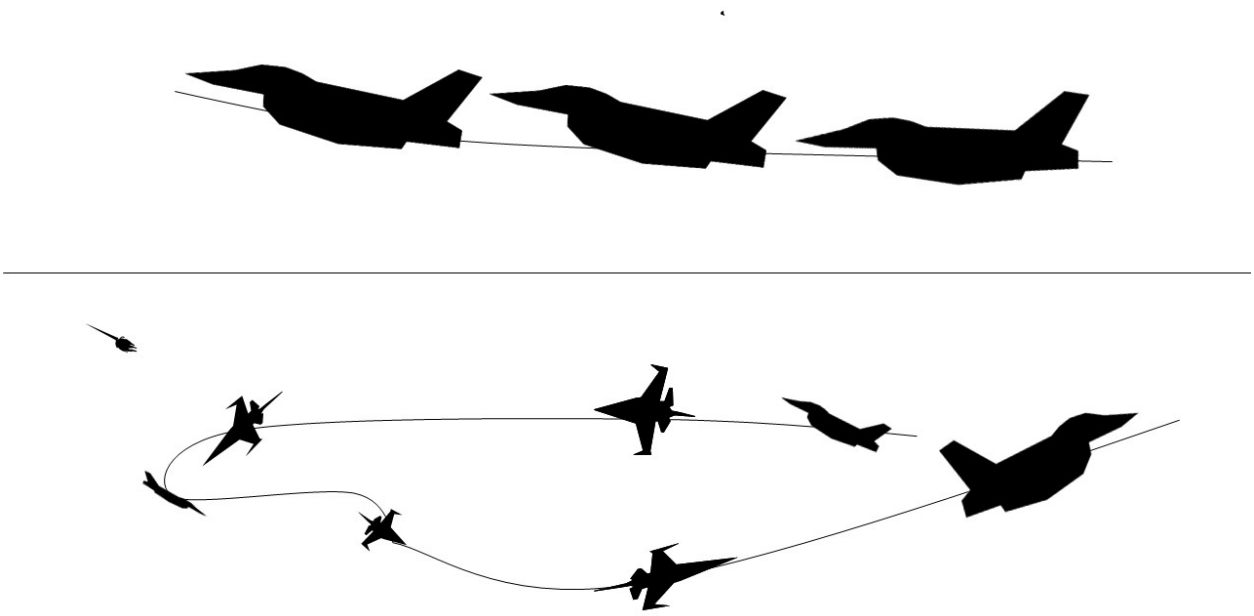

Figure 2.8: A contrast between a linear and nonlinear maneuver

   (a) in the controls,

   (b) in the state,

   (c) in both.

4. The performance index can be far more complex than a quadratic function. Referring to Figure 2.8, the performance of the system will be dictated by the performance criterion, and as the diagram suggests, a sophisticated choice of performance criterion in contrast to a naive selection can make the difference between life and death.

5. Uncertainty might exist in the following:

   (a) the dynamics,

   (b) the initial conditions.

6. Exogenous effects can introduce error.

7. Lastly, the command could be an implicit function of the time and state.

To generalize the results from linear systems to nonlinear system, we must employ a powerful tool for the solution of continuous-time optimization problems: the calculus of variations and optimal control. While the calculus of variations minimizes over a set of differentiable curves, optimal control optimizes a functional constrained by a set of differential equations.

2.2.2 Problem Formulation

We will address a more general formulation for this optimal control problem. This formulation is necessarily more formal than those previously discussed. This section demonstrates why practitioners can greatly benefit from optimizing a system constrained to differential equations.

First, we state the formal definition of a *Control System* from [50].

Definition 2.2.1 (Control System)**.** *A control system is a* 4*-tuple* $\Sigma = (M, U, f, \mathcal{U})$ *consisting of the state space,* M*, a control set,* U*, the dynamics,* f*, and a class of admissible controls,* $\mathcal{U}$*. In this dissertation, the following simplifying specifications are made:*

1. *M is a smooth manifold.*
2. *U is a subset of $\mathbb{R}^N$, $U \subset \mathbb{R}^N$.*
3. *The dynamics, f, is a continuously differentiable function,*

$$f : \mathbb{R} \times M \times U \to \mathbb{R}^n, \quad (t, x, u) \mapsto f(t, x, u). \tag{2.47}$$

4. *The class of admissible controls, $\mathcal{U}$, consists of all locally bounded, Lebesgue measurable functions $u : [t_0, T] \to U, t \mapsto u(t)$ with values in the control set, U, for which the solution of the corresponding initial value problem,*

$$\dot{x}(t) = f(t, x(t), u(t)), \quad x(t_0) = x_0,$$

exists over the full interval time interval, $I = [t_0, T]$, with t_0, the initial time, and T, the final time. The solution pair, (x, u), is called an admissible controlled trajectory of the system.

The main constraint on a control system emerges from its dynamics. Additionally, the formulation of the control set incorporates possible limitations on the control.

Furthermore, constraints on the state of the system are often present as well. For example, rather than explicitly specifying the final state of the system via a command, the *terminal constraint,* which is the zero level set of a function, Ψ, explicitly specifies a set of terminal conditions and final times. The system transfers the state from the initial condition, $x(0) = x_0$, to the terminal condition, $x(T) = x_T$ over I. The final time is constrained when the terminal constraint explicitly depends on time. Otherwise it is free.

Definition 2.2.2 (Terminal Constraint)**.** *The* terminal set $N \subset \mathbb{R} \times M$ *is:*

$$N = \{(t, x) \in \mathbb{R} \times M : \ \Psi(t, x) = 0\} \tag{2.48}$$

where Ψ *is a twice continuously differentiable mapping in all variables* (t, x)*,*

$$\Psi : \mathbb{R} \times M \to \mathbb{R}^{n-k}, \quad (t, x) \mapsto \Psi(t, x) = (\psi_1(t, x), \ldots, \psi_{n-k}(t, x))^T, \tag{2.49}$$

such that the gradients of the functions ψ_i*,* $i = 1, \ldots, n-k$*, with respect to* (t, x) *are linearly independent everywhere on* N*. These assumptions on* Ψ *guarantee that the terminal set is a* $k + 1$ *dimensional embedded submanifold of* $\mathbb{R} \times M$*.*

In the previous discussion of linear systems, we assumed that the performance criterion was a quadratic form. Now, we replace the familiar quadratic criteria with a general functional. The performance criterion is called the *objective*. The objective function in "Bolza" form sums two quantities. The Lagrangian is the term under an integral. The other is the terminal penalty.

Definition 2.2.3 (Lagrangian)**.** *The Lagrangian is a continuously differentiable function,*

$$L : \mathbb{R} \times M \times U \to \mathbb{R}, \quad (t, x, u) \mapsto L(t, x, u). \tag{2.50}$$

Definition 2.2.4 (Terminal Penalty)**.** *The terminal penalty,* φ*, is given by a twice continuously differentiable function of all variables defined on the terminal set,*

$$\varphi : N \subseteq \mathbb{R} \times M \to \mathbb{R}, \quad (t, x) \mapsto \varphi(t, x). \tag{2.51}$$

Definition 2.2.5 (Objective)**.** *The objective, J, is given in Bolza form as:*

$$J(u) = \varphi(T, x(T)) + \int_{t_0}^{T} L(s, x(s), u(s))ds, \tag{2.52}$$

with u, an admissible control, and x, the corresponding trajectory.

An *optimal control problem* consists in the selection among all admissible controlled trajectories, of one that minimizes an objective while achieving a state transfer from the initial condition to the terminal manifold.

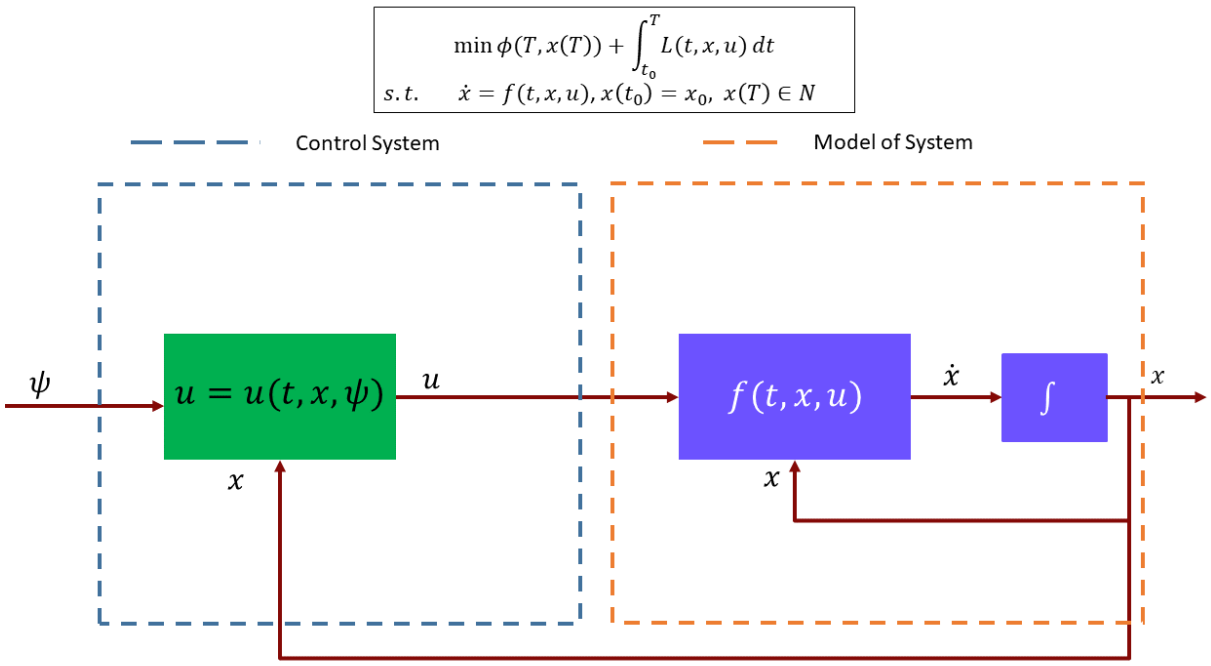

Figure 2.9: A nonlinear optimal control system.

More formally:

[OC] Minimize the objective, $J = J(u)$, over all admissible controlled trajectories (x, u) that satisfy the terminal constraint, $(T, x(T)) \in N$.

Next, we summarize the basic features of the problem, as depicted in Figure 2.9:

1. We desire to maneuver a system from some fixed initial condition, x_0, to a terminal condition on the terminal manifold, $x_T \in N$, over the interval, I.

2. The states belong to the manifold, M, and the controls are functions from the class of admissible controls, $\mathcal{U}$, taking values in the control set, U, over the interval, I.

3. The system is nonlinear, and its dynamics is described by $\dot{x} = f(t, x, u)$.

4. Along the maneuver, the optimal control trajectory (x, u) minimizes,

$$\mathcal{J} = \phi(T, x(T)) + \int_{t_0}^{T} L(t, x, u)\mathrm{d}t \tag{2.53}$$

   over all admissible controls.

5. Additionally, state and controls may be individually or simultaneously restricted later in the dissertation.

2.3 Necessary Conditions for Optimality for Optimal Control Problems

The Pontryagin Maximum Principle gives the first-order necessary condition for optimality of an optimal control problem. It aids the solution of optimal control problems, winnowing selection to only those functions that satisfy the Maximum Principle.

The *Hamiltonian* function, H, of the optimal control problem [OC] is defined as:

$$H(t, \lambda_0, \lambda, x, u) = \lambda_0 L(t, x, u) + \lambda f(t, x, u). \tag{2.54}$$

We quote the formulation from [50]:

Theorem 2.3.1 (Pontryagin Maximum Principle)**.** *Let $(x_\star, u_\star)$ be a controlled trajectory defined over the interval $[t_0, T]$ with the control $u_\star$ piecewise continuous. If $(x_\star, u_\star)$ is optimal, then there exists a constant $\lambda_0 \geq 0$ and a covector $\lambda : [t_0, T] \to (\mathbb{R}^n)^*$, the so-called adjoint variable, such that the following conditions are satisfied:*

1. *Nontrivially of the multiplier* $(\lambda_0, \lambda(t)) \neq 0$ *for all* $t \in [t_0, T]$

2. *Adjoint equation: the adjoint variable* λ *is a solution to the time varying differential equation*

$$\dot{\lambda}(t) = -\frac{\partial H}{\partial x}\left(t, \lambda_0, \lambda(t), x_*(t), u_\star(t)\right) \tag{2.55}$$

3. *Minimizing condition: everywhere in* $[t_0, T]$ *we have that*

$$H(t, \lambda_0, \lambda(t), x_\star(t), u_\star(t)) = \min_{v \in U} H(t, \lambda_0, \lambda(t), x_\star(t), v). \tag{2.56}$$

If the Lagrangian L *and the dynamics* f *are continuously differentiable in* t*, then the function*

$$h : t \mapsto H(t, \lambda_0, \lambda(t), x_\star(t), u_\star(t)) \tag{2.57}$$

is continuously differentiable with derivative given by

$$\dot{h} = \frac{\mathrm{d}h}{\mathrm{d}t}(t) = \frac{\partial H}{\partial t}\left(t, \lambda_0, \lambda(t), x_\star(t), u_\star(t)\right).$$

4. *Transversality condition: at the endpoint of the controlled trajectory, the convector*

$$(H + \lambda_0 \phi_t, -\lambda + \lambda_0 \phi_x)$$

is orthogonal to the terminal constraint N*, i.e. there exists a multiplier* $\nu \in \left(\mathbb{R}^{n+1-k}\right)^\star$ *such that*

$$H + \lambda_0 \phi_t + \nu D_t \Psi = 0 \quad \textit{and} \quad \lambda = \lambda_0 \phi_x + \nu D_x \Psi \ \textit{ at } (T, x_\star(T)) \tag{2.58}$$

Corollary 2.3.1. *If the Lagrangian* L *and the dynamics* f *are not explicit functions of the independent variable, then the function* $h : t \mapsto H(t, \lambda_0, \lambda(t), x_\star(t), u_\star(t))$ *is constant. If* ϕ *and* Ψ *also do not depend on* t *(and in this case the terminal time* T *necessarily is free), then for any multiplier* (λ_0, λ) *that satisfies the conditions of the maximum principle, the Hamiltonian* H *vanishes identically along the optimal controlled trajectory*

$$H(t, \lambda_0, \lambda(t), x_\star(t), u_\star(t)) \equiv 0. \tag{2.59}$$

If the parameter λ_0 is positive, it is possible to normalize it to $\lambda_0 = 1$ by dividing all equations by λ_0. Extremals of this type are called normal. Extremals with $\lambda_0 = 0$ are called abnormal. Even the simplest time-optimal control problems show that optimal abnormal extremals may exist.

2.4 Sufficient Conditions for Optimality in Optimal Control Theory: Dynamic Programming and the Hamilton-Jacobi-Bellman Equation

As described earlier, the Maximum Principle provides only necessary conditions for optimality in an optimal control problem. However, in engineering, we also seek sufficient conditions for optimality.

To emphasize the difference, suppose we created an optimum control law to transfer a satellite from Earth into orbit. To ensure efficacy, the solution should minimize transit time and maximize terminal speed and should not maximize transit time and minimize terminal speed.

Sufficient conditions provide the tools to construct feedback solutions. They allow the engineer to consider the change in the objective as a function of the starting and ending conditions in the state space. The mathematician Richard Bellman [6] devised this technique to solve optimization problems in his theory of "Dynamic Programming."

He considered "control policies" to be transformations of a state, and an optimal control problem to be a sequence of control policies, $\{u_k\}$, driving the system towards a maximum or minimum. He asserted a "Principle of Optimality" as follows:

> [Bellman] An optimal policy has the property that whatever the initial state and initial decisions are, the remaining decisions must constitute an optimal policy with regard to the state resulting from the first decisions.

The overarching theme is that the optimal objective, referred to as the value, cannot have an arbitrary form. Instead, the value evolves constrained to a differential equation, and knowledge of the value yields an optimal control.

These considerations, within some technical conditions, apply to continuous-time optimal control problems. We define these concepts [50] as follows.

Definition 2.4.1 (Value Function)**.** *The value function, $V(t,x)$, is the best possible cost function for admissible trajectories of an optimal control problem as a function of the initial condition, (t,x), i.e.:*

$$V(t,x) = \inf_{u \in \mathcal{U}} J(t,x,u), \tag{2.60}$$

where the optimization occurs over all admissible controls.

The principle of optimality provides a sufficient condition for an optimum control. To see this, we start from a candidate trajectory, divide the trajectory at an intermediate state, and continue from the intermediate state to the terminal manifold. Formally, we write,

$$V(t_0, x(t_0)) = \min_{u \in \mathcal{U}} \left\{ \int_{t_0}^{T} L(t,x,u)\mathrm{d}u + \phi(T, x(T)) \right\}. \tag{2.61}$$

If an arbitrary control, u, is used over the interval, $[t_0, t_0 + \delta t_0]$, then by the principle of optimality, the following inequality holds for this control:

$$V(t_0, x(t_0)) \leq \int_{t_0}^{t_0+\delta t_0} L(t,x,u)\mathrm{d}s + V(t_0, \delta t_0, x(t_0 + \delta t_0)). \tag{2.62}$$

Under the assumption that the value function is C^1, using (2.61) and (2.62) to compute the derivative in δt_0, it follows that

$$0 \leq \frac{\partial V}{\partial x}(t,x) f(t,x,u) + \frac{\partial V}{\partial t}(t,x) + L(t,x,u), \qquad \forall u \in U, \tag{2.63}$$

and equality holds for an optimum control. The resulting equation (2.64) is the Hamilton-Jacobi-Bellman (HJB) equation,

$$0 = \frac{\partial V}{\partial t}(t,x) + \min_{u \in U}\{\frac{\partial V}{\partial x}(t,x) f(t,x,u) + L(t,x,u)\}. \tag{2.64}$$

We show that the solution of the value function yields an optimum control, *i.e.* a sufficient condition for optimality.

Definition 2.4.2 (Admissible Feedback Controls)**.** *[8] For a region, G, in (t,x) space, a feedback control $u : G \to U, (t,x) \mapsto u(t,x)$ is admissible for the an optimum control problem if for every initial condition, $(t,x) \in G$, the initial value problem,*

$$\dot{x} = f(t,x,u(t,x)), \quad \xi(t) = x,$$

has a unique solution $x : [t,T] \to \mathbb{R}^n$.

For the classical solution to the HJB equation, we quote the following sufficient condition for an optimal control problem, again taken from [50].

Theorem 2.4.1 (Sufficient Condition for Optimal Control)**.** *Suppose there exists the pair $(V, u_\star)$, for which $u_\star$ is an admissible control and V is a C^1 solution to the Hamilton-Jacobi Equation,*

$$0 = \frac{\partial V}{\partial t}(t,x) + \min_{u \in U}\left\{\frac{\partial V}{\partial x}(t,x) f(t,x,u) + L(t,x,u)\right\}, \tag{2.65}$$

with equality holding for $u_\star$. Then $u_\star$ is an optimal control, and V is the value function for the problem.

While this result concisely provides a sufficient condition for optimality, use of this condition presents serious challenges. Equation (2.65) combines the solution of a first order partial differential equation (PDE) with a minimization condition.

For a general problem, the minimization condition leads to admissible feedback controls which switch discontinuously. When the switch occurs, the value need not remain continuously differentiable. Though some problems permit solution of the value function by

separation of variables under the minimization condition, most problems remain fraught with difficulty because solving the minimization problem in (2.65) often leads to a highly nonlinear PDE.

An alternative approach to solving the HJB equation identifies the quantity under minimization with the Hamiltonian and converts the single partial differential equation to a system of ordinary differential equations. To convert a single partial differential equation to a system of ordinary differential equations, we employ the method of characteristics from the theory of partial differential equations. The simultaneous minimization of the Hamiltonian-like quantity then yields the value function.

Chapter 3

Fields of Extremals for Optimal Control Problems with Terminal Constraints and Free Terminal Time

In this chapter, we extend the method of characteristics for first-order PDE's to optimal control to yield a constructive procedure that calculates a field of extremals for optimal control problems with terminal constraints and free terminal time. In these problems, the value function has a singularity at the terminal point, and a parameter desingularizes the value function near the terminal manifold. In this dissertation, after presenting this required background material, we apply a rigorous mathematics treatment to perturbation feedback control to establish a novel connection between the the engineering literature and classical, mathematical theory.

3.1 The Method of Characteristics of First Order Partial Differential Equation

The discussion here follows the treatment presented in [32]. The method of characteristics is a procedure to reduce first order partial differential equations to a system of ordinary differential equations. This method, at its core, does not solve an optimization problem, however, when applied to an optimization problem, the resulting value function, derived by the method, yields an optimal control.

The general method of characteristics seeks an integral surface–a geometric description of solutions to first order linear PDE's. On the integral surface, each point is associated with a tangent cone, a set of directions which are tangent to the surface. The idea of an integral manifold is that if we parameterize the surface, z, in coordinates, say x and y, as a function of t, then a curve which starts on a strip evolves for all time on the surface.

These strips are known as the characteristics strips, and the characteristic directions are the directions of characteristics curves, which lie on the integral surface. Consequently, the characteristic equations are the differential equations which describe the evolution in time of the characteristic curves.

For example, given the form of a first order partial differential equation in two dimensions,

$$F\left(x, y, \frac{\partial V}{\partial x}, \frac{\partial V}{\partial y}, V\right) \equiv 0, \tag{3.1}$$

we can take the integral surface, z, as a function of the coordinates x, y, where we define

$$z = V(x, y), \qquad p = \frac{\partial V}{\partial x}(x, y), \qquad \text{and } q = \frac{\partial V}{\partial y}(x, y), \tag{3.2}$$

transforming (3.1) to an equation in 5 variables, p, q, x, y, z :

$$F\left(x, y, z, p, q, \right) \equiv 0. \tag{3.3}$$

The method converts the PDE described by (3.3) to a system of 5 ordinary differential equations in the parameters p, q, x, y, z each evolving according to the parameter t.

The total differential along a curve, γ, on the integral surface is given by:

$$\frac{\mathrm{d}F}{\mathrm{d}t} = F_x \frac{\mathrm{d}x}{\mathrm{d}t} + F_y \frac{\mathrm{d}y}{\mathrm{d}t} + F_z \frac{\mathrm{d}z}{\mathrm{d}t} + F_p \frac{\mathrm{d}p}{\mathrm{d}t} + F_q \frac{\mathrm{d}q}{\mathrm{d}t}. \tag{3.4}$$

We seek 5 ordinary differential equations whose solutions are equivalent to the solution of the single PDE in the 5 variable partial differential equation.

On the surface, $z = V(x, y)$, the tangent plane at a point on the integral surface is given by:

$$z - z_0 = \nabla V \begin{bmatrix} x - x_0 \\ y - y_0 \end{bmatrix} = \begin{bmatrix} p & q \end{bmatrix} \begin{bmatrix} x - x_0 \\ y - y_0 \end{bmatrix}. \tag{3.5}$$

The total differential of the surface at a fixed point in x and y relates first order changes in each of these coordinate on the integral surface as in:

$$\mathrm{d}z = p\mathrm{d}x + q\mathrm{d}y. \tag{3.6}$$

For a point on the tangent plane of the surface, we have $\mathrm{d}z = 0$, and thus (3.7) below defines characteristic curves:

$$\frac{dy}{dx} = -\frac{p}{q}. \tag{3.7}$$

If the surface, z, is parameterized by a free parameter, which is a function, $u = G(x, y)$, then we can generate tangent planes by considering an envelope or union of the surfaces. Parameterizing each surface by u according to

$$z = V(x, y, u), \qquad \text{and} \qquad 0 = \frac{\partial V}{\partial u}(x, y), \tag{3.8}$$

then for fixed x, y, z, the tangent plane can be constructed from the system of equations, as the direction of the tangent to the surface is given by,

$$(p, q, -1) = \left(\frac{\partial V}{\partial x} + \frac{\partial V}{\partial u}\frac{\partial u}{\partial x}, \frac{\partial V}{\partial y} + \frac{\partial V}{\partial u}\frac{\partial u}{\partial y}, -1 \right) = (V_x, V_y, -1). \tag{3.9}$$

Again from (3.8), the minimum condition of the calculus of variations is immediately recognizable. Consider the necessary condition in the maximum principle: H is minimized in u. If we treat u as the parameter for the envelope of surfaces, the minimization condition chooses the characteristic surface, which solves for an optimization problem.

Now using this information for the surface, we can define the differential equations for the surface so that everywhere in time (3.7) holds, by taking the total differential of the surface

in time:

$$\frac{\mathrm{d}x}{\mathrm{d}t} = F_p, \qquad \frac{\mathrm{d}y}{\mathrm{d}t} = F_q, \tag{3.10}$$

where $\frac{\partial z}{\partial x} = p$ and $\frac{\partial z}{\partial y} = q$ and therefore,

$$\frac{\mathrm{d}z}{\mathrm{d}t} = pF_p + qF_q. \tag{3.11}$$

Hence, z satisfies (3.7), but constitutes an under-determined system.

The remaining two parameters evolve according to differential equations that satisfy the original PDE (3.1), whereby we differentiate with respect to x and y to yield equations which can be solved in terms of p and q.

Suppose that we start at a point on the integral surface, (x, y, z). There, the curve γ is parameterized by p and described by:

$$\frac{\mathrm{d}F}{\mathrm{d}x} = \frac{\partial F}{\partial x} + \frac{\partial F}{\partial z}\frac{\partial z}{\partial x} + \frac{\partial F}{\partial p}\frac{\partial p}{\partial x} + \frac{\partial F}{\partial q}\frac{\partial q}{\partial x} = 0, \tag{3.12}$$

$$\frac{\mathrm{d}F}{\mathrm{d}y} = \frac{\partial F}{\partial y} + \frac{\partial F}{\partial z}\frac{\partial z}{\partial y} + \frac{\partial F}{\partial p}\frac{\partial p}{\partial y} + \frac{\partial F}{\partial q}\frac{\partial q}{\partial y} = 0, \tag{3.13}$$

so that

$$\frac{\partial F}{\partial p}\frac{\partial p}{\partial x} + \frac{\partial F}{\partial q}\frac{\partial q}{\partial x} = -\frac{\partial F}{\partial x} - \frac{\partial F}{\partial z}\frac{\partial z}{\partial x}, \tag{3.14}$$

$$\frac{\partial F}{\partial p}\frac{\partial p}{\partial y} + \frac{\partial F}{\partial q}\frac{\partial q}{\partial y} = -\frac{\partial F}{\partial y} - \frac{\partial F}{\partial z}\frac{\partial z}{\partial y}, \tag{3.15}$$

Using the partial differential equation to remove the dependence on p and q, we can take the total differentials in x and y of (3.3) to arrive at

$$\frac{\mathrm{d}p}{\mathrm{d}t} = \frac{\partial p}{\partial x}F_p + \frac{\partial p}{\partial y}F_q = -\frac{\partial F}{\partial x} - \frac{\partial F}{\partial z}p, \tag{3.16}$$

$$\frac{\mathrm{d}q}{\mathrm{d}t} = \frac{\partial q}{\partial x}F_p + \frac{\partial q}{\partial y}F_q = -\frac{\partial F}{\partial y} - \frac{\partial F}{\partial z}q. \tag{3.17}$$

As a result, $\frac{\mathrm{d}F}{\mathrm{d}t} = 0$ in (3.4) remains satisfied.

The method can be applied to the Hamilton-Jacobi-Bellman equation. To see this, we start with the equation,

$$F\left(t, x, z, \tau, \lambda\right) = 0, \tag{3.18}$$

where the integral surface is the action denoted by S, with integral surface $z = S(t, x)$, parameterized by the coordinates $\tau = \frac{\partial S}{\partial t}(t, x)$ and $\lambda = \frac{\partial S}{\partial x}(t, x)$. The HJB equation takes the following form:

$$\tau + H\left(t, x, \lambda\right) = 0, \tag{3.19}$$

where we define the HJB with coordinate x to avoid confusion.

As a result,

$$\frac{\mathrm{d}t}{\mathrm{d}s} = \frac{\partial F}{\partial \tau} = 1 \Rightarrow t = s, \tag{3.20}$$

$$\frac{\mathrm{d}x}{\mathrm{d}t} = \frac{\partial F}{\partial \lambda} = \frac{\partial H}{\partial \lambda}, \tag{3.21}$$

$$\frac{\mathrm{d}z}{\mathrm{d}t} = \tau + \lambda\frac{\partial H}{\partial \lambda} = \frac{\partial S}{\partial t} + \lambda\frac{\mathrm{d}x}{\mathrm{d}t}, \tag{3.22}$$

$$\frac{\mathrm{d}\tau}{\mathrm{d}t} = -\frac{\partial H}{\partial t}, \tag{3.23}$$

$$\frac{\mathrm{d}\lambda}{\mathrm{d}t} = -\frac{\partial H}{\partial x}. \tag{3.24}$$

The system of equations again yields the canonical equations (3.21) and (3.24). We conclude that the characteristic equations are the dynamics of the system and the adjoint equation.

Furthermore, the parameter, λ, is the spatial rate of change of the integral surface in its total derivative, as represented in (3.22), This concept will be applied later in this dissertation to problems in optimal control in a result called the Shadow Price Lemma. For the system, it holds that:

$$\frac{\mathrm{d}S}{\mathrm{d}t} = \frac{\partial S}{\partial t} + \frac{\partial S}{\partial x}\frac{\mathrm{d}x}{\mathrm{d}t} + \frac{\partial S}{\partial z}\frac{\mathrm{d}z}{\mathrm{d}t} + \frac{\partial S}{\partial \tau}\frac{\mathrm{d}\tau}{\mathrm{d}t} + \frac{\partial S}{\partial \lambda}\frac{\mathrm{d}\lambda}{\mathrm{d}t} = 0, \tag{3.25}$$

after we relabel terms to match (3.4).

One difference which emerges when the method of characteristics is applied to an optimal control problem is that we must satisfy both boundary conditions and the maximization property. Analogously, if we consider the envelope of surfaces of the value function, the minimum condition of the maximum principle selects amongst the choice of parameters which define an optimum surface.

Starting from a point on the surface, trajectories evolve backwards in time according to the characteristic equations. In the following section, we will formally develop the solution to the optimal control problem with the method of characteristics.

3.2 Parametrization of Extremals

Calculating a single optimal trajectory for an optimal control problem often requires considerable effort and computation time. Various conditions impact the behavior of a system executing an optimal control. Combining a nominal control with linear feedback, allows us to recalculate trajectories which would ordinarily be prohibitively expensive.

Here, we aim to show that variations in the parameters generate locally optimal solutions, which neighbor the nominal trajectory. We think of this as constructing a gain schedule, which is a map from changes of the current state to nearby controlled maneuvers. We schedule solutions by tabulating the control as a function of some parameter, p.

The schedule depends on time and evolves along the maneuver. The situation is depicted in figure 3.1:

The family of controlled trajectories must satisfy the conditions of the maximum principle in order to be locally optimal. The following two definitions taken from [50] formalize these principles. The first describes a family of trajectories that is not necessarily extremal. The second defines an family of trajectories that is necessarily extremal.

Definition 3.2.1 (C^r-Parameterized Family of Controlled Trajectories)**.** *Given an open subset P of $\mathbb{R}^d$ with $0 \leq d \leq n$, let*

$$t_- : P \to \mathbb{R}, p \mapsto t_-(p) \text{ and } t_+ : P \to \mathbb{R}, p \mapsto t_+(p) \tag{3.26}$$

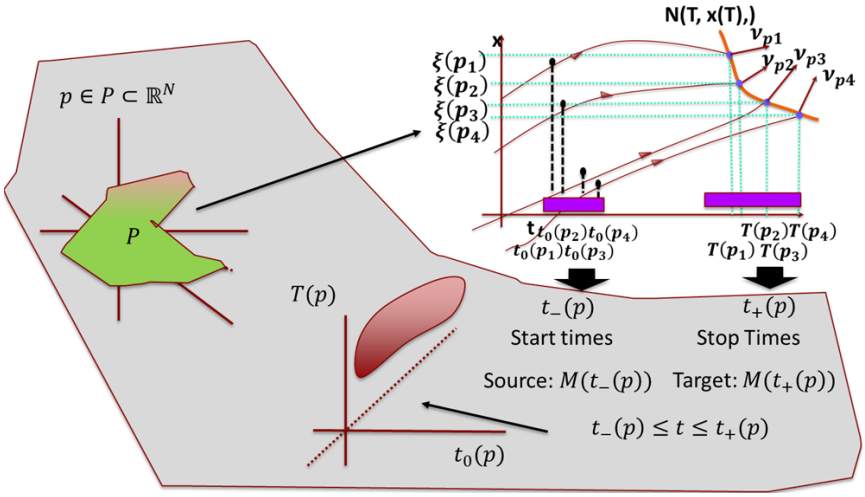

Figure 3.1: A depiction of a parameterized family

be two r-times continuously differentiable functions, $t_\pm \in C^r(P)$ *that satisfy* $t_-(p) \le t_+(p)$ *for all* $p \in P$*. We call* t_- *and* t_+ *the initial and terminal times of the parametrization and define its domain as*

$$D = \{(t,p) : p \in P, t_-(p) \le t \le t_+(p)\}\,. \tag{3.27}$$

Let

$$\xi_- : P \to \mathbb{R}^n, p \mapsto \xi_-(p) \text{ and } \xi_+ : P \to \mathbb{R}^n, p \mapsto \xi_+(p), \tag{3.28}$$

be r-times continuously differentiable functions, $\xi_\pm \in C^r(P)$*. A d-dimensional,* C^r *parameterized family of* $\mathcal{T}$ *of controlled trajectories with domain* D*, initial conditions* ξ_- *and terminal conditions* ξ_+ *consists of*

1. *Admissible controls,* $u : D \to U, (t,p) \mapsto u(t,p)$*, which are continuous and r-times continuously differentiable in* p *on* D*.*

2. *Corresponding trajectories,* $x : D \to \mathbb{R}^n, (t,p) \mapsto x(t,p)$*, i.e. solutions of the dynamics,*

$$\dot{x}(t,p) = f(t, x(t,p), u(t,p)), \tag{3.29}$$

which exist over the full interval $[t_-(p), t_+(p)]$ *and satisfy the initial condition*

$$x(t_-(p), p) = \xi_-(p) \tag{3.30}$$

and terminal condition

$$x(t_+(p), p) = \xi_+(p). \tag{3.31}$$

The definition of a C^r parameterized family of controlled trajectories leads to the analogous definition for extremals, which assumes that the trajectories satisfy the conditions of the maximum principle.

Essentially, the following definition establishes a parameterized version of the Pontryagin Maximum Principle:

Definition 3.2.2 ([50] C^r-Parameterized Family of Extremals)**.** *A* C^r*-parameterized family of extremals defined with domain* D *and parameter set* P *consists of:*

1. *a* C^r *parameterized family* $\mathcal{T}$ *of controlled trajectories* (x, u),
2. *a nonnegative multiplier* $\lambda_0 \in C^{r-1}(P)$ *and costate* $\lambda : D \to (\mathbb{R}^N)^\star, \lambda = \lambda(t, p)$, *such that* $(\lambda_0(p), \lambda(t, p)) \neq (0, 0)$ *for all* $(t, p) \in D$ *and the adjoint equation,*

$$\dot{\lambda}(t, p) = -\lambda_0(p) L_x(t, x(t, p), u(t, p)) - \lambda(t, p) f_x(t, x(t, p), u(t, p)),$$

is satisfied on the interval $[\tau_-(p), \tau_+(p)]$ *with boundary condition* $\lambda_-(p) = \lambda(\tau_-(p), p)$ *(respectively,* $\lambda_+(p) = \lambda(\tau_+(p), p)$ *given by an (r-1) times continuously differentiable function of* p *satisfying the following:*

   (a) *with* $h(t, p) = H(t, \lambda_0, \lambda(t, p), x(t, p), u(t, p))$, *the controls* $u = u(t, p)$ *solve the minimization problem*

$$h(t, p) = \min_{u \in U} H(t, \lambda_0(p), \lambda(t, p), x(t, p), u); \tag{3.32}$$

(b) with $h_\pm(p) = h(t_\pm(p), p)$ the following transversality condition holds at the source (respectively target)

$$\lambda_\pm(p)\frac{\partial \xi_\pm}{\partial p}(p) = \lambda_0(p)\frac{\partial \gamma}{\partial p}(p) + h_\pm(p)\frac{\partial t_\pm}{\partial p}(p); \tag{3.33}$$

(c) if the target N_+ is a part of the terminal manifold N, $N_+ \in N$, then setting $T(p) = t_+(p)$ and $\xi_+(p) = x(T(p), p)$ we have that $\gamma_+(p) = \phi(T(p), \xi_+(p))$; furthermore, there exists an $(r-1)$ times continuously differentiable multiplier $\nu : P \to \left(\mathbb{R}^{n+1-k}\right)^\star$ such that the following transversality conditions are satisfied

$$\lambda(T(p), p) = \lambda_0(p)\frac{\partial \phi}{\partial x}(T(p), \xi_+(p)) + \nu(p)\frac{\partial \Psi}{\partial x}(T(p), \xi_+(p)), \tag{3.34}$$

$$-h(T(p), p) = \lambda_0(p)\frac{\partial \phi}{\partial t}(T(p), \xi_+(p)) + \nu(p)\frac{\partial \Psi}{\partial t}(T(p), \xi_+(p)). \tag{3.35}$$

Additionally, we define the following function from [8]. Let Υ be the function defined by:

$$\Upsilon : N \times (\mathbb{R}^{n-k})^* \to \mathbb{R}, \quad (\tau, \xi, \nu) \mapsto \Upsilon(\tau, \xi, \nu) = \phi(\tau, \xi) + \nu\Psi(\tau, \xi). \tag{3.36}$$

The function, Υ, is considered the "Total Terminal Constraint," in that it contains in a single quantity both the "soft-constraint" *i.e.* the terminal penalty, ϕ, and the "hard-constraint," Ψ. Note, (3.34) reads

$$\lambda(\tau, \xi, \nu) = \frac{\partial \Upsilon}{\partial x}(\tau, \xi, \nu) = \frac{\partial \phi}{\partial x}(\tau, \xi) + \nu\frac{\partial \Psi}{\partial x}(\tau, \xi). \tag{3.37}$$

for a normal extremal with $\lambda_0(p) = 1$.

3.3 Fields of Extremals

Given a parameterized family of extremals, the associated cost $C(t, p)$—the cost-to-go function of this family — is the cost along the extremal with initial condition $(t, x(t, p))$. To prove optimality of the extremals we first determine whether it is possible to identify the parameterized cost, $C(t, p)$, with the actual value $V = V(t, x)$ of the optimal control problem. As shown in [50] below, the so-called Shadow Price Lemma is key to this inquiry.

Lemma 3.3.1 (Shadow Price Lemma)**.** *Let $\mathcal{E}$ be a C^1-parameterized family of extremal lifts with domain D, then for all $(t,p) \in D$,*

$$\lambda_0(p)\frac{\partial C}{\partial p}(t,p) = \lambda(t,p)\frac{\partial x}{\partial p}(t,p). \tag{3.38}$$

As a result, the gradient of C is equivalent to the gradient of the value function if the flow of trajectories associated with the parameterized family of extremals is injective. The optimal control problems are time-dependent and their flow is defined in terms of the graphs of trajectories, *i.e* as

$$\digamma : D \to \mathbb{R} \times \mathbb{R}^n, \quad (t,p) \mapsto \digamma(t,p) = \begin{pmatrix} t \\ x(t,p) \end{pmatrix}. \tag{3.39}$$

A parameterized family of extremals for which the flow map, $\digamma$, is injective, is called a parameterized field of extremals.

We aim to find conditions for which a parameterized family of extremals is a field of extremals. Loosely, by perturbing the conditions of an extremal at the end point, the inverse function theorem can construct a tube of extremals, which satisfy the maximum principle starting from a region of end points. We construct this tube of extremals around our reference extremal to define a feedback control around a reference trajectory. The idea is captured in the following in Figure 3.2:

More precisely, the following result holds [50]:

Theorem 3.3.1. *Let $\mathcal{E}$ be a C^r parameterized family of normal extremals for a time-dependent optimal control problem and suppose the restriction of its flow $\digamma$ to some open set $Q \subset D$ is a $C^{1,r}$ differomorphism onto an open subset*

$$G \subset \mathbb{R} \times \mathbb{R}^n \tag{3.40}$$

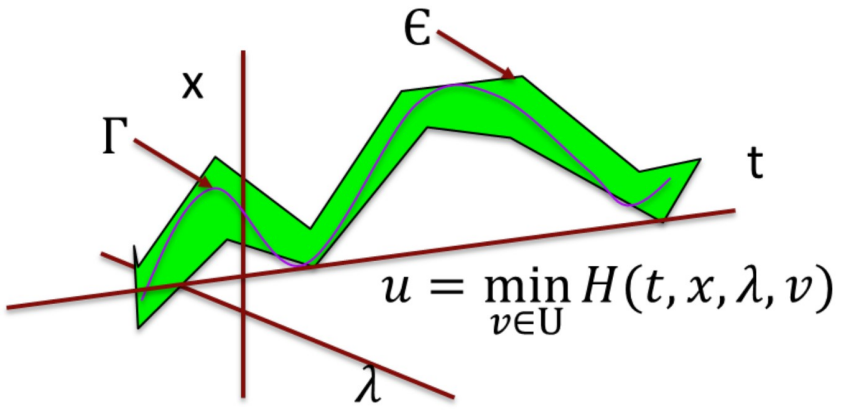

Figure 3.2: A reference extremal, Γ, embedded in a family, $\mathcal{E}$.

of the (t, x)-space. Then the value $V^{\mathcal{E}}$ of the parameterized family $\mathcal{E}$,

$$V^{\mathcal{E}} : G \to \mathbb{R}, \quad V^{\mathcal{E}} = C \circ F^{-1}, \tag{3.41}$$

is continuously differentiable in (t, x) and $r-$times continuously differentiable in x for fixed t. The function

$$u_\star : G \to \mathbb{R}, \quad u_\star = u \circ F^{-1}, \tag{3.42}$$

is an admissible feedback control that is continuous and r-times continuously differentiable in x for fixed t. Together, the pair $\left(V^{\mathcal{E}}, u_\star\right)$ is a classical solution to the Hamilton-Jacobi-Bellman equation

$$\frac{\partial V}{\partial t}(t, x) + \min_{u \in U} \left\{ \frac{\partial V}{\partial x}(t, x) f(t, x, u) + L(t, x, u) \right\} \equiv 0 \tag{3.43}$$

on G. Furthermore, the following identities hold in the parameter space on Q :

$$\frac{\partial V^{\mathcal{E}}}{\partial t}(t, x(t, p)) = -H(t, \lambda(t, p), x(t, p), u(t, p)), \tag{3.44}$$

$$\frac{\partial V^{\mathcal{E}}}{\partial x}(t, x(t, p)) = \lambda(t, p). \tag{3.45}$$

If $\mathcal{E}$ is nicely C^r parameterized, i.e. if λ is r-times continuously differentiable, then $V^{\mathcal{E}}$ is $r+1$-times continuously differentiable in x on G, and we also have that

$$\frac{\partial^2 V^{\mathcal{E}}}{\partial x^2}(t, x(t,p)) = \frac{\partial \lambda^T}{\partial p}(t,p)\left(\frac{\partial x}{\partial p}(t,p)\right)^{-1}. \tag{3.46}$$

The key relation here is (3.45), which allows us to identify the multiplier, $\lambda(t,p)$, of the parameterized family of extremals with the gradient $\frac{\partial V}{\partial x}(t, x(t,p))$, of the value function. This identification transforms the minimum condition (2.56) of the Pontryagin Maximum principle (2.3.1) into the statement of the Hamilton-Jacobi-Bellman equation. The following optimality statement then is an immediate consequence [50].

Corollary 3.3.1. *Let $\mathcal{F}$ be a C^r-parameterized local field of extremals with target N_T in the terminal manifold N, $N_T \subset N$, and assume that its associated flow covers a domain G. Then, given any initial condition $(t_0, x_0) \in G$, $x_0 = x(t_0, p_0)$, the open loop control $\bar{u}(t) = u(t, p_0)$, $t_0 \le t \le T(p_0)$, is optimal when compared with any other admissible control u for which the corresponding trajectory x (respectively its graph) lies in G, i.e. $\mathcal{J}(\bar{u}) \le \mathcal{J}(u)$.*

3.4 The Variational Equations and Conjugate Points

The optimality of the control, $u = u(t,p)$ in a parameterized family of extremals depends on the injectivity of the associated flow of trajectories. The local injectivity of the Jacobian matrix of the flow can be determined according to:

$$D\mathcal{F}(t,p) = \begin{bmatrix} 1 & 0 \\ \frac{\partial x}{\partial t}(t,p) & \frac{\partial x}{\partial p}(t,p) \end{bmatrix}, \tag{3.47}$$

which is non-singular if and only if the matrix $\frac{\partial x}{\partial p}(t,p)$ is nonsingular.

This matrix is the solution to the variational equation for the state. More generally, it helps to define a set of differential equations which describe first order changes in states, controls, and multipliers with respect to the parameters. These differential equations are referred to as the sensitivity equations and are useful in the study of stability and numerical calculation.

These equations inform a linear approach to flight control, where design employs a separate set of differential equations derived from a linearization of the true equations of motions. Linearization leads to simple relationships, which control engineers can use to develop linear controls systems. Sensitivities to the control inputs or the states are measured, and gains are calculated from these linear relationships.

As an example, consider the straight and level flight of an aircraft or projectile spinning flight. In the first situation, the axes of the aircraft may be distinct. In the other situation, the axes of the aircraft may all be inextricably linked. Linearizing an aircraft about its motion, we can examine the changes to first order in all of the maneuvers with respect to the parameters of the problem. Applying linearization in straight and level flight produces different linear dynamics than linearization in rolling flight. These dynamics show that the aircraft states associated with motions for rolling and yawing can be neglected from those of pitching. In the case of a spinning projectile, the linearization shows that the rate of spin of the projectile about its longitudinal axis contributes stability in pitching motions. Consequently, the linearization is a useful process to lay bare the dynamics of a system with complex behavior.

In fact, the same linear differential equations used in basic flight control design can justify sufficiency arguments for optimization. According to [36], where t is the independent variable, x is the state, and p is some parameter,

$$\dot{x} = f(t, x, p), \qquad x(t_0) = x_0, \tag{3.48}$$

such that the Jacobians of f with respect to x, p yield

$$A(t,p) = \frac{\partial f}{\partial x}(t, x(t,p), p), \qquad \text{and} \qquad B(t,p) = \frac{\partial f}{\partial p}(t, x(t,p), p), \tag{3.49}$$

so that

$$\frac{\mathrm{d}}{\mathrm{d}t}\left(\frac{\partial x}{\partial p}\right) = \frac{\partial \dot{x}}{\partial p} = \frac{\partial f}{\partial p}\left(t, x(t,p), p\right) = A(t,p)\frac{\partial x}{\partial p}(t,p) + B(t,p), \tag{3.50}$$

with $\frac{\partial x}{\partial p}(t_0, p) = 0$.

These are the sensitivity equations of the state with respect to the parameters. When the sensitivity equations are applied to the necessary conditions for an optimal control problem, they are called variational equations. These include:

1. the variational equation of the dynamics,
2. the variational equation of the adjoint.

This dissertation focuses on controlled extremals whose controls and trajectories stay away from control or state-space constraints. In the engineering literature such extremals are called non-singular [34]. Here, we quote from [50].

Definition 3.4.1 (Nonsingular Extremal)**.** *A normal extremal $\Lambda = ((x, u), \lambda)$ consisting of a controlled trajectory $\Gamma = (x, u)$ defined over an interval $[\tau, T]$ with corresponding multiplier λ is said to be nonsingular if for all $t \in [\tau, T]$ we have that*

$$\frac{\partial H}{\partial u}\left(t, \lambda(t), x(t), u(t)\right) \equiv 0 \tag{3.51}$$

and the matrix

$$\frac{\partial^2 H}{\partial u^2}\left(t, \lambda(t), x(t), u(t)\right) \tag{3.52}$$

is positive definite. As in the calculus of variations, in this case we say that the strengthened Legendre condition is satisfied along the extremal Λ.

Continuing the quotation [50], if the control, $u(t)$, of a normal extremal, Λ, lies in the interior of the control set, then it is an immediate consequence of the actual minimization condition of the maximum principle that $\frac{\partial H}{\partial u}\left(t, \lambda(t), x(t), u(t)\right) \equiv 0$ and that the matrix $\frac{\partial^2 H}{\partial u^2}\left(t, \lambda(t), x(t), u(t)\right)$ is positive semi-definite. This property is the Legendre condition.

In our development, we make the following assumptions.

- We assume that the maximum principle has been used to construct an extremal, *i.e.*, that the reference corresponding to parameter value, p_0, satisfies all conditions of the maximum principle.

- The reference trajectory is non-singular. It is normal and satisfies the strengthened Legendre condition .
- We assume that the reference trajectory remains away from constraints.

Suppose now that we have solved for some controlled trajectories and that these trajectories are parameterized by the parameter, p. For a parameterized family of extremals we make perturbations with respect to p to first order. Starting with the dynamics,

$$\dot{x}(t,p) = f(t, x(t,p), u(t,p)), \tag{3.53}$$

we have that

$$\frac{\mathrm{d}}{\mathrm{d}t}\left(\frac{\partial x}{\partial p}\right) = \frac{\partial f}{\partial x}\frac{\partial x}{\partial p} + \frac{\partial f}{\partial u}\frac{\partial u}{\partial p}. \tag{3.54}$$

From the definition of the Hamiltonian as $H = L + \lambda f$, we also have that

$$\frac{\partial}{\partial \lambda}\frac{\partial H}{\partial x} = \frac{\partial f^T}{\partial x}. \tag{3.55}$$

We need the aforementioned relationship to perturb the adjoint equation. Also, since we need to combine the equations, here we differentiate the column vector, λ^T,

$$\frac{\mathrm{d}}{\mathrm{d}t}\left(\frac{\partial \lambda^T}{\partial p}\right) = \frac{\partial^2 H}{\partial x^2}\frac{\partial x}{\partial p} + \frac{\partial^2 H}{\partial u \partial x}\frac{\partial u}{\partial p} + \frac{\partial f^T}{\partial x}\frac{\partial \lambda^T}{\partial p}. \tag{3.56}$$

Similarly, from the instantaneous minimization condition, we have

$$\frac{\partial H}{\partial u}(t, \lambda(t,p), x(t,p), u(t,p) \equiv 0. \tag{3.57}$$

Recognizing that

$$\frac{\partial}{\partial \lambda}\frac{\partial H}{\partial u} = \frac{\partial f^T}{\partial u}, \tag{3.58}$$

we obtain that

$$0 = \frac{\partial^2 H}{\partial x u}\frac{\partial x}{\partial p} + \frac{\partial^2 H}{\partial u^2}\frac{\partial u}{\partial p} + \frac{\partial f^T}{\partial x}\frac{\partial \lambda}{\partial p}. \tag{3.59}$$

Summarizing the three equations, we have that

$$\frac{\mathrm{d}}{\mathrm{d}t}\left(\frac{\partial x}{\partial p}\right) = f_x \frac{\partial x}{\partial p} + f_u \frac{\partial u}{\partial p}, \tag{3.60}$$

$$\frac{\mathrm{d}}{\mathrm{d}t}\left(\frac{\partial \lambda^T}{\partial p}\right) = H_{xx}\frac{\partial x}{\partial p} + H_{xu}\frac{\partial u}{\partial p} + f_x^T \frac{\partial \lambda}{\partial p}, \tag{3.61}$$

$$0 = H_{ux}\frac{\partial x}{\partial p} + H_{uu}\frac{\partial u}{\partial p} + f_u^T \frac{\partial \lambda}{\partial p}. \tag{3.62}$$

Since the extremals are non-singular, we can solve equation (3.62) for $\frac{\partial u}{\partial p}$. Substituting the result into equations (3.60) and (3.61) results in the following classical form of the variational equations for state and costate along a nonsingular extremal. We have quoted this from [50]:

Proposition 3.4.1. *Given a C^r parameterized family of nonsingular extremals, the matrices $\frac{\partial x}{\partial p}(t,p)$ and $\frac{\partial \lambda^T}{\partial p}(t,p)$ are solutions to the homogeneous linear matrix differential equation*

$$\begin{bmatrix} \frac{\mathrm{d}}{\mathrm{d}t}\left(\frac{\partial x}{\partial p}\right) \\ \frac{\mathrm{d}}{\mathrm{d}t}\left(\frac{\partial \lambda^T}{\partial p}\right) \end{bmatrix} = \begin{bmatrix} \frac{\partial f}{\partial x} - \frac{\partial f}{\partial u}\left(\frac{\partial^2 H}{\partial u^2}\right)^{-1}\frac{\partial^2 H}{\partial x \partial u} & -\frac{\partial f}{\partial u}\left(\frac{\partial^2 H}{\partial u^2}\right)^{-1}\frac{\partial f^T}{\partial u} \\ -\frac{\partial^2 H}{\partial x^2} - \frac{\partial^2 H}{\partial u \partial x}\left(\frac{\partial^2 H}{\partial u^2}\right)^{-1}\frac{\partial^2 H}{\partial x \partial u} & -\frac{\partial f}{\partial x} - \frac{\partial f}{\partial u}\left(\frac{\partial^2 H}{\partial u^2}\right)^{-1}\frac{\partial^2 H}{\partial x \partial u} \end{bmatrix} \begin{bmatrix} \frac{\partial x}{\partial p} \\ \frac{\partial \lambda^T}{\partial p} \end{bmatrix}. \tag{3.63}$$

All functions are evaluated along the parameterized extremal $\Gamma_p = (x(\cdot,p), u(\cdot,p), \lambda(\cdot,p))$. The notation has been set up for column vectors, and we note that, for example, differentiating the m-dimensional column vector H_u^T with respect to x, one obtains an $m \times n$ matrix whose row vectors are the x-gradients of the components of H_u^T. This matrix is denoted H_{ux}. In particular, under our general differentiability assumptions, the mixed partial derivatives are equal and we have that $H_{xu} = H_{ux}^T$.

The variational equations and especially the invertibility of the matrix $\frac{\partial x}{\partial p}$ have a direct connection with a matrix Riccati differential equation which is given in the classical result below quoted from [50]:

Proposition 3.4.2. *Suppose $A(\cdot), B(\cdot), M(\cdot)$, and $N(\cdot)$ are continuous $n \times n$ matrices defined on $[0,T]$ and let $(X,Y)^T$ be the solution to the initial value problem*

$$\begin{bmatrix} \dot{X} \\ \dot{Y} \end{bmatrix} = \begin{bmatrix} A & -M \\ -N & -B \end{bmatrix} \begin{bmatrix} X \\ Y \end{bmatrix}, \qquad \begin{bmatrix} X(0) \\ Y(0) \end{bmatrix} = \begin{bmatrix} X_0 \\ Y_0 \end{bmatrix} \tag{3.64}$$

Suppose X_0 is nonsingular. Then the solution $X(t)$ is nonsingular on the full interval $[0,T]$ if and only if the solution S to the Riccati equation

$$\dot{S} + SA(t) + B(t)S - SM(t)S + N(t) \equiv 0, \qquad S(0) = Y_0 X_0^{-1} \tag{3.65}$$

exists on the full interval $[0,T]$, and in this case we have that

$$Y(t) = S(t)X(t).$$

The solution S to the Riccati equation has a finite escape time at $t = \tau$ if and only if τ is the first time when the matrix $X(t)$ becomes singular.

The Riccati differential equation arises naturally from the canonical equations of optimal control. Resuming the discussion from earlier, consider a canonical system which satisfies the differential equations for a quadratic Hamiltonian in the control and in the state

$$\begin{bmatrix} \dot{x}(t) \\ \dot{\lambda}^T(t) \end{bmatrix} = \begin{bmatrix} A(t) & -B(t) \\ -C(t) & -A^T(t) \end{bmatrix} \begin{bmatrix} x(t) \\ \lambda^T(t) \end{bmatrix}. \tag{3.66}$$

We can now compare the form of the equations in (3.66) to (3.62). Suppose the variational equation for optimality holds true. The system of equations that remain composed of the variational equation of the state and the variational equation of the adjoint yields the canonical system of differential equations (3.66).

Rather than using a similarity transform to transform the 2nd order system to normal form, we make the "*ansatz*," $x = S\lambda^T$, for a nontrivial solution, λ, and a symmetric matrix. This

gives

$$\dot{x}(t) = \dot{S}(t)\lambda(t) + S(t)\dot{\lambda}(t), \tag{3.67}$$

$$A(t)x(t) - B(t)\lambda(t) = \dot{S}(t)\lambda(t) - S(t)C(t)x(t) - S(t)A^T(t)\lambda(t), \tag{3.68}$$

$$A(t)S(t)\lambda(t) - B(t)\lambda(t) = \dot{S}(t)\lambda(t) - S(t)C(t)S(t)\lambda(t) - S(t)A^T(t)\lambda(t), \tag{3.69}$$

with the result that

$$\dot{S}(t) = S(t)C(t)S(t) + A^T(t)S(t) + S(t)A(t) - B(t). \tag{3.70}$$

By Proposition 3.4.2, the non-existence of a solution, $S(t)$, indicates that singularities exist in the solutions to the canonical system.

We can also link the variational equations to a quadratic cost function by considering the second variation of the cost function for an optimal control problem or a problem in the calculus of variations. Here, we have that

$$I^2[h] = \int_a^b \begin{bmatrix} h & \dot{h} \end{bmatrix} \begin{bmatrix} L_{xx} & L_{\dot{x}x} \\ L_{x\dot{x}} & L_{\dot{x}\dot{x}} \end{bmatrix} \begin{bmatrix} h \\ \dot{h} \end{bmatrix} \mathrm{d}t. \tag{3.71}$$

This mimics the situation in the calculus of variations where the second variation takes this form. The cross terms can be integrated by parts to give

$$\int_a^b L_{\dot{x}x}\dot{h}h\mathrm{d}t = -\int_a^b \frac{\mathrm{d}}{\mathrm{d}t}L_{\dot{x}x}h^2\mathrm{d}. \tag{3.72}$$

This gives the definition of the quadratic forms analogous to

$$\mathcal{Q}(h) = \int_a^b \Big(Q(t)h(t)^2 + R(t)\dot{h}(t)\Big)\,\mathrm{d}t, \tag{3.73}$$

where $Q(h) = L_{xx} - \frac{\mathrm{d}}{\mathrm{d}t}L_{\dot{x}x}$ and $R(t) = L_{\dot{x}\dot{x}}$.

In the calculus of variations, the strengthened Legendre condition states that $L_{\dot{x}\dot{x}} > 0$ for all time $t \in [a, b]$. Under the assumption of the strengthened Legendre condition, Jacobi noted

that the quadratic form, $\mathcal{Q}(h)$, need not be positive definite. Rather, additional necessary, respectively, sufficient conditions, now known as the Jacobi conditions must hold.

Essentially, if there exists non-trivial solutions, y, to the Jacobi equation which has a zero at some time $c \in (a, b]$,

$$\frac{\mathrm{d}}{\mathrm{d}t}\left(R\dot{y}\right) = Qy, \qquad y(a) = 0, \quad \dot{y}(a) = 1, \tag{3.74}$$

then $\mathcal{Q}$ will not be positive-definite. The time, c, is called conjugate to a and the point, $x(c)$, is a conjugate point. In optimal control theory, the analogue of these equations is given by (3.63). Therefore, the variational equation of the cost function gives a necessary condition for optimality in terms of nonexistence of a conjugate point. The construction of a field of extremals employs the same idea.

Figure 3.3 depicts the propagation of the changes in the parameter on through to the change in the extremal Γ.

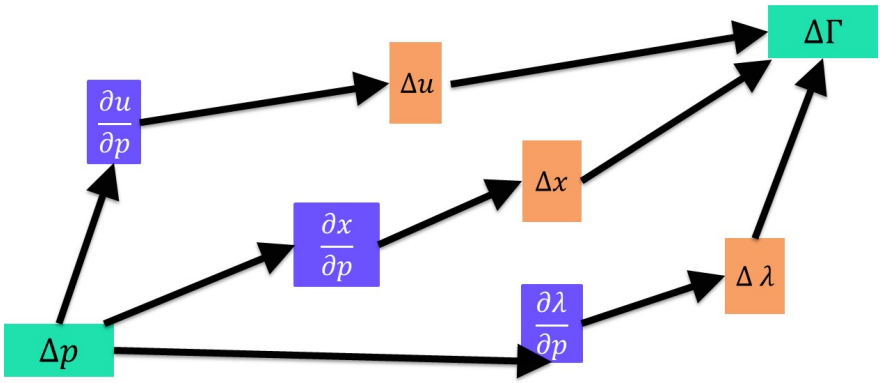

Figure 3.3: Propagation of Parameter Changes to Extremal Changes

3.5 A Backward Sweep of the Variational Equations of the Extremals

The remainder of this chapter of the thesis presents novel material and captures the main theoretical contributions of the dissertation. These results have already been published in [8]. They provide a mathematically clear formulation of the construction of a parameterized family of extremals. They also investigate when this family constitutes a field around a nonsingular extremal for an optimal control problem with terminal constraints and free terminal time. The terminal constraint causes the flow to be singular at the terminal time. Consequently, desingularizing of the parameterization is necessary to construct a field of extremals.

To achieve this result, we seek the conditions which guarantee that a nonsingular extremal can be embedded into a field of extremals. These conditions are developed in a formal way in Chapter 6 of the textbook by Bryson and Ho [34], based on research done in the 1960s, in connection with the space program (*e.g.*, [15, 14, 41]). Here, we revisit those formal procedures and apply a mathematically rigorous standing in terms of local fields of extremals. At the same time, we also clarify some of the implicitly made assumptions in the formal calculations.

In a first step, we construct a canonical C^1-parameterized family of normal extremals by parameterizing extremals through a section of the normal bundle to the terminal manifold, N.

Let τ denote the terminal time, ξ the terminal point of a non-singular extremal, and ν the corresponding multiplier in the transversality condition. The multiplier, λ, is then simply given by

$$\lambda(\tau,\xi,\nu) = \frac{\partial \Upsilon}{\partial x}(\tau,\xi,\nu) = \frac{\partial \varphi}{\partial x}(\tau,\xi) + \nu \frac{\partial \Psi}{\partial x}(\tau,\xi). \tag{3.75}$$

However, the transversality condition on the terminal time also needs to be satisfied. Since the reference extremal is non-singular, we can employ the implicit function theorem to solve the equation

$$\frac{\partial H}{\partial u}(\tau, \lambda(\tau,\xi,\nu), \xi, u) = 0$$

for u by a differentiable function, $u = u(\tau, \xi, \nu)$, near the reference control. Thus, we need to impose the following condition on the parameterization:

$$H(\tau, \lambda(\tau, \xi, \nu), \xi, u(\tau, \xi, \nu)) + \frac{\partial \Upsilon}{\partial t}(\tau, \xi; \nu) \equiv 0. \tag{3.76}$$

Let $\Omega : N \times (\mathbb{R}^{n-k})^* \to \mathbb{R}$ denote the function of (τ, ξ, ν) defined by this relation, and assume that the gradient of Ω is non-zero at the endpoint of the reference extremal. We shall compute this gradient below. The equation (3.76) locally defines a hypersurface, $\tilde{N}$ (an n-dimensional embedded submanifold of $N \times (\mathbb{R}^{n-k})^*$), which provides us with coordinates for all terminal points which satisfy the transversality conditions of the maximum principle.

Choosing an appropriate coordinate chart for $\tilde{N}$ at the endpoint of the reference extremal, it follows that there exists an open set $P \subset \mathbb{R}^n$, such that the inverse coordinate map (the parameterization)

$$\omega : P \to \tilde{N}, \qquad p \mapsto (\tau(p), \xi(p), \nu(p)) \tag{3.77}$$

is a differomorphism, and reduces to the endpoint of the reference extremal for some $p_0 \in P$.

Proposition 3.5.1. *Let $\bar{\Gamma} = ((\bar{x}, \bar{u}), \bar{\lambda})$ be a nonsingular extremal for problem* [OC] *defined over $[t_0, T]$. Suppose that the following assumption [A] is satisfied, i.e.,*

1. *for every $t \in [t_0, T]$ the control $\bar{u}(t)$ lies in the interior of the control set U and is the unique minimizer of the function $v \mapsto H(t, \bar{\lambda}(t), \bar{x}(t), v)$ over the control set U;*
2. *the gradient of the function $\Omega = H + \frac{\partial \Upsilon}{\partial t}$ is non-zero at the terminal point of the reference extremal.*

Then the set $\tilde{N}$ of all endpoints $(\tau, \xi) \in N$ and multipliers $\nu \in (\mathbb{R}^{n-k})^*$ for which the transversality conditions of the maximum principle are satisfied is an n-dimensional embedded submanifold of $N \times (\mathbb{R}^{n-k})^*$ and there exists a canonical C^1-parameterized family of nonsingular extremals $\mathcal{E}$ with domain $D = \{(t, p) : p \in P,\, t_-(p) \le t \le \tau(p)\}$ that contains the reference extremal for $p_0 \in P$:

$$x(t, p_0) \equiv \bar{x}(t), \quad u(t, p_0) \equiv \bar{u}(t), \quad \lambda(t, p_0) \equiv \bar{\lambda}(t) \qquad \text{for all } t \in [t_0, T]. \tag{3.78}$$

The reference extremal, $\bar{\Gamma}$, is embedded into the parameterized family, $\mathcal{E}$. The condition that $\bar{u}(t)$ is the unique minimizer is important in the construction. It prevents switching of the control in a neighborhood of the reference value p_0. If switching were to occur, then the smoothness properties that we assumed would not be satisfied, and different parameterized families of extremals would need to be patched together. Condition (1) is satisfied, for instance, if the Hamiltonian H is strictly convex in u.

Proof. The following proof adapts the proof of Theorem 5.3.1 found in [50]. Here, only the main steps are given. If ρ denotes the lift of the graph of the controlled trajectory, $\bar{x}$, into the cotangent bundle defined by the extremal, Γ, *i.e.*,

$$\rho : [t_0, T] \to [t_0, T] \times \mathbb{R}^n \times (\mathbb{R}^n)^*, \qquad t \mapsto \rho(t) = (t, \bar{x}(t), \bar{\lambda}(t)),$$

then the strengthened Legendre condition implies that there exists a function, $u = u(t, x, \lambda)$, defined, continuous and continuously differentiable in (x, λ) in a tubular neighborhood V of the curve ρ, which is the unique solution of the equation $H_u(t, \lambda, x, u) = 0$ on V. By choosing a small enough neighborhood V , we can guarantee that $u(t, x, \lambda)$ still is the unique minimizer of the function

$$\eta : U \to \mathbb{R}, \quad v \mapsto \eta(v) = H(t, \lambda, x, v).$$

This solves the minimization problem on the Hamiltonian in the control. This step applies assumption (1) to the reference control.

We define the trajectories, $x = x(t, p)$, and costates, $\lambda = \lambda(t, p)$, by integrating the combined dynamics,

$$\dot{x} = f(t, x, u(t, x, \lambda)), \tag{3.79}$$

$$\dot{\lambda} = -L_x(t, x, u(t, x, \lambda)) - \lambda f_x(t, x, u(t, x, \lambda)), \tag{3.80}$$

backward from the terminal manifold with terminal conditions,

$$x(\tau(p), p) = \xi(p) \quad \text{and} \quad \lambda(\tau(p), p) = \frac{\partial \Upsilon}{\partial x}(\tau(p), \xi(p), \nu(p)). \tag{3.81}$$

The control $u(t,p)$ is given by

$$u(t,p) = u(t, x(t,p), \lambda(t,p)). \tag{3.82}$$

From the continuous dependence of solutions to ordinary differential equations on initial conditions and parameters, it follows that $x(\cdot,p)$ and $\lambda(\cdot,p)$ exist and are continuously differentiable in the parameter p over some interval $[t_-(p), \tau(p)]$.

The construction reveals that all parameterized controlled trajectories $(x(\cdot,p), u(\cdot,p))$ are extremals with multiplier $\lambda(\cdot,p)$. This defines a C^1-parameterized family of nonsingular extremals $\mathcal{E}$ which contains the reference extremal. □

Denote the domain of this canonical C^1-parameterized family of nonsingular extremals $\mathcal{E}$ by $D = \{(t,p) : p \in P,\, t_-(p) \le t \le \tau(p)\}$ with $t_-(p_0) = t_0$ and $\tau(p_0) = T$. Recall that the flow $\digamma$ corresponding to the parameterized family $\mathcal{E}$ is defined by

$$\digamma : D \to \mathbb{R} \times \mathbb{R}^n, \quad (t,p) \longmapsto \digamma(t,p) = \begin{pmatrix} t \\ x(t,p) \end{pmatrix}, \tag{3.83}$$

i.e., in terms of the graphs of the corresponding trajectories. If the Jacobian matrix, $D\digamma(t,p_0)$ (equivalently, $\frac{\partial x}{\partial p}(t,p_0)$), is nonsingular on the interval, $[t_0,T)$, *i.e.*, aside from the final times where there may exist overlaps), then for every time, t, in this interval, there exists a neighborhood O_t of (t,p_0), $O_t \subset D$, such that the restriction of the flow map, $\digamma$, to O_t is a C^1-differomorphism. Thus, if we define

$$G = \bigcup_{\tau \le t < T} \digamma(O_t), \tag{3.84}$$

then G is an open set which, except for the terminal point $(T, \bar{x}(T))$, contains the graph of the controlled reference trajectory, $(\bar{x}, \bar{u})$. The following corollary results:

Corollary 3.5.1. *[50] The canonical C^1-parameterized family of nonsingular extremals $\mathcal{E}$ constructed in Proposition 3.5.1 defines a* local field *of extremals around the reference trajectory if and only if the Jacobian matrix $\frac{\partial x}{\partial p}(t,p_0)$ is nonsingular over the interval $[t_0,T)$. In this case, the reference extremal is optimal when compared with all other controlled trajectories $\Gamma = (x,u)$ for which the graph of the trajectory lies in G.* □

For reference, we record the gradient of the function Ω of (τ, ξ, ν), defined by equation (3.37), which describes the transversality condition on the terminal time.

These formulas can be expressed in a compact form if, for a (vector-valued) function $\zeta = \zeta(t, x)$, we make consistent use of the notation

$$\frac{d\zeta}{dt}(t,x) = \frac{\partial \zeta}{\partial t}(t,x) + \frac{\partial \zeta}{\partial x}(t,x) f(t,x,u) \tag{3.85}$$

for the time-derivative of ζ along solutions of the dynamics.

Lemma 3.5.1. *The gradient of* $\Omega = H + \frac{\partial \Upsilon}{\partial t}$ *is given by*

$$\frac{\partial \Omega}{\partial \tau} = \frac{\partial H}{\partial t} + \frac{d}{dt}\left(\frac{\partial \Upsilon}{\partial t}\right), \quad \frac{\partial \Omega}{\partial \xi} = \frac{\partial H}{\partial x} + \frac{d}{dt}\left(\frac{\partial \Upsilon}{\partial x}\right), \quad \frac{\partial \Omega}{\partial \nu} = \frac{d\Psi}{dt}, \tag{3.86}$$

with all functions evaluated at (τ, ξ, ν).

Proof. In this calculation, all functions are evaluated at the point (τ, ξ, ν). This includes the multiplier, λ, and the control, u, arising in the Hamiltonian, H. When differentiating, we treat all variables as column vectors and thus differentiate with respect to λ^T and ν^T. For example, we have that $\frac{\partial H}{\partial \lambda^T} = f^T$ by the adjoint equation and we note that all partial derivatives $\frac{\partial H}{\partial u}$ vanish along a nonsingular extremal. Differentiating equation (3.37) gives

$$\begin{aligned}
\frac{\partial \Omega}{\partial \tau} &= \frac{\partial H}{\partial t} + \frac{\partial H}{\partial \lambda^T}\frac{\partial \lambda^T}{\partial \tau} + \frac{\partial H}{\partial u}\frac{\partial u}{\partial \tau} + \frac{\partial}{\partial \tau}\left(\frac{\partial \Upsilon}{\partial t}\right) \\
&= \frac{\partial H}{\partial t} + f^T \frac{\partial}{\partial t}\left(\frac{\partial \Upsilon}{\partial x}\right)^T + \frac{\partial^2 \Upsilon}{\partial t^2} \\
&= \frac{\partial H}{\partial t} + \frac{\partial}{\partial x}\left(\frac{\partial \Upsilon}{\partial t}\right) f + \frac{\partial^2 \Upsilon}{\partial t^2} = \frac{\partial H}{\partial t} + \frac{d}{dt}\left(\frac{\partial \Upsilon}{\partial t}\right),
\end{aligned}$$

$$\begin{aligned}
\frac{\partial \Omega}{\partial \xi} &= \frac{\partial H}{\partial \lambda^T}\frac{\partial \lambda^T}{\partial \xi} + \frac{\partial H}{\partial x} + \frac{\partial H}{\partial u}\frac{\partial u}{\partial \xi} + \frac{\partial}{\partial \xi}\left(\frac{\partial \Upsilon}{\partial t}\right) \\
&= f^T \frac{\partial}{\partial x}\left(\frac{\partial \Upsilon}{\partial x}\right)^T + \frac{\partial H}{\partial x} + \frac{\partial^2 \Upsilon}{\partial t \partial x} \\
&= \frac{\partial H}{\partial x} + \frac{\partial^2 \Upsilon}{\partial x^2} f + \frac{\partial^2 \Upsilon}{\partial t \partial x} = \frac{\partial H}{\partial x} + \frac{d}{dt}\left(\frac{\partial \Upsilon}{\partial x}\right),
\end{aligned}$$

and

$$\begin{aligned}\frac{\partial \Omega}{\partial \nu^T} &= \frac{\partial H}{\partial \lambda^T}\frac{\partial \lambda^T}{\partial \nu^T} + \frac{\partial H}{\partial u}\frac{\partial u}{\partial \nu^T} + \frac{\partial}{\partial \nu^T}\left(\frac{\partial \Upsilon}{\partial t}\right)^T \\ &= f^T\left(\frac{\partial \Psi}{\partial x}\right)^T + \left(\frac{\partial \Psi}{\partial t}\right)^T = \left(\frac{d\Psi}{dt}\right)^T,\end{aligned}$$

which is equivalent to the last expression in equation (3.86). □

We aim to establish conditions which guarantee that the matrix $\frac{\partial x}{\partial p}(t, p_0)$ is nonsingular for $t_0 \leq t < T$. These conditions are based on the variational equations. The formulas are identical with the ones given in [34, Chapter 6], but we arrive at them from a different point of view. We give their complete derivation in contrast to the brief development in [34].

The matrices, $\frac{\partial x}{\partial p}$ and $\frac{\partial \lambda^T}{\partial p}$, satisfy the variational equations (3.63) of the dynamics and adjoint equation, respectively.

The parametrization at the terminal point determines the terminal values for the partial derivatives $\frac{\partial x}{\partial p}$ and $\frac{\partial \lambda^T}{\partial p}$. These computations are extensive and to avoid burying their meaning in notation, we drop the arguments. Thus, in the calculations below, τ, ξ and ν and their derivatives are always evaluated at p; x, u and λ are evaluated at $(\tau(p), p)$; f is evaluated at $(\tau(p), x(\tau(p), p), u(\tau(p), p))$; and all gradients of Υ are evaluated at $\omega(p) = (\tau(p), \xi(p), \nu(p))$. Differentiating the terminal conditions

$$x(\tau(p), p) \equiv \xi(p) \quad \text{and} \quad \lambda(\tau(p), p) \equiv \frac{\partial \Upsilon}{\partial x}(\tau(p), \xi(p), \nu(p)),$$

it follows that

$$\frac{\partial x}{\partial p}(\tau(p), p) = \frac{\partial \xi}{\partial p} - \frac{\partial x}{\partial \tau}\frac{\partial \tau}{\partial p} = \frac{\partial \xi}{\partial p} - f\frac{\partial \tau}{\partial p}, \tag{3.87}$$

and

$$\begin{aligned}
\frac{\partial \lambda^T}{\partial p}(\tau(p),p) &= \frac{d}{dp}\left(\frac{\partial \Upsilon}{\partial x}\right)^T - \frac{\partial \lambda^T}{\partial \tau}\frac{\partial \tau}{\partial p} \\
&= \left(\frac{\partial}{\partial \tau}\left(\frac{\partial \Upsilon}{\partial x}\right)^T - \dot{\lambda}^T\right)\frac{\partial \tau}{\partial p} + \frac{\partial}{\partial \xi}\left(\frac{\partial \Upsilon}{\partial x}\right)^T \frac{\partial \xi}{\partial p} + \frac{\partial}{\partial \nu^T}\left(\frac{\partial \Upsilon}{\partial x}\right)^T \frac{\partial \nu^T}{\partial p} \\
&= \left(\frac{\partial}{\partial t}\left(\frac{\partial \Upsilon}{\partial x}\right) + \frac{\partial H}{\partial x}\right)^T \frac{\partial \tau}{\partial p} + \frac{\partial^2 \Upsilon}{\partial x^2}\left(\frac{\partial x}{\partial p} + f\frac{\partial \tau}{\partial p}\right) + \left(\frac{\partial \Psi}{\partial x}\right)^T \frac{\partial \nu^T}{\partial p} \\
&= \frac{\partial^2 \Upsilon}{\partial x^2}\frac{\partial x}{\partial p} + \frac{\partial \nu}{\partial p}\frac{\partial \Psi}{\partial x} + \left(\frac{\partial}{\partial t}\left(\frac{\partial \Upsilon}{\partial x}\right) + f^T\frac{\partial^2 \Upsilon}{\partial x^2} + \frac{\partial H}{\partial x}\right)^T \frac{\partial \tau}{\partial p} \\
&= \frac{\partial^2 \Upsilon}{\partial x^2}\frac{\partial x}{\partial p} + \frac{\partial \nu}{\partial p}\frac{\partial \Psi}{\partial x} + \left(\frac{d}{dt}\left(\frac{\partial \Upsilon}{\partial x}\right) + \frac{\partial H}{\partial x}\right)^T \frac{\partial \tau}{\partial p}.
\end{aligned}$$

Observing that the term multiplying $\frac{\partial \tau}{\partial p}$ is the transpose of $\frac{\partial \Omega}{\partial \xi}$ (Lemma 3.5.1), we therefore have the following relation at the endpoint $(\tau(p), p)$:

$$\frac{\partial \lambda^T}{\partial p} = \frac{\partial^2 \Upsilon}{\partial x^2}\frac{\partial x}{\partial p} + \frac{\partial \nu}{\partial p}\frac{\partial \Psi}{\partial x} + \left(\frac{\partial \Omega}{\partial \xi}\right)^T \frac{\partial \tau}{\partial p}. \tag{3.88}$$

Differentiating the following conditions

1. the endpoint needs to lie in the terminal manifold,
2. the transversality condition for the terminal time needs to be satisfied,

gives two further equality relations between the derivatives, $\frac{\partial x}{\partial p}(\tau(p), p)$, $\frac{\partial \nu}{\partial p}(p)$ and $\frac{\partial \tau}{\partial p}(p)$. Differentiating $\Psi(\tau(p), \xi(p)) \equiv 0$, and using equation (3.87), gives us that

$$0 = \frac{\partial \Psi}{\partial x}\frac{\partial x}{\partial p} + \frac{d\Psi}{dt}\frac{\partial \tau}{\partial p}. \tag{3.89}$$

Lastly, differentiating the identity $\Omega(\tau(p), \xi(p), \nu(p)) \equiv 0$ and using the formulas from Lemma 3.5.1 yields

$$\begin{aligned}
0 &= \frac{\partial \Omega}{\partial \tau}\frac{\partial \tau}{\partial p} + \frac{\partial \Omega}{\partial \xi}\frac{\partial \xi}{\partial p} + \frac{\partial \Omega}{\partial \nu^T}\frac{\partial \nu^T}{\partial p} \\
&= \left[\frac{\partial H}{\partial t} + \frac{d}{dt}\left(\frac{\partial \Upsilon}{\partial t}\right)\right]\frac{\partial \tau}{\partial p} + \frac{\partial \Omega}{\partial \xi}\left(\frac{\partial x}{\partial p} + f\frac{\partial \tau}{\partial p}\right) + \left(\frac{d\Psi}{dt}\right)^T\frac{\partial \nu^T}{\partial p} \\
&= \frac{\partial \Omega}{\partial \xi}\frac{\partial x}{\partial p} + \frac{\partial \nu}{\partial p}\frac{d\Psi}{dt} + \left[\frac{\partial H}{\partial t} + \frac{d}{dt}\left(\frac{\partial \Upsilon}{\partial t}\right) + \left(\frac{\partial H}{\partial x} + \frac{d}{dt}\left(\frac{\partial \Upsilon}{\partial x}\right)\right)f\right]\frac{\partial \tau}{\partial p}.
\end{aligned}$$

The coefficient multiplying $\frac{\partial \tau}{\partial p}$ in this equation can be expressed in a simpler form. By differentiating Υ along the trajectory in time, we have that

$$\begin{aligned}
\frac{d^2\Upsilon}{dt^2} &= \frac{d}{dt}\left(\frac{d\Upsilon}{dt}\right) = \frac{d}{dt}\left(\frac{\partial \Upsilon}{\partial t} + \frac{\partial \Upsilon}{\partial x}\frac{dx}{dt}\right) \\
&= \frac{d}{dt}\left(\frac{\partial \Upsilon}{\partial t}\right) + \frac{d}{dt}\left(\frac{\partial \Upsilon}{\partial x}\right)f + \frac{\partial \Upsilon}{\partial x}\frac{d^2x}{dt^2} \\
&= \frac{d}{dt}\left(\frac{\partial \Upsilon}{\partial t}\right) + \frac{d}{dt}\left(\frac{\partial \Upsilon}{\partial x}\right)f + \lambda\ddot{x}. \qquad (3.90)
\end{aligned}$$

Hence, it follows that

$$\frac{\partial H}{\partial t} + \frac{d}{dt}\left(\frac{\partial \Upsilon}{\partial t}\right) + \left(\frac{\partial H}{\partial x} + \frac{d}{dt}\left(\frac{\partial \Upsilon}{\partial x}\right)\right)f = \frac{\partial H}{\partial t} + \frac{\partial H}{\partial x}f + \frac{d^2\Upsilon}{dt^2} - \lambda\ddot{x}. \qquad (3.91)$$

Similarly, using equation (3.90) while computing the total time derivative of the function, Ω, along a trajectory gives the same result:

$$\begin{aligned}
\frac{d\Omega}{dt} &= \frac{dH}{dt} + \frac{d}{dt}\left(\frac{\partial \Upsilon}{\partial t}\right) \\
&= \frac{\partial H}{\partial t} + \frac{\partial H}{\partial \lambda^T}\frac{d\lambda^T}{dt} + \frac{\partial H}{\partial x}\frac{dx}{dt} + \frac{\partial H}{\partial u}\frac{du}{dt} + \left[\frac{d^2\Upsilon}{dt^2} - \frac{d}{dt}\left(\frac{\partial \Upsilon}{\partial x}\right)f - \frac{\partial \Upsilon}{\partial x}\frac{d^2x}{dt^2}\right] \\
&= \frac{\partial H}{\partial t} + f^T\dot{\lambda}^T + \frac{\partial H}{\partial x}f + \frac{d^2\Upsilon}{dt^2} - \dot{\lambda}f - \lambda\ddot{x} \\
&= \frac{\partial H}{\partial t} + \frac{\partial H}{\partial x}f + \frac{d^2\Upsilon}{dt^2} - \lambda\ddot{x}. \qquad (3.92)
\end{aligned}$$

Consequently, the coefficient multiplying $\frac{\partial \tau}{\partial p}$ is simply given by this total derivative, $\frac{d\Omega}{dt}$. Hence,

$$0 = \frac{\partial \Omega}{\partial \xi}\frac{\partial x}{\partial p} + \frac{\partial \nu}{\partial p}\frac{d\Psi}{dt} + \frac{d\Omega}{dt}\frac{\partial \tau}{\partial p}. \tag{3.93}$$

In summary, we have verified the following identities between the partial derivatives of the time, state and multipliers at the final time:

Proposition 3.5.2. *In the hypersurface $\tilde{N}$ the following relations hold identically in p:*

$$\begin{pmatrix} \frac{\partial \lambda^T}{\partial p}(\tau(p),p) \\ \\ 0 \\ \\ 0 \end{pmatrix} = \begin{pmatrix} \frac{\partial^2 \Upsilon}{\partial x^2} & \left(\frac{\partial \Psi}{\partial x}\right)^T & \left(\frac{\partial \Omega}{\partial \xi}\right)^T \\ \\ \frac{\partial \Psi}{\partial x} & 0 & \frac{d\Psi}{dt} \\ \\ \frac{\partial \Omega}{\partial \xi} & \left(\frac{d\Psi}{dt}\right)^T & \frac{d\Omega}{dt} \end{pmatrix} \begin{pmatrix} \frac{\partial x}{\partial p}(\tau(p),p) \\ \\ \frac{\partial \nu^T}{\partial p}(p) \\ \\ \frac{\partial \tau}{\partial p}(p) \end{pmatrix}. \tag{3.94}$$

The partial derivatives of Ψ are evaluated at $(\tau(p), \xi(p))$ and the partial derivatives of Ω and Υ are evaluated at $\omega(p) = (\tau(p), \xi(p), \nu(p))$. □

While the notation in terms of the function Ω and its partial and total derivatives is convenient in the sense that it gives compact expressions, equations (3.86) and (3.92) are more useful for computation.

In the *backward sweep method*, the relations in Proposition 3.5.2 are propagated backward from the terminal condition. Let $S = S(t,p) \in \mathbb{R}^{n\times n}$ be the solution to the matrix Riccati differential equation

$$\dot{S} + Sf_x + f_x^T S + H_{xx} - (Sf_u + H_{xu})H_{uu}^{-1}(H_{ux} + f_u^T S) \equiv 0, \tag{3.95}$$

with terminal condition

$$S(\tau(p),p) = \frac{\partial^2 \Upsilon}{\partial x^2}(\omega(p)). \tag{3.96}$$

Here, and below, all partial derivatives of f and H are evaluated along the extremal $\Gamma_p = (x(\cdot,p),u)\cdot,p),\lambda(\cdot,p))$. The Riccati equation (3.95) can equivalently be expressed in the form

$$\dot{S} + S\left(f_x - f_u H_{uu}^{-1}H_{ux}\right) + \left(f_x - f_u H_{uu}^{-1}H_{ux}\right)^T S - Sf_u H_{uu}^{-1} f_u^T S + H_{xx} - H_{xu}H_{uu}^{-1}H_{ux} \equiv 0.$$

The local solution, S, to this Riccati equation with a terminal condition, (3.96), will be used to desingularize the transversality conditions near the terminal point. Given S defined on an open interval I_p that contains $\tau(p)$, there exist solutions $R = R(t,p) \in \mathbb{R}^{(n-k)\times n}$ and $r \in (\mathbb{R}^n)^*$ to the linear differential equations,

$$\dot{R} = R\left(-f_x + f_u H_{uu}^{-1} H_{ux} + f_u H_{uu}^{-1} f_u^T S\right) \tag{3.97}$$

$$\dot{r} = r\left(-f_x + f_u H_{uu}^{-1} H_{ux} + f_u H_{uu}^{-1} f_u^T S\right), \tag{3.98}$$

with terminal conditions

$$R(\tau(p),p) = \frac{\partial \Psi}{\partial x}(\tau(p),\xi(p)) \qquad \text{and} \qquad r(\tau(p),p) = \frac{\partial \Omega}{\partial \xi}(\omega(p)). \tag{3.99}$$

Furthermore, let $Q = Q(t,p) \in \mathbb{R}^{(n-k)\times(n-k)}$, $q = q(t,p) \in \mathbb{R}^{n-k}$ and $a = a(t,p) \in \mathbb{R}$ denote the following integrals:

$$\dot{Q} = R f_u H_{uu}^{-1} f_u^T R^T, \qquad \dot{q} = R f_u H_{uu}^{-1} f_u^T r^T, \qquad \dot{a} = r f_u H_{uu}^{-1} f_u^T r^T, \tag{3.100}$$

with terminal conditions

$$Q(\tau(p),p) = 0, \qquad q(\tau(p),p) = \frac{d\Psi}{dt}(\tau(p),\xi(p)), \qquad a(\tau(p),p) = \frac{d\Omega}{dt}(\omega(p)). \tag{3.101}$$

If we define the time varying matrices, (where, as always, all the partial derivatives are evaluated along the extremals),

$$A = f_x - f_u H_{uu}^{-1} H_{ux}, \qquad B = f_u H_{uu}^{-1} f_u^T, \qquad \text{and} \qquad C = H_{xx} - H_{xu} H_{uu}^{-1} H_{ux}, \tag{3.102}$$

these equations can also be expressed in the form,

$$\dot{S} + SA + A^T S - SBS + C = 0, \tag{3.103}$$

$$\dot{R} = R(-A + BS), \qquad \dot{r} = r(-A + BS), \tag{3.104}$$

$$\dot{Q} = RBR^T, \qquad \dot{q} = RBr^T, \qquad \dot{a} = rBr^T. \tag{3.105}$$

Defining

$$\mathcal{Q}(t,p) = \begin{pmatrix} Q(t,p) & q(t,p) \\ \\ q^T(t,p) & a(t,p) \end{pmatrix} \qquad \text{and} \qquad \mathcal{R}(t,p) = \begin{pmatrix} R(t,p) \\ \\ r(t,p) \end{pmatrix}, \tag{3.106}$$

these equations simply become

$$\dot{\mathcal{R}} = \mathcal{R}(-A + BS) \qquad \text{and} \qquad \dot{\mathcal{Q}} = \mathcal{R}B\mathcal{R}^T. \tag{3.107}$$

Theorem 3.5.1. ***(backward sweep)*** *For all $t \in I_p$ we have that*

$$\begin{pmatrix} \frac{\partial \lambda^T}{\partial p}(t,p) \\ \\ 0 \\ \\ 0 \end{pmatrix} = \begin{pmatrix} S(t,p) & R^T(t,p) & r^T(t,p) \\ \\ R(t,p) & Q(t,p) & q(t,p) \\ \\ r(t,p) & q^T(t,p) & a(t,p) \end{pmatrix} \begin{pmatrix} \frac{\partial x}{\partial p}(t,p) \\ \\ \frac{\partial \nu^T}{\partial p}(p) \\ \\ \frac{\partial \tau}{\partial p}(p) \end{pmatrix}. \tag{3.108}$$

Proof. Define

$$\begin{aligned} \Delta_1(t,p) &= \frac{\partial \lambda^T}{\partial p}(t,p) - S(t,p)\frac{\partial x}{\partial p}(t,p) - \frac{\partial \nu}{\partial p}(p)R(t,p) - r^T(t,p)\frac{\partial \tau}{\partial p}(p), \\ \Delta_2(t,p) &= R(t,p)\frac{\partial x}{\partial p}(t,p) - \frac{\partial \nu}{\partial p}(p)Q(t,p) - q(t,p)\frac{\partial \tau}{\partial p}(p), \\ \Delta_3(t,p) &= r(t,p)\frac{\partial x}{\partial p}(t,p) - \frac{\partial \nu}{\partial p}(p)q(t,p) - a(t,p)\frac{\partial \tau}{\partial p}(p). \end{aligned}$$

Fix the parameter p. It follows from Proposition 3.5.2 that $\Delta_i(\tau(p),p) = 0$ for $i = 1,2,3$. Hence the result follows by verifying that $\frac{d\Delta_i}{dt}(t,p) \equiv 0$ for all $t \in I_p$ and $i = 1,2,3$. A direct computation shows that the differential equations on S, R, r, Q, q and a have been defined in a way so that this holds (see also [34], [50]).

3.6 Sufficient Conditions for a Local Minimum

We now use the backward sweep to establish sufficient conditions for a strong local minimum. It follows from Corollary 3.5.1 that the controlled reference trajectory, $(x(\cdot,p),u(\cdot,p))$, corresponding to the parameter value, p, is a relative extremum over the interval $[t_0,\tau(p)]$, if the matrix, $\frac{\partial x}{\partial p}(\cdot,p)$, is nonsingular over the interval, $[t_0,\tau(p))$, with the interval open at the end-point. In this case, it follows, from the general theory presented in section 3.3, that the Hessian matrix of the value function $V^{\mathcal{E}}$ of the canonical parameterized field of extremals is given by

$$\frac{\partial V^{\mathcal{E}}}{\partial x^2}(t,x(t,p)) = \frac{\partial \lambda^T}{\partial p}(t,p)\left(\frac{\partial x}{\partial p}(t,p)\right)^{-1} = S^{\#}(t,p) \tag{3.109}$$

with $S^{\#}(t,p)$ defined by the last relation. This matrix thus exists on $[t_0,\tau(p))$ and it is a classical result (and a matter of direct verification) that it is a solution of the Riccati differential equation, (3.95), along $(x(t,p),u(t,p),\lambda(t,p))$. This is a direct consequence of the variational equations, (3.63).

However, $S^{\#}(t,p)$ and $S(t,p)$ are different. For optimal control problems with terminal constraints, the solution $S^{\#}(t,p)$ blows up in certain directions at the terminal time, since the matrix, $\frac{\partial x}{\partial p}(t,p)$, becomes singular as $t\to\tau(p)$. The matrix, S, desingularizes the behavior of $S^{\#}(t,p)$ near the terminal time, but it is the matrix $S^{\#}(t,p)$, (not $S(t,p)$), which matters for conjugate points and local optimality. The following statement is classical (*e.g.*, see Proposition 2.4.1 in [50]):

Proposition 3.6.1. *Suppose $t_1<\tau(p)$ and the matrix $\frac{\partial x}{\partial p}(t_1,p)$ is nonsingular. Let*

$$\sigma = \inf\left\{t : \frac{\partial x}{\partial p}(s,p) \text{ is nonsingular for all } s\in[t,t_1]\right\}.$$

Then $\sigma<t_0$ if and only if the solution $S^{\#}(t,p)$ to the Riccati matrix differential equation (3.95) along $(x(t,p),u(t,p),\lambda(t,p))$ with terminal condition

$$S^{\#}(t_1,p) = \frac{\partial \lambda^T}{\partial p}(t_1,p)\left(\frac{\partial x}{\partial p}(t_1,p)\right)^{-1}$$

exists over the full interval $[t_0, t_1]$. *In this case, for all such times* t *we have that*

$$S^{\#}(t,p) = \frac{\partial \lambda^T}{\partial p}(t,p)\left(\frac{\partial x}{\partial p}(t,p)\right)^{-1}.$$

Thus the 'first' time σ *(when integrated backward) where the matrix* $\frac{\partial x}{\partial p}(\sigma,p)$ *becomes singular is the 'first' time where the solution* $S^{\#}(t,p)$ *has a finite escape.* □

The existence of the solutions $S^{\#}(t,p)$ and $S(t,p)$ over the interval $[t_0, \tau(p))$ is not equivalent. The solution, $S(t,p)$, which has the finite terminal condition, $\frac{\partial^2 \Upsilon}{\partial x^2}(\omega(p))$, may blow up at a time $\tilde{\sigma} \in (t, \tau(p))$ while the flow of extremals remains injective, and the solution $S^{\#}(\tilde{\sigma}, p)$ is well-defined. A classical example of this is the problem of connecting two points, P and Q, on the sphere $S^2 \subset \mathbb{R}^3$, with a curve of shortest length (see [34, Example 2, Sect. 6.3]). Thus, finite explosion times of the solution $S(t,p)$ do not necessarily correspond to conjugate points. When the flow mapping undergoes singularities, which are typically fold points, these are related to the invertibility of the matrix $\frac{\partial x}{\partial p}(\cdot, p)$.

The matrix solution, $S(t,p)$, desingularizes the flow of extremals near the terminal manifold. Clearly, this matrix is well-defined over a sufficiently small interval, $[t_1, \tau(p)]$, and this allows us to separate the behavior at the terminal point from the behavior over the full interval. After ensuring that the matrix $\frac{\partial x}{\partial p}(\cdot, p)$ is non-singular over a small interval, $[t_1, \tau(p))$, we can revert to the classical result above.

Proposition 3.6.2. *Suppose the solution* $S(\cdot, p)$ *to the Riccati differential equation (3.95) with terminal condition (3.96) exists on the interval* $[t_1, \tau(p)]$. *If the matrix* $\mathcal{Q}(t,p)$ *is non-singular for* $t \in [t_1, \tau(p))$, *then also the matrix* $\frac{\partial x}{\partial p}(t,p)$ *is nonsingular for* $t \in [t_1, \tau(p))$.

Proof. Suppose $\frac{\partial x}{\partial p}(s,p)$ is singular for some time $s \in [t_1, \tau(p)]$. Then, there exists a nonzero vector, z, in the null-space of this matrix, $\frac{\partial x}{\partial p}(s,p)z = 0$. We claim that

$$\begin{pmatrix} \frac{\partial \nu^T}{\partial p}(p) \\ \\ \frac{\partial \tau}{\partial p}(p) \end{pmatrix} z \neq 0.$$

If this vector vanishes, it follows from Theorem 3.5.1 that also $\frac{\partial \lambda^T}{\partial p}(s,p)z = 0$. But then $\frac{\partial \lambda^T}{\partial p}(t,p)$ and $\frac{\partial x}{\partial p}(t,p)$ are solutions to the homogenous linear differential equation (3.63), which vanish for $t = s$. Hence, they vanish identically.

At the terminal point, we thus have

$$\frac{\partial \xi}{\partial p}(p)z = \left(\frac{\partial x}{\partial t}(\tau(p),p)\frac{\partial \tau}{\partial p}(p) + \frac{\partial x}{\partial p}(\tau(p),p)\right) z = 0.$$

This implies that the columns of the matrix $\frac{\partial \omega}{\partial p}(p)$ are linearly dependent. This contradicts the fact that ω is a local differomorphism on $\tilde{N}$, which implies that

$$\frac{\partial \omega}{\partial p}(p) = \left(\frac{\partial \xi}{\partial p}(p), \frac{\partial \nu^T}{\partial p}(p), \frac{\partial \tau}{\partial p}(p)\right)^T \tag{3.110}$$

has rank n.

Having proved the claim, the relation

$$\mathcal{Q}(t,p)\begin{pmatrix} \frac{\partial \nu^T}{\partial p}(p) \\ \\ \frac{\partial \tau}{\partial p}(p) \end{pmatrix} z = -\mathcal{R}(t,p)\frac{\partial x}{\partial p}(s,p)z = 0 \tag{3.111}$$

implies that the matrix $\mathcal{Q}(t,p)$ is singular. □

If the matrix, $\mathcal{R}(t,p)$, has maximal rank $n-k+1$ at the terminal time, $\tau(p)$, then the invertibility of $\mathcal{Q}(t,p)$ is equivalent to the invertibility of $\frac{\partial x}{\partial p}(t,p)$. For, $\mathcal{R}(t,p)$ is the solution to the homogenous linear matrix differential equation (3.104), and thus it has constant rank for all times t. If the rank is maximal and $\frac{\partial x}{\partial p}(t,p)$ is nonsingular, it follows that the product

$$\mathcal{Q}(t,p)\begin{pmatrix} \frac{\partial \nu^T}{\partial p}(p) \\ \\ \frac{\partial \tau}{\partial p}(p) \end{pmatrix}$$

is of full rank and thus each factor is of rank $n+1-k$. This implies that $\mathcal{Q}(t,p)$ is nonsingular, and also the mapping $p \mapsto \left(\frac{\partial \nu^T}{\partial p}(p), \frac{\partial \tau}{\partial p}(p)\right)^T$ is of maximal rank. In particular, in this case

the multiplier ν and the terminal time τ can be introduced as free parameters with the remaining $k-1$ coordinates made from states on the manifold, $\tilde{N}$.

If the matrix $\mathcal{Q}(t,p)$ is nonsingular over $[t_1,\tau(p))$, then for $t \in [t_1,\tau(p))$ it follows from Theorem 3.5.1 that

$$\mathcal{Q}^{-1}(t,p)\mathcal{R}(t,p) = -\begin{pmatrix} \frac{\partial \nu^T}{\partial p}(p) \\ \\ \frac{\partial \tau}{\partial p}(p) \end{pmatrix} \left(\frac{\partial x}{\partial p}(t,p)\right)^{-1}$$

and thus

$$\begin{aligned} S^{\#}(t,p) &= S(t,p) - \mathcal{R}^T(t,p)\mathcal{Q}^{-1}(t,p)\mathcal{R}(t,p) \\ &= S(t,p) - \left(R^T(t,p), r^T(t,p)\right) \begin{pmatrix} Q(t,p) & q(t,p) \\ \\ q^T(t,p) & a(t,p) \end{pmatrix}^{-1} \begin{pmatrix} \frac{\partial \nu^T}{\partial p}(p) \\ \\ \frac{\partial \tau}{\partial p}(p) \end{pmatrix}. \end{aligned} \tag{3.112}$$

This formula then defines $S^{\#}(t_1,p)$ and we can use Proposition 3.6.2 to compute conjugate points for times $t < t_1$.

The following Lemma describes the inverse of $\mathcal{Q}$ in terms of its principal minor $Q(t,p)$:

Lemma 3.6.1. *The matrix $\mathcal{Q}(t,p)$ is nonsingular if and only if one of the following two conditions are satisfied: (i) $Q(t,p)$ is nonsingular and $a(t,p) \neq q^T(t,p)Q^{-1}(t,p)q(t,p)$ or (ii) the null space of $Q(t,p)$ is 1-dimensional and if $z(t,p)$ is a basis vector for this null-space, then $q^T(t,p)z(t,p) \neq 0$.*

Proof. For notational simplicity, we drop the argument (t,p). If the rank of Q is full, then we have the decomposition

$$\mathcal{Q} = \begin{pmatrix} Q & q \\ \\ q^T & a \end{pmatrix} = \begin{pmatrix} Q & 0 \\ \\ q^T & 1 \end{pmatrix} \begin{pmatrix} \mathrm{Id} & Q^{-1}q \\ \\ 0 & a - q^TQ^{-1}q \end{pmatrix}.$$

In this case, $\mathcal{Q}$ is nonsingular if and only if $a \neq q^TQ^{-1}q$.

If the rank of Q is equal to $n-k-1$, then Q has a 1-dimensional kernel and we denote a basis vector for this null-space by z. The matrix $\mathcal{Q}$ is singular if and only if there exists a nonzero vector, $(w,b)^T \in \mathbb{R}^{n-k+1}$, such that

$$0 = \begin{pmatrix} Q & q \\ \\ q^T & a \end{pmatrix} \begin{pmatrix} w \\ \\ b \end{pmatrix} = \begin{pmatrix} Qw + qb \\ \\ q^T w + ab \end{pmatrix}.$$

If $b = 0$, this is equivalent to w being a multiple of z, and that $q^T z = 0$. If $b \neq 0$, then we can normalize $b = -1$, and, as a result, these conditions are equivalent to $q = Qw$ and $a = q^T w$. The first relation again implies that $z^T q = z^T Q w = 0$. Hence, if the rank of Q is $n-k-1$, then the matrix $\mathcal{Q}$ is nonsingular if and only if $z^T q \neq 0$.

Finally, it is clear that $\mathcal{Q}$ is singular if the rank of Q is less that $n-k-1$. This proves the lemma. □

The invertibility of the principal minor $Q(t,p)$ is related to the linearized system's local controllability properties. If $Q(s,p)$ is singular for some $s < \tau(p)$ and z is a vector in its null space, then

$$0 = z^T Q(s,p) z = -\int_s^{\tau(p)} z^T \dot{Q}(t,p) z \; dt = -\int_s^{\tau(p)} z^T R f_u H_{uu}^{-1} f_u^T R^T z \; dt \leq 0,$$

and, thus, since H_{uu} is positive definite, it follows that

$$z^T R(t,p) f_u(t, x(t,p), u(t,p)) \equiv 0 \qquad \text{for all} \quad t \in [s, \tau(p)].$$

Indeed, this argument shows that the matrix $Q = Q(t,p)$ is negative semi definite. It results that $z^T Q(t,p) \equiv 0$ for all $t \in [s, \tau(p)]$ and, furthermore,

$$\frac{d}{dt} z^T q(t,p) = z^T R B r^T = z^T R f_u H_{uu}^{-1} f_u^T \equiv 0,$$

so that $z^T q(t,p)$ is constant.

In particular, if we define $\mu(t,p) = z^T R(t,p)$, then it follows from (3.97) that μ is a nontrivial solution of the linear adjoint equation,

$$\dot{\mu} = z^T R\left(-f_x + f_u H_{uu}^{-1} H_{ux} + f_u H_{uu}^{-1} f_u^T S\right) = -z^T R f_x = -\mu f_x,$$

which satisfies

$$\mu(t,p) f_u(t, x(t,p), u(t,p)) \equiv 0 \qquad \text{for} \quad \text{all} \quad t \in [s, \tau(p)].$$

This connects the invertibility of Q with the following classical characterization for the controllability of a time-varying linear system (*e.g.*, see [35, 38]). A time-varying linear system $\dot{y} = A(t)y + B(t)v$ is controllable over an interval $[\tau, T]$ if and only if, for every nontrivial solution, μ, of the adjoint equation, $\dot{\mu} = -\mu A(t)$, the function, $\mu(t)B(t)$, does not vanish identically on the interval, $[\tau, T]$.

If Q is nonsingular over the interval, $[t_1, \tau(p))$, then the sweep method can be simplified by eliminating the multiplier from the second equation in (3.108). In that scenario,

$$\frac{\partial \nu^T}{\partial p}(p) = -Q^{-1}(t,p)\left(R(t,p)\frac{\partial x}{\partial p}(t,p) + q(t,p)\frac{\partial \tau}{\partial p}(p)\right),$$

and substituting this relation into the first and third equation in (3.108), and again dropping the arguments (t,p) and p gives us that

$$\begin{aligned}\frac{\partial \lambda^T}{\partial p} &= S\frac{\partial x}{\partial p} - R^T Q^{-1}\left(R\frac{\partial x}{\partial p} + q\frac{\partial \tau}{\partial p}\right) + r^T\frac{\partial \tau}{\partial p} \\ &= \left(S - R^T Q^{-1} R\right)\frac{\partial x}{\partial p} + \left(r^T - R^T Q^{-1} q\right)\frac{\partial \tau}{\partial p},\end{aligned}$$

and

$$\begin{aligned}0 &= r\frac{\partial x}{\partial p} - q^T Q^{-1}\left(R\frac{\partial x}{\partial p} + q\frac{\partial \tau}{\partial p}\right) + a\frac{\partial \tau}{\partial p} \\ &= \left(r - q^T Q^{-1} R\right)\frac{\partial x}{\partial p} + \left(a - q^T Q^{-1} q)\right)\frac{\partial \tau}{\partial p}.\end{aligned}$$

Hence, and with all expressions evaluated at (t,p),

$$\frac{\partial \lambda^T}{\partial p} = \left(S - R^T Q^{-1} R - \frac{\left(r - qQ^{-1}R\right)^T \left(r - qQ^{-1}R\right)}{a - q^T Q^{-1} q} \right) \frac{\partial x}{\partial p}. \tag{3.113}$$

If we define

$$\tilde{S} = S - R^T Q^{-1} R, \quad \tilde{r} = r - q^T Q^{-1} R, \quad \text{and} \quad \tilde{a} = a - q^T Q^{-1} q, \tag{3.114}$$

direct calculations verify that $\tilde{S}$ satisfies the same matrix Riccati differential equation (3.95) and $\tilde{r}$ and $\tilde{a}$ obey the same relations as r and a, respectively. Therefore, we have the formulas,

$$\begin{aligned}
\dot{\tilde{r}} &= \dot{r} - \dot{q}^T Q^{-1} R - q^T \frac{d}{dt}\left(Q^{-1}\right) R - q^T Q^{-1} \dot{R} \\
&= r(-A + BS) - (RBr^T)^T Q^{-1} R + q^T Q^{-1} \dot{Q} Q^{-1} R - q^T Q^{-1} R(-A + BS) \\
&= r(-A + BS) - rBR^T Q^{-1} R + q^T Q^{-1} RBR^T Q^{-1} R - q^T Q^{-1} R(-A + BS) \\
&= (r - q^T Q^{-1} R)(-A + BS - BR^T Q^{-1} R) = \tilde{r}(-A + B\tilde{S})
\end{aligned}$$

and

$$\begin{aligned}
\dot{\tilde{a}} &= \dot{a} - \dot{q}^T Q^{-1} q - q^T \frac{d}{dt}\left(Q^{-1}\right) q - q^T Q^{-1} \dot{q} \\
&= rBr^T - (RBr^T)^T Q^{-1} q + q^T Q^{-1} \dot{Q} Q^{-1} q - q^T Q^{-1} RBr^T \\
&= rBr^T - rBR^T Q^{-1} q + q^T Q^{-1} RBR^T Q^{-1} q - q^T Q^{-1} RBr^T \\
&= \left(r - q^T Q^{-1} R\right) B \left(r - q^T Q^{-1} R\right)^T = \tilde{r} B \tilde{r}^T.
\end{aligned}$$

In this notation, we have that $S^{\#} = \tilde{S} - \frac{\tilde{r}^T \tilde{r}}{\tilde{a}}$. In accordance with Lemma 3.6.1, $\mathcal{Q}(t,p)$ is nonsingular and $S^{\#}$ exists if and only if $\tilde{a} \neq 0$. We therefore have the following statement:

Corollary 3.6.1. *Suppose the solution $S(\cdot,p)$ to the Riccati differential equation (3.95) with terminal condition (3.96) exists on the interval $[t_1, \tau(p)]$. If, for $t \in [t_1, \tau(p))$, the matrix $Q(t,p)$ is nonsingular and $a(t,p) \neq q^T(t,p) Q^{-1}(t,p) q(t,p)$, then $\frac{\partial x}{\partial p}(t,p)$ is nonsingular over the interval $[t_1, \tau(p))$ and, with all expressions evaluated at (t,p) we have that*

$$S^{\#} = \tilde{S} - \frac{\tilde{r}^T \tilde{r}}{\tilde{a}} = S - R^T Q^{-1} R - \frac{\left(r - qQ^{-1}R\right)^T \left(r - qQ^{-1}R\right)}{a - q^T Q^{-1} q}. \tag{3.115}$$

The backward sweep of the variational equations will also be simplified if the last diagonal entry a in $\mathcal{Q}$ does not vanish [34]. This is the only special case considered in the classical engineering literature. It is a second-order necessary condition for optimality on the terminal time that $a(\tau(p), p) \geq 0$. However, it is not a necessary condition for optimality that $a(t, p)$ remains positive as the extremals are integrated backward. But, if $a(\tau(p), p) > 0$, then, on a sufficiently small interval, $[t_1, \tau(p))$, we can simply solve the equation which defines the transversality condition on the terminal time (*i.e.*, the third equation in (3.108)) for the partial derivative, $\frac{\partial \tau}{\partial p}(p)$, and reduce the calculations to the first two terms. This process involves the following Schur complements of the matrices S, R and Q:

$$\bar{S} = S - \frac{r^T r}{a}, \quad \bar{R} = R - \frac{qr}{a}, \quad \text{and} \quad \bar{Q} = Q - \frac{qq^T}{a}. \tag{3.116}$$

As long as $a(t, p) > 0$, it follows from the third relation in (3.108) that

$$\frac{\partial \tau}{\partial p}(p) = -\frac{1}{a(t,p)} \left(r(t,p) \frac{\partial x}{\partial p}(t,p) + q^T(t,p) \frac{\partial \nu^T}{\partial p}(p) \right).$$

Substituting this into the first two relations, and, dropping the arguments (t, p) and p, gives us that

$$\begin{aligned} \frac{\partial \lambda^T}{\partial p} &= S \frac{\partial x}{\partial p} + R^T \frac{\partial \nu^T}{\partial p} - \frac{r^T}{a} \left(r \frac{\partial x}{\partial p} + q^T \frac{\partial \nu^T}{\partial p} \right) & (3.117) \\ &= \left(S - \frac{r^T r}{a} \right) \frac{\partial x}{\partial p} + \left(R^T - \frac{r^T q^T}{a} \right) \frac{\partial \nu^T}{\partial p} = \bar{S} \frac{\partial x}{\partial p} + \frac{\partial \nu}{\partial p} \bar{R} & (3.118) \end{aligned}$$

and

$$\begin{aligned} 0 &= R \frac{\partial x}{\partial p} + Q \frac{\partial \nu^T}{\partial p} - \frac{q}{a)} \left(r \frac{\partial x}{\partial p} + q^T \frac{\partial \nu^T}{\partial p} \right) & (3.119) \\ &= \left(R - \frac{qr}{a} \right) \frac{\partial x}{\partial p} + \left(Q - \frac{qq^T)}{a} \right) \frac{\partial \nu^T}{\partial p} = \bar{R} \frac{\partial x}{\partial p} + \frac{\partial \nu}{\partial p} \bar{Q}. & (3.120) \end{aligned}$$

In matrix form, it follows that

$$\begin{pmatrix} \frac{\partial \lambda^T}{\partial p}(t,p) \\ \\ 0 \end{pmatrix} = \begin{pmatrix} \bar{S}(t,p) & \bar{R}^T(t,p) \\ \\ \bar{R}(t,p) & \bar{Q}(t,p) \end{pmatrix} \begin{pmatrix} \frac{\partial x}{\partial p}(t,p) \\ \\ \frac{\partial \nu^T}{\partial p}(p) \end{pmatrix}. \tag{3.121}$$

These equations are identical to the equations for a fixed terminal time (*c.f.*, [50, Section 5.3.2]). The matrices $\bar{S}$, $\bar{R}$ and $\bar{Q}$ satisfy the same matrix differential equations as the original terms S, R and Q. Only the terminal values have changed. For example, using the notation (3.102), we have that

$$\begin{aligned}
\dot{\bar{S}} &= \dot{S} - \frac{1}{a}\left(\dot{r}^T r + r^T \dot{r}\right) + \frac{\dot{a}}{a} r^T r \\
&= -SA - A^T S + SBS - C - \frac{1}{a}\left((-A + BS)^T r^T r + r^T r(-A + BS)\right) + \frac{rBr^T}{a} r^T r \\
&= -\left(S - \frac{r^T r}{a}\right) A - A^T \left(S - \frac{r^T r}{a}\right) + \left(S - \frac{r^T r}{a}\right) B \left(S - \frac{r^T r}{a}\right) - C \\
&= -\bar{S}A - A^T \bar{S} + \bar{S}B\bar{S} - C.
\end{aligned}$$

Therefore, all the considerations from the case with a fixed terminal time, T, carry over. Additionally, as long as $a(t,p) \neq 0$, the matrix, $\mathcal{Q}(t,p)$, is nonsingular if and only if the matrix, $\bar{Q}(t,p)$, is nonsingular. This is immediate from the decomposition,

$$\begin{pmatrix} Q & q \\ q^T & a \end{pmatrix} = \begin{pmatrix} Q - \frac{qq^T}{a} & \frac{q}{a} \\ 0 & 1 \end{pmatrix} \begin{pmatrix} \mathrm{Id} & 0 \\ q^T & a \end{pmatrix}.$$

Thus, we also have the following statement:

Corollary 3.6.2. [34] *If $a(\tau(p), p) > 0$ and $\bar{Q}(t,p)$ is nonsingular over a sufficiently small interval $[t_1, \tau(p)]$, then $\frac{\partial x}{\partial p}(t,p)$ is nonsingular over $[t_1, \tau(p))$ and we have that*

$$\begin{aligned}
S^{\#}(t,p) &= \bar{S}(t,p) + \bar{R}^T(t,p) \frac{\partial \nu^T}{\partial p}(p) \left(\frac{\partial x}{\partial p}(t,p)\right)^{-1} \\
&= \bar{S}(t,p) - \bar{R}^T(t,p) \bar{Q}(t,p)^{-1} \bar{R}(t,p).
\end{aligned} \tag{3.122}$$

The problem is equivalent to a formulation with fixed terminal time, T. As long as $a(t,p)$ remains positive, one is able to solve the equation that defines the transversality condition for the terminal time, τ, as a function of ξ and ν.

As a result, the parameterization can be achieved through $p = (\xi, \nu)$ and $\tau = \tau(p)$; in other words, *we can choose coordinates on the terminal manifold, N, and solve for the terminal time, τ.*

Thus, both Q is nonsingular and $a \neq 0$, then we have that

$$\det \mathcal{Q}(t,p) = \det \bar{Q}(t,p)a(t,p) = \det Q(t,p)\tilde{a}(t,p), \tag{3.123}$$

and the two conditions derived above are equivalent. Note that $\bar{Q} = Q - \frac{qq^T}{a}$ is a rank 1 correction of Q and, if Q is nonsingular, then $\bar{Q}$ is invertible if and only if $a \neq q^T Q^{-1} q$.

3.7 A Summary of the Novel Contribution

In this chapter, we developed sufficient conditions for the local optimality of a controlled reference trajectory for an optimal control problem with terminal constraints and free terminal time. Mathematically, this problem is more complex than when the terminal time is fixed. In the engineering literature, [34], there exist formal approaches to this problem; by means of making unnecessary assumptions, these reduce the problem and calculations to the much simpler problem with a fixed final time.

This, however, is unnecessary. Rather, we use a desingularization of the flow of extremals near the terminal point to establish a general framework. In particular, we establish the role of the matrix, $\mathcal{Q}$, in the construction and of the solution, $S^{\#}$, to the Riccati equation (3.65) with the correct terminal condition.

Chapter 4

A Mathematical Formulation of Flight Control

This chapter review the basics of flight and aerodynamics for the purpose of introducing a mathematical model of flight control. The discussion of basic aerodynamics comes from [3] and continuum mechanics are found in [5]. The discussion of the basics of flight dynamics are found in [55].

It discusses the basic terms modeled in the equations and how they are practically calculated. The F-16 model is taken from the work of [43]. The chapter also derives a simplified version of flight path angle dynamics. It explains how a flight control system controls the flight path angle of the aircraft. To facilitate the optimization problem, the dynamics are simplified by reducing the state space. In the chapter that follows, perturbation feedback control is applied to the simplified model derived in this chapter.

4.1 The Dynamics of Flight Control

A flight control system controls flight.

Flight is a dynamics described by Newton's laws:

$$m\dot{V} = \omega \times V + F + mg \tag{4.1}$$

$$J\dot{\omega} = -\omega \times J\omega + M. \tag{4.2}$$

According to (4.1) and (4.2), a flight control system controls the aircraft states of flight, which are the velocity, V, and angular velocities, ω, in the so-called body axes. Body axes are Euclidean coordinates fixed to the aircraft. The parameters m and J are the aircraft's mass and inertia matrix. The force F and torque M are external influences that induce accelerations. The function g represents gravity.

The dynamics, at first, seem mundane and conventional. After all, the equations (4.1) and (4.2) are generic. They describe *any* rigid body with coordinates on the body in a gravity field with 6 degrees of freedom.

The forces, F, and moments, M, express the complicated, fascinating, and unique equations expressing the aerodynamic and propulsive forces on an aircraft; we will collectively refer to them as the aerodynamics.

For example, the propulsion of an aircraft through the air results from internal aerodynamic forces and the resulting torques. Internal combustion and airflow, driven by components like fans, turbomachinery, and nozzles, cause these forces. The aircraft engine accelerates the air inside the aircraft and propels the plane through the sky. At the aft end of the aircraft, plumes of combusting fuel may spurt from nozzles into the exhaust, igniting afterburners that allow certain fighter aircraft to aggressively accelerate.

The term F in (4.1) contains the net propulsive force on the aircraft, the thrust, T.

4.2 Basic Aerodynamics

The shape of an aircraft determines its aerodynamics. Aerodynamics is the study of the fluid mechanics of lift and drag, forces which arise whenever a fluid flows past a body. The aircraft's shape maximizes the lift force and minimizes the drag force for the aircraft's design flight condition.

Aerodynamics result from distributed pressure and shear stress on the surface of a body. The net force vector on a body, resolved into components, and with axes defined according to the velocity vector of the body, yields the orientation of the drag axis. The lift axis is perpendicular to the drag axis.

Drag forces oppose the direction of the velocity vector of the body. Their action slows the velocity of a moving body in a fluid. The lift forces act orthogonally to the velocity vector. Lift opposes the force of gravity for a straight-and-level plane flying through the air. Lift "lifts" the aircraft. Drag slows it.

As the aircraft changes orientation and speed, the air pressure distributions around the wings and outer moldline induce lift and drag on the body. The location and magnitude of the net pressure force moves around the aircraft. As a result, the air torques the aircraft in flight.

The Navier-Stokes equations [21] describe the aerodynamic forces of the airflow on the aircraft. These equations are nearly intractable. In principle, predicting the aerodynamic forces and moments, F and M, from these equations requires integration by a computational fluid dynamics (CFD) software. However, practical aerodynamics uses empirical methods to estimate the aerodynamics.

The Navier-Stokes equations are coupled, nonlinear PDE's that relate the density, ρ, pressure, p, Reynold's number, Re, Prandtl Number, Pr, heat flow, q, shear stress,τ, energy, E_t, and velocities in the x, y, and z directions u, v, and w, respectively, for a fluid as follows:

$$0 = \frac{\partial \rho}{\partial t} + \frac{\partial (\rho u)}{\partial x} + \frac{\partial (\rho v)}{\partial y} + \frac{\partial (\rho w)}{\partial z}, \tag{4.3}$$

$$\frac{\partial \rho u}{\partial t} + \frac{\partial \rho u^2}{\partial x} + \frac{\partial \rho uv}{\partial y} + \frac{\partial \rho uw}{\partial z} = -\frac{\partial p}{\partial x} + \frac{1}{Re}\left[\frac{\partial \tau_{xx}}{\partial x} + \frac{\partial \tau_{xy}}{\partial y} + \frac{\partial \tau_{xz}}{\partial z}\right], \tag{4.4}$$

$$\frac{\partial \rho u}{\partial t} + \frac{\partial \rho uv}{\partial x} + \frac{\partial \rho v^2}{\partial y} + \frac{\partial \rho vw}{\partial z} = -\frac{\partial p}{\partial y} + \frac{1}{Re}\left[\frac{\partial \tau_{xy}}{\partial x} + \frac{\partial \tau_{yy}}{\partial y} + \frac{\partial \tau_{yz}}{\partial z}\right], \tag{4.5}$$

$$\frac{\partial \rho w}{\partial t} + \frac{\partial \rho uw}{\partial x} + \frac{\partial \rho uw}{\partial y} + \frac{\partial \rho w^2}{\partial z} = -\frac{\partial p}{\partial z} + \frac{1}{Re}\left[\frac{\partial \tau_{xz}}{\partial x} + \frac{\partial \tau_{yz}}{\partial y} + \frac{\partial \tau_{zz}}{\partial z}\right], \tag{4.6}$$

$$\begin{aligned}
&\frac{\partial E_t}{\partial t} + \frac{\partial u E_t}{\partial x} + \frac{\partial v E_t}{\partial y} + \frac{\partial w E_t}{\partial z} = \\
&-\frac{\partial up}{\partial x} - \frac{\partial vp}{\partial y} - \frac{\partial wp}{\partial z} - \frac{1}{RePr}\left\{\frac{\partial q_x}{\partial x} + \frac{\partial q_y}{\partial y} + \frac{\partial q_z}{\partial z}\right\} \\
&+ \frac{1}{Re}\left\{\frac{\partial}{\partial x}\left(u\tau_{xx} + v\tau_{xy} + w\tau_{xz}\right) + \frac{\partial}{\partial y}\left(u\tau_{xy} + v\tau_{yy} + w\tau_{yz}\right) + \frac{\partial}{\partial z}\left(u\tau_{xz} + v\tau_{yz} + w\tau_{zz}\right)\right\}.
\end{aligned} \tag{4.7}$$

Equation (4.3) represents the equation of continuity that describes how a compressible fluid changes density with velocity. The next three equations apply momentum balance to a fluid, yielding the pressure distribution. The last equation, (4.7), describes the energy balance for the fluid. Boundary conditions on the surface are taken to be the geometry of the body of an aircraft, and boundary conditions at infinity are taken to be the free stream airflow and pressure of the air undisturbed by the body.

These equations inform aircraft design and tend to be used for diagnosing complex problems in flow, but, for the purpose of practical design, assumptions about and approximation to these equations are a first resort. Wind tunnels and system identification are the main tools for empirical estimation of the forces and moments.

A wind tunnel uses the principles of flow similarity or dimensional analysis to simulate airflow at flight conditions. A small-scale model of the aircraft in the simulated airflow applies forces and moments to strain gauges. Scaling the resulting forces and moments yields approximations of those on the full-size aircraft.

These equations (4.3) to (4.7) determine the pressure distribution, p, around a body. Pressure distributions determine forces normal to fluid surface. Surface forces to the body resolve into a coordinate frame aligned with the body. The axial force, A, is parallel to a coordinate frame that is usually a reference line on the body. The normal force, N, is accordingly normal to the axial force. The normal vector of area in the surface integrals, $\mathrm{d}S$, is, by convention, taken to be pointing out of the surface and tangent to the surface, $\mathrm{d}T$.

$$\begin{bmatrix} A \\ N \end{bmatrix} = -\oiint_S p \mathrm{d}S + \oiint_S \tau \mathrm{d}T \tag{4.8}$$

From (4.8), we calculate the lift and drag forces using a coordinate transformation defined by two angles, α and β.

The angle of attack, α, is the angle between the airflow on the body and a reference line in a 2-dimensional flow. When resolved into three dimensions, the angle β is the sideslip, which is the analogous angle of attack in the other axes.

To empirically estimate the unknown functions representing forces and moments, F and M, from flight test measurements, we apply the principles of system identification directly. By using the aircraft's outputs and inputs, we can estimate F and M to gauge the aircraft's true dynamics. Here, the state variables of the aircraft are taken to be the parameters of interest in flight. The equations of motion of an aircraft are taken to be the assumed dynamics.

To give some context to α and β, consider the simplest object of study in aerodynamics, the airfoil. The airfoil is an infinitely long, cross-section of a wing. A symmetric airfoil is perfectly aligned with oncoming airflow. As a result, the airflow generates no lift. It only generates drag, which is due to viscosity. If the orientation of the airfoil changes and increases the angle of attack, both the lift and drag correspondingly increase on the airfoil.

As with most things, ceaselessly increasing the angle of attack does not continue to produce lift. Rather, there are diminishing returns. At some point, the airfoil begins to stall, which is marked by a corresponding decrease in lift and a dramatic increase in drag.

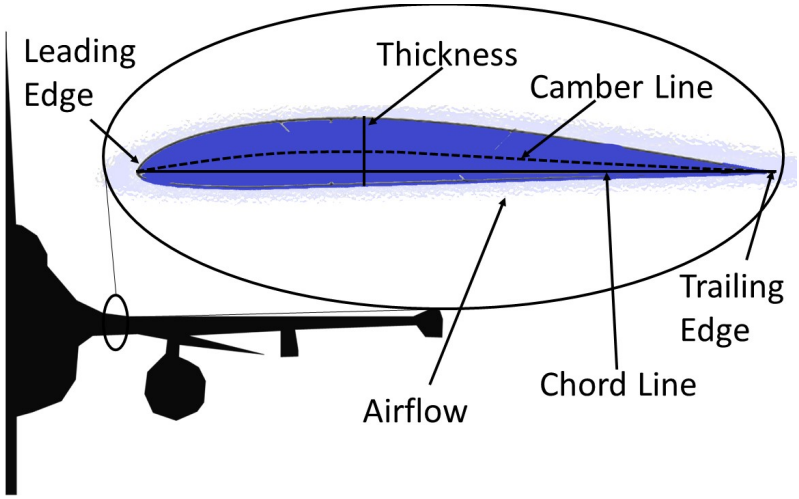

Figure 4.1: A diagram of an airfoil, which is an idealized cross-section of a wing in a 2-dimensional airflow with an infinite length out of the plane of the page. The basic geometry of an airfoil described by its chord, thickness, and mean camber line. The airflow around the airfoil induces forces on the airfoil. By Newton's third law, the airfoil induces forces on the flow. For this reason, the airflow is often depicted moving along a stationary airfoil.

The leading edge is the point, LE, on the airfoil that first impacts the airfoil. The point that last impacts the airfoil is the trailing edge, TE. The angle, θ, parameterizes the curve of the airfoil, where the pressure on the upper section is denoted p_U and the pressure on the

lower section is dubbed p_l. Similarly, The angle of the surface, which is considered positive in a clockwise rotation, parameterizes the shear stress distributions on the upper and lower surfaces, τ_U and τ_L .

The axial and normal forces, A and N, relate to the lift and drag, L and D, through the angle of attack, α :

$$\begin{bmatrix} A \\ N \end{bmatrix} = \int_{LE}^{TE} \begin{bmatrix} \cos\theta & -\sin\theta \\ \sin\theta & \cos\theta \end{bmatrix} \begin{bmatrix} \tau_L \mathrm{d}s_L(1) - \tau_U \mathrm{d}s_U(1) \\ p_U \mathrm{d}s_L(1) - p_L \mathrm{d}s_U(1) \end{bmatrix} \tag{4.9}$$

$$\begin{bmatrix} D \\ L \end{bmatrix} = \begin{bmatrix} \cos\alpha & -\sin\alpha \\ \sin\alpha & \cos\alpha \end{bmatrix} \begin{bmatrix} A \\ N \end{bmatrix} \tag{4.10}$$

In the equations, (1) indicates a 2-dimensional object's depth is of unit dimension. The change in lift and drag associated with the angle of attack results from the change in forces due to the rotated geometry.

The pressure distributions, and shear stress distributions are functions of the angle of attack. Figure 4.2 demonstrates the phenomenon. Precise control of the aircraft angles requires control of the forces and moments along the body of an aircraft as control surfaces. Control surfaces are essentially movable wings, which alter the course of a flying body. The figure depicts the change in the net force as a result of the angle of attack changes for an airfoil.

In the design of an aircraft, each part added to the outer mold line adds drag. As a result, unless a component is "wing like," any increases in the lift are negligible. Additionally, a major difference between a finite wing and an infinite airfoil is the addition of 'induced drag. Induced drag is extra drag associated with increased lift for a finite wing. Most aircraft have a parabolic relationship between drag and lift.

A drag polar is the classical representation of lift versus drag as a function of the angle of attack. Figure 4.3 depicts the drag polar for an F-16. The drag polar also describes another consequence of increasing the angle of attack. Increasing the angle of attack beyond a certain value can stall a lifting body, and lead to a marked increase in drag and a decrease in lift.

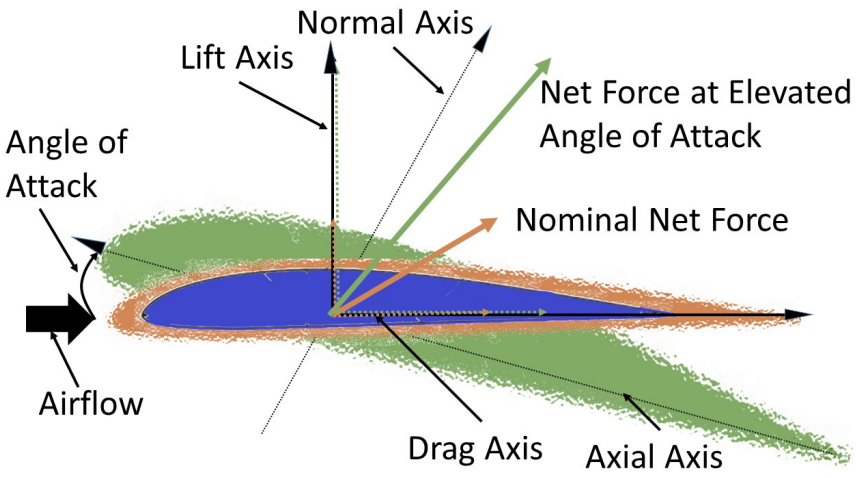

Figure 4.2: A diagram of an airfoil which shows that as the angle of attack of an airfoil changes, the net force components, lift and drag, change their magnitudes.

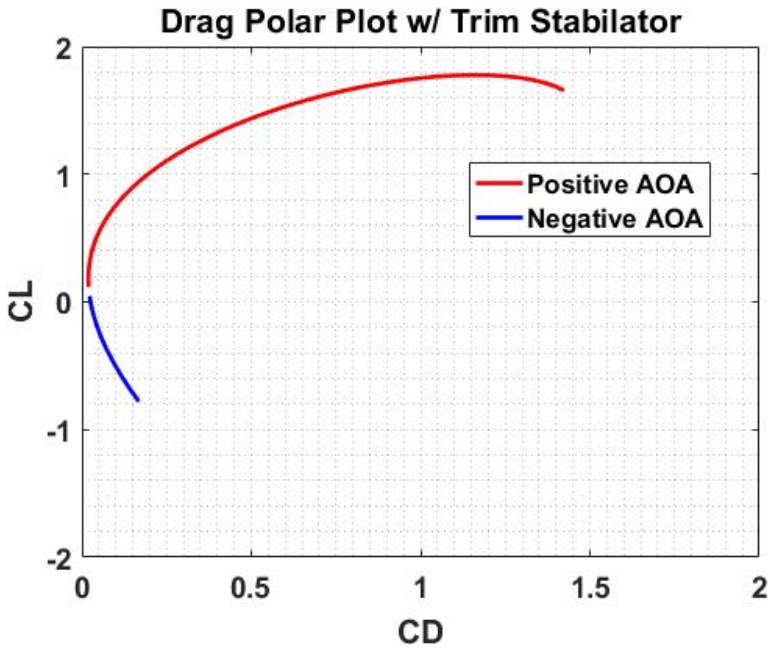

Figure 4.3: A graph of the lift plotted against drag for the trimmed F-16. The variables are a function of the angle of attack. Positive angles of attack increase the lift on the surface until the surface stalls. The stall is the flat part of the graph on the positive AOA locus, which shows that, at some point, drag increases for no corresponding increase in lift. Stall dramatically slows the aircraft and causes the aircraft to lose lift.

4.3 Flow Similarity

Because knowledge of the pressure distribution and velocity distribution is equivalent to knowledge of the lift and drag, determination of solutions to the Navier-Stokes equations is a principle focus of aerodynamics. However, as previously stated, these equation are an intractable partial differential equation. The primary methods of attack are usually approximations, simplifications, or numerical computation. For this reason, engineers often sidestep the solution of the Navier-Stokes equations, and, instead, empirically normalize and nondimensionalize estimates of lift and drag, as functions of many parameters. These parameters describe flow around the body.

The Buckingham Pi theorem [3] shows that the main parameters governing pressure and shear stress distributions are the speed of sound, a, the Mach number, M, the fluid density, ρ, the mean aerodynamic chord, c, the wingspan, b, the wing's planform area, S, the Reynolds number, Re, and the ratio of specific heats, γ. In addition to those parameters already listed, the angle of attack and the angle of sideslip, α and β, respectively, are the angles between a reference axis on the body and the flow. These last two parameters are the most important for flight control.

Dimensionless coefficients describe forces on a body by geometric properties, like angles and lengths, and flow properties, like density and velocity. The most important parameters for flow similarity are the Reynolds numbers and the Mach number. Any two flows around a similarly shaped body will have the same Reynolds and Mach numbers.

A Newtonian fluid's viscosity, $\vec{\tau}_{visc}$ is described by:

$$\tau_{visc} = \mu \left(\frac{\partial v}{\partial x} \right). \tag{4.11}$$

This means that shear stress is proportional to the change in its velocity gradient, $\frac{\partial v}{\partial x}$. The parameter, μ, is called the viscosity coefficient. Viscosity describes the frictional effects of a fluid as particles flow past each other. The Reynold's number is a ratio of inertial to viscous

forces for a body moving in a fluid:

$$Re = \frac{\text{Inertial Forces}}{\text{Viscous Forces}} = \frac{\rho V c}{\mu}, \tag{4.12}$$

where ρ is the fluid density, V is the fluid speed, μ is the viscosity coefficient, and c is a reference length for the body or aircraft.

The Reynolds number, Re, quantifies the relative importance of inertial forces to viscous forces. One infers from the form of the equation, (4.12), that as the Reynolds number of a flow increases, the inertial effects tend to dominate. Low Reynold's number flows are laminar, while high Reynold's number flows are turbulent.

Wind tunnels approximate a flow with an identical Reynolds number to yield a dynamically similar one. The similar flow around a smaller body in a test section of the tunnel imparts forces on the section. Strain gauges measure the force imparted on the miniature body, and a velocity rake measures the velocity distribution downstream of the tunnel.

This combination of the velocity and pressure information is used to estimate the lift and drag forces on the body. The aerodynamic forces on a body are, in general, complicated functions of many parameters. As a result, empirical methods have a distinct advantage over computational approaches.

The dimensionless force coefficients are given in Table 4.1.

Coefficient	Symbol	Dynamic Coefficient	Symbol
X Force Coefficient	C_X	X Force Dynamic Coefficient	C_{X_q}
Z Force Coefficient	C_Z	Z Force Dynamic Coefficient	C_{Z_q}
Pitch Moment Coefficient	C_M	Pitch Damping Coefficient	C_{M_q}

Table 4.1: Table of Coefficients

The most standard way to retrieve force from these dimensionless quantities is to scale the forces by flow properties, dynamic pressure, $\bar{q}$, and reference dimensions, such as wing planform area, S, and the chord, c. It holds that

$$\bar{q} = \frac{1}{2}\rho V^2 \tag{4.13}$$

$$F_X = f_1(\bar{q}, c, S, C_X, C_{X_q}) \tag{4.14}$$

$$F_Z = f_2(\bar{q}, c, S, C_Z, C_{Z_q}) \tag{4.15}$$

$$F_M = f_3(\bar{q}, c, S, C_M, C_{M_q}) \tag{4.16}$$

The dynamic pressure is the pressure of a fluid due to its velocity ignoring compressibility effects. Conventionally, we use this concept rather than the equivalent compressible concept, impact pressure.

4.4 F-16 Aerodynamic Model

The F-16 is currently produced by Lockheed Martin. The United States Air Force is the F-16's primary user. The F-16 was designed as a cheap alternative to the air superiority fight aircraft of the time period, the F-15. The clean aircraft weight is 18,900 lbs, and its maximum take-off weight is 42,300 lbs with stores. This is approximately half of the corresponding weights for the F-15. The aircraft has a wing area of 300 feet squared.

From a control engineer's point of view, the shape of the F-16 causes the aircraft to be statically unstable. Static instability means that small changes in orientation tend to grow if compensating motions do not occur in the flight control surfaces. The advantage of static instability is agility. For a pilot to control the aircraft, an automatic flight control system, called fly-by-wire, automatically neutralizes unstable motions to aid flight.

The aerodynamic model for the F-16 presented in [43] identifies the aircraft's aerodynamics and estimates parameters in a form convenient for the calculations that follow. The equations are described by δ_e, the deflection of the elevator flight surfaces. The terms x_{FS} and x_{ref} are the location of the center of gravity and aerodynamic reference. The aerodynamics are referenced to a fixed point on the aircraft called the aerodynamic reference. The aircraft's center of gravity varies with its loadout.

The model, in which we neglect the damping terms and set $\beta = 0$, estimates the body axis coefficients C_X,C_Z, and C_M as follows:

$$C_X = a_0 + a_1\alpha + a_2\delta_e^2 + a_3\delta_e + a_4\alpha\delta_e + a_5\alpha^2 + a_6\alpha^3, \tag{4.17}$$

$$C_Z = f_0 + f_1\alpha + f_2\alpha^2 + f_3\alpha^3 + f_4\alpha^4 + f_5\delta_e, \tag{4.18}$$

$$\begin{aligned} C_M =& m_0 + m_1\alpha + m_2\delta_e + m_3\alpha\delta_e + m_4\delta_e^2 + m_5\alpha^2\delta_e m_6\delta_e^3 + m_7\alpha\delta_e^2 \\ &+ \left(f_0 + f_1\alpha + f_2\alpha^2 + f_3\alpha^3 + f_4\alpha^4 + f_5\delta_e\right)\left(x_{ref} - x_{FS}\right), \end{aligned} \tag{4.19}$$

with the constants taken from [43].

a_0	-1.943367E-2	f_0	-1.378278E-1	m_0	-2.029370E-2
a_1	2.136104E-1	f_1	-4.211369E0	m_1	4.660702E-2
a_2	-2.903457E-1	f_2	4.775187E0	m_2	-6.012308E-1
a_3	-3.348641E-3	f_3	-1.026225E1	m_3	-8.062977E-2
a_4	-2.060504E-1	f_4	8.399763E1	m_4	8.320429E-2
a_5	6.988016E-1	f_5	-4.354000E-1	m_5	5.018538E-1
a_6	-9.035381E-1			m_6	6.378864E-1
				m_7	4.226356E-1

Table 4.2: Morelli's Parameters for the Global Nonlinear F-16 Model [43]

From here, we can define quantities that are used in the example application. The transformation from the aircraft's body axis to stability axis is as follows:

$$\begin{bmatrix} C_D \\ C_L \end{bmatrix} = \begin{bmatrix} -\cos\alpha & -\sin\alpha \\ \sin\alpha & -\cos\alpha \end{bmatrix} \begin{bmatrix} C_X \\ C_Z \end{bmatrix}. \tag{4.20}$$

The following equations are used in the next chapter in the variational equations and arise from derivatives of the original equations of motion:

$$\frac{\partial C_X}{\partial \alpha} = a_1 + a_4\delta_e + 2a_5\alpha + 3a_6\alpha^2 \qquad \frac{\partial C_Z}{\partial \alpha} = 2f_2 + 6f_3\alpha + 12f_4\alpha^2, \tag{4.21}$$

$$\frac{\partial C_X^2}{\partial^2 \alpha} = 2a_5 + 6a_6\alpha \qquad \frac{\partial C_Z^2}{\partial^2 \alpha} = f_1 + 2f_2\alpha + 3f_3\alpha^2 + 4f_4\alpha^3, \tag{4.22}$$

$$\frac{\partial^2 C_x}{\partial \delta_e \partial \alpha} = a_4 \qquad \frac{\partial^2 C_z}{\partial \delta_e \partial \alpha} = 0, \tag{4.23}$$

$$\frac{\partial^2 C_x}{\partial \delta_e^2} = 2a_2 \qquad \frac{\partial^2 C_z}{\partial \delta_e^2} = 0, \tag{4.24}$$

$$\frac{\partial C_x}{\partial \delta_e} = 2a_2\delta_e + a_3 + a_4\alpha \qquad \frac{\partial C_z}{\partial \delta_e} = f_5. \tag{4.25}$$

The body-axis derivatives relate to the lift-drag axis derivatives via the following equations, which are also used in the next chapter:

$$\begin{bmatrix} \frac{\partial C_D}{\partial \alpha} \\ \frac{\partial C_L}{\partial \alpha} \end{bmatrix} = \begin{bmatrix} \sin\alpha & -\cos\alpha \\ \cos\alpha & \sin\alpha \end{bmatrix} \begin{bmatrix} C_X \\ C_Z \end{bmatrix} + \begin{bmatrix} -\cos\alpha & -\sin\alpha \\ \sin\alpha & -\cos\alpha \end{bmatrix} \begin{bmatrix} \frac{\partial C_X}{\partial \alpha} \\ \frac{\partial C_Z}{\partial \alpha} \end{bmatrix}, \tag{4.26}$$

$$\begin{bmatrix} \frac{\partial^2 C_D}{\partial \alpha^2} \\ \frac{\partial^2 C_L}{\partial \alpha^2} \end{bmatrix} = \begin{bmatrix} \cos\alpha & \sin\alpha \\ -\sin\alpha & \cos\alpha \end{bmatrix} \begin{bmatrix} C_X - \frac{\partial^2 C_X}{\partial \alpha^2} \\ C_Z - \frac{\partial^2 C_Z}{\partial \alpha^2} \end{bmatrix} + 2 \begin{bmatrix} \sin\alpha & -\cos\alpha \\ \cos\alpha & \sin\alpha \end{bmatrix} \begin{bmatrix} \frac{\partial C_X}{\partial \alpha} \\ \frac{\partial C_Z}{\partial \alpha} \end{bmatrix}, \tag{4.27}$$

$$\begin{bmatrix} \frac{\partial C_D}{\partial \delta_e \partial \alpha} \\ \frac{\partial C_L}{\partial \delta_e \partial \alpha} \end{bmatrix} = \begin{bmatrix} \sin\alpha & -\cos\alpha \\ \cos\alpha & \sin\alpha \end{bmatrix} \begin{bmatrix} \frac{\partial C_X}{\partial \delta_e} \\ \frac{\partial C_Z}{\partial \delta_e} \end{bmatrix} + \begin{bmatrix} -\cos\alpha & -\sin\alpha \\ \sin\alpha & -\cos\alpha \end{bmatrix} \begin{bmatrix} \frac{\partial^2 C_X}{\partial \delta_e \partial \alpha} \\ \frac{\partial^2 C_Z}{\partial \delta_e \partial \alpha} \end{bmatrix}, \tag{4.28}$$

$$\begin{bmatrix} \frac{\partial^2 C_D}{\partial \delta_e^2} \\ \frac{\partial^2 C_L}{\partial \delta_e^2} \end{bmatrix} = \begin{bmatrix} -\cos\alpha & -\sin\alpha \\ \sin\alpha & -\cos\alpha \end{bmatrix} \begin{bmatrix} \frac{\partial^2 C_X}{\partial \delta_e^2} \\ \frac{\partial^2 C_Z}{\partial \delta_e^2} \end{bmatrix}. \tag{4.29}$$

Graphs of these quantities are provided in the following Figures 4.4, 4.5, and 4.6. They plot the important forces as a function of change in the control surface position and the angle of attack.

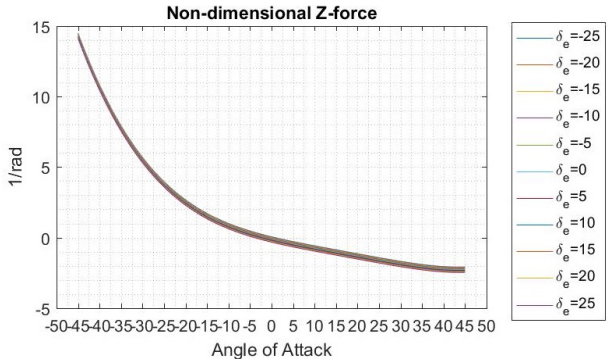

Figure 4.4: Z forces as a function of elevator deflection. The lines which remains close to one another are the elevator deflection changes. These indicate that the elevators do not have a substantial effect on lift compared to the change in angle of attack.

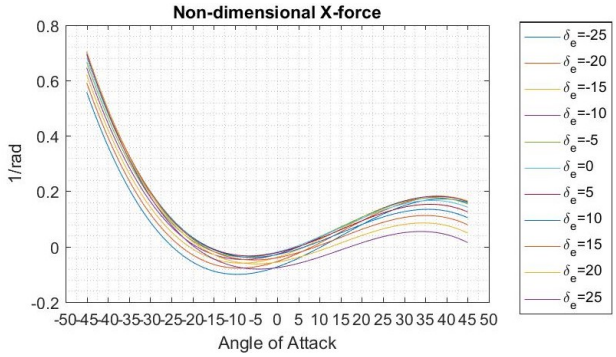

Figure 4.5: X forces as a function of elevator deflection. Here, the lines spread out further, and indicate that the elevators strongly contribute to drag. The cost to any control will be the extra drag contribution from the elevator deflections.

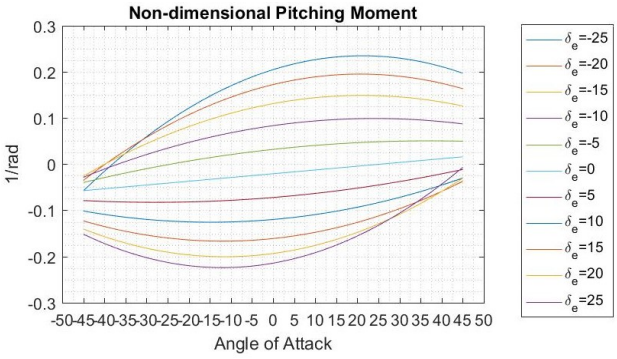

Figure 4.6: Pitching moment as a function of elevator deflection. The elevators directly influence the pitching moment of the aircraft. The trend in the graph shows the strongest correlation with elevator deflection.

4.5 Flight Control Systems

A flight control system safely flies or aids flight. It achieves these functions by synthesizing information about the aircraft's location, flight condition, kinematics, and mass properties. Using this information, a flight control system accepts inputs from a pilot and electromechanically transforms them into control surface motions to change its orientation, speed, and flight path, subject to the dynamics (4.1) and (4.2).

The control surfaces are miniature wings that apply aerodynamic forces and torques to the aircraft. Automatic feedback corrects deviations from the pilot's desired command by constantly repositioning the control surfaces. It rejects disturbances from exogenous influences such as turbulence and wind. It even overrides a pilot's command in dangerous or extreme situations.

Pilots have several available inputs to control the aircraft. In the cockpit, a pilot can control the aircraft's orientation by deflecting a control stick or pushing on a foot pedal. Electrical or mechanical connections between the pilot's input cause changes in the aircraft's engines and the aircraft's control surfaces.

Control inputs mechanically or electrically connect to surfaces on an aircraft or the engine's control system. As a result, changing the throttles, stick position, or pedals' positions change the propulsive and aerodynamic forces on the aircraft.

The aerodynamic torques initiated by stick and pedal deflections change the orientation of the aircraft. Each torque initiates a type of motion. Longitudinal stick inputs control the pitching motion, lateral stick inputs control rolling motion, and the pedals control the yawing motion. A picture of the pitch, roll, and yaw motions is shown in Figure 4.7.

The throttles increase the aircraft's energy state. Higher energy states can be used to increase velocity or increase altitude. For a constant orientation, the throttles can therefore be flight path effectors, and will determine which the aircraft flies relative to the horizon.

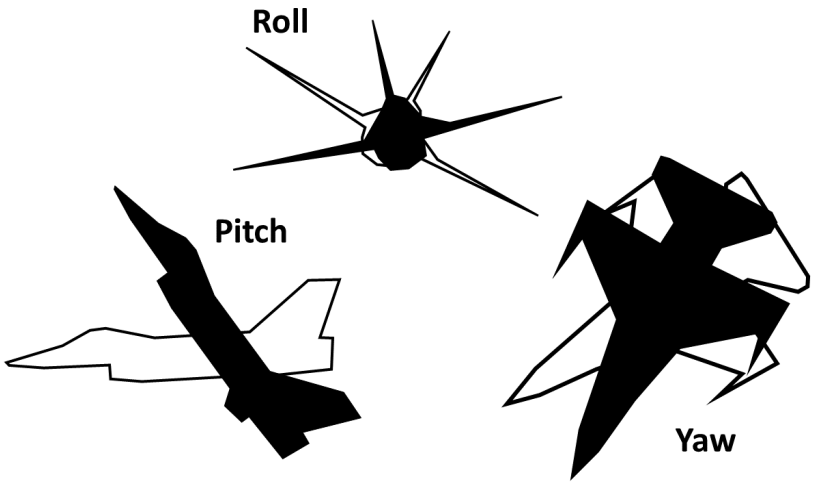

Figure 4.7: The motions of pitch, roll, and yaw.

4.6 Flight Control

A flight control problem is the challenge of controlling the dynamics, (4.1) and (4.2), with complete or partial knowledge of the forces and moments.

To illustrate flight control, consider an F-16 flying above a "flat earth," which is a two dimensional plane. The two directions of interest on this flat earth are the Up and East direction. In this idealized world, the gravitational field is constantly opposite the Up direction. In this inertial frame, Newton's Laws dictate the flight of the aircraft. The linear and angular accelerations are the result of the sum of forces and sum of torques.

The F-16's lift and drag in dimensionless form are C_L and C_D, which were defined in (4.26). The directions of lift and drag define a coordinate system relative to the velocity of a rigid body. The diagram in Figure 4.8 depicts the definitions of these forces.

The velocity of the rigid body relative to air, airspeed, may not be the same as the velocity of the rigid body to the ground, ground speed. When there are winds, headwinds increase the relative velocity of the body to the air and, contrastingly, tail winds decrease the relative velocity of the body to the air. The airspeed, not the ground speed, matters for the determination of the aerodynamic forces of lift and drag. The acceleration of the aircraft is

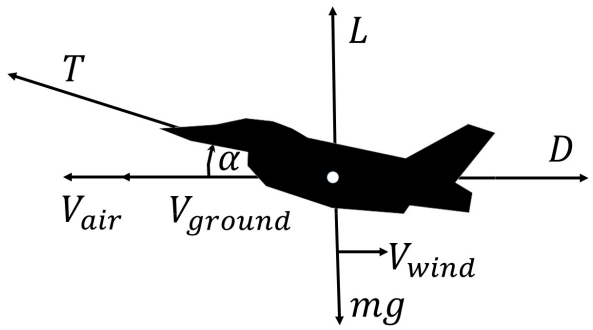

Figure 4.8: The force body diagram. The velocity vector defines the directions of lift and drag.

the result of the sum of these four forces. They are described in the force body diagram in Figure 4.8.

Using the force body diagram, we can conveniently sum the forces in the Lift and Drag axes. Using α, we can define the transformation $R(\alpha)$ from the body axis forces to the lift-drag axis.

$$\begin{bmatrix} \sum F_D \\ \sum F_L \end{bmatrix} = R(\alpha) \begin{bmatrix} \sum F_X \\ \sum F_Z \end{bmatrix} = \begin{bmatrix} -\cos\alpha & -\sin\alpha \\ \sin\alpha & -\cos\alpha \end{bmatrix} \begin{bmatrix} T + F_x \\ F_z \end{bmatrix} \tag{4.30}$$

Applying the rotation matrix to the functions of C_x and C_z yields C_L and C_D. The graphs of these dimensionless lift and drag coefficients are included in Figure 4.9.

4.7 Trim of Moments

The key to the control of any aircraft is the careful balance of moments and forces. When the sum of all moments and forces balance, the aircraft is in a steady-state. To solve the equations of motion to yield a steady-state solution is to trim the aircraft, and the aircraft's equilibria are the trim points.

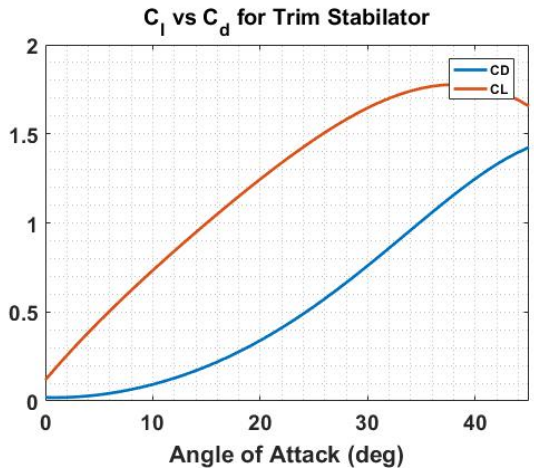

Figure 4.9: A diagram showing the result of applying the the transformation, $R(\alpha)$, to the coefficients, C_x and C_z, to yield C_L and C_D.

Mathematically, given a system of differential equations such as

$$\dot{x} = f(x, u), \tag{4.31}$$

trim entails solving for the control inputs u which set $\dot{x} = 0$.

To simplify the problem at hand, we will trim the aircraft so that the moment equation is zero. If q represents the pitch rate, then the moment equation is given by Newton's laws:

$$\begin{aligned} I_y \dot{q} =& \bar{q} S_{ref} c_{ref} \left(C_m(\alpha, \delta_h) + C_{m_q}(\alpha) \hat{q} \right) \\ &+ \bar{q} S_{ref} c_{ref} \left(x_{aero} - x_{cg} \right) \left(C_z(\alpha, \delta_h) + C_{z_q}(\alpha) \hat{q} \right) \end{aligned} \tag{4.32}$$

True trim conditions also ensure that the force equations are exactly balanced, which would entail manipulating the thrust so that the vehicle does not lose or gain speed. For the purposes of this dissertation, we will seek steady conditions where the vehicle will balance the torques, with the assumption that there is no rotation on the aircraft, and we will neglect the speed trim in order to avoid modeling thrust inputs.

The elevator deflection can be solved so that

$$0 = \dot{q}|_{q=0} = C_m(\alpha, \delta_h) + \left(x_{aero} - x_{cg} \right) C_z(\alpha, \delta_h) = 0 \tag{4.33}$$

Without rotation about the roll axis, the body axis pitch rate would be exactly the Euler angle pitch rate. Also, the moments of inertia when used in the body axis are constants. This is not true in other frames.

A plot of the trim stabilator, and the resulting moment balance, is shown in Figure 4.10. The trim stabilator is the value of the stabilator angle, which is required to prevent the aircraft from rotating at a sustained level of acceleration. It is the steady-state elevator setting to pull-G's on the aircraft. To quickly summarize, the equation that describes pitch acceleration can be written simply

$$I_y \dot{q} = M\left(\alpha, \delta_h, \hat{q}\right). \tag{4.34}$$

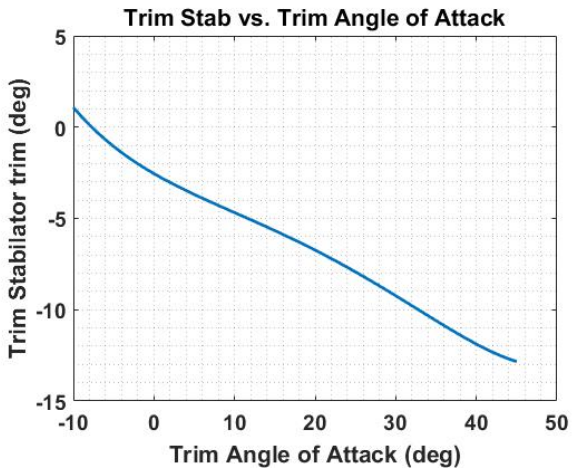

Figure 4.10: A graph showing the stabilator trim required to set the $\dot{q}$ equation to zero when pitch rate, q, is assumed to be zero and α is specified on the x-axis of the figure. Note as the vehicle increases in angle of attack, the stabilator takes negative values. These values move the surfaces of the left and right stabilators trailing edge up. Trailing edge motion decreases lift at the tail. The decrease of lift at the tail counter-balances the increased lift generated by the wing from the increased angle of attack. This delicate balancing act is the challenge of flight control.

4.8 Derivation of Flight Path Angle Dynamics

Consider the force on the aircraft in a frame affixed to the center of gravity of the vehicle in polar coordinates. The radial vector is the velocity and the angle coordinate is the flight path angle. We describe the force balance equations from this frame.

Examine Figure 4.11, where vectors parallel to the velocity vector are on the real axis, and vectors orthogonal to the velocity vector are on the imaginary axis.

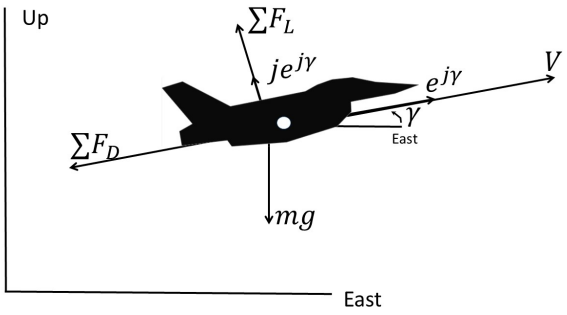

Figure 4.11: A diagram showing how polar coordinates is used to derive dynamics. The radial vector is the real axis along the velocity, V, which is the direction of tangential accelerations. The vector normal to it is the imaginary axis, j, used to represent the normal acceleration.

The acceleration of the aircraft in this equation follows from Newton's laws:

$$\vec{F} = m\frac{\mathrm{d}\vec{V}}{\mathrm{d}t} = \left(-\sum F_D - mg\sin\gamma\right) + j\left(\sum F_L - mg\cos\gamma\right). \tag{4.35}$$

The acceleration is described by the tangential and normal components as follows. Let $\vec{V}$ describe the vector and V the magnitude of the velocity,

$$\frac{\mathrm{d}\vec{V}}{\mathrm{d}t} = \frac{\mathrm{d}}{\mathrm{d}t}\left(Ve^{\hat{j}\gamma}\right) = \frac{\mathrm{d}V}{\mathrm{d}t}e^{\hat{j}\gamma} + \hat{j}\dot{\gamma}Ve^{\hat{j}\gamma}. \tag{4.36}$$

Therefore we sum the equations along components to get:

$$m\dot{V} = -\sum F_D - mg\sin\gamma, \tag{4.37}$$

$$m\dot{\gamma}V = \sum F_L - mg\cos\gamma. \tag{4.38}$$

Since the angle of attack is the transformation from the body axis to the velocity vector, and the body axis pitch rate is given by q, we can write:

$$\dot{\alpha} + \dot{\gamma} = q. \tag{4.39}$$

A summary of all the axes are described in Figure 4.12.

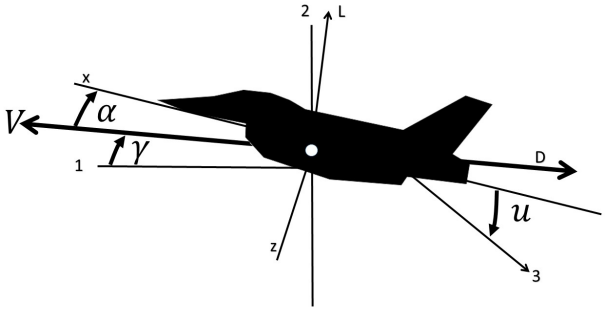

Figure 4.12: A diagram of different axes and angles through a mock-up F16 center of gravity. 1 represents the zero-lift axis of the aircraft; 2 represents the horizon axis; 3 represents the zero-lift axis of the stabilators; 4 represents the normal axis (which is opposite the body z-axis); and, 5 represents the altitude axis. The angle α is defined relative to the velocity vector.

4.9 Reduction of the State Space

The dynamics are ascertained from the equations described previously. Explicit arguments for the controls are specified, as follows:

$$\dot{h} = V \sin\gamma, \tag{4.40}$$

$$\dot{V} = -\sum F_D\left(\alpha, \delta_h, \hat{q}\right) - mg\sin\gamma, \tag{4.41}$$

$$mV\dot{\gamma} = \sum F_L\left(\alpha, \delta_h, \hat{q}\right) - mg\cos\gamma, \tag{4.42}$$

$$\dot{\gamma} + \dot{\alpha} = q, \tag{4.43}$$

$$I_y\dot{q} = M\left(\alpha, \delta_h, \hat{q}\right). \tag{4.44}$$

We wish to split these dynamics into fast dynamics and slow dynamics. The fast dynamics are generally called the "short period," which is the natural high frequency oscillatory behavior of an aircraft as it flies.

The "short period" dynamics are generally stabilized by a flight control system or an autopilot. The short period equations, (4.43) and (4.44), ensures that any angle of attack which can be sustained is constantly trimmed, *i.e.*, the $\dot{q}$ differential equation is zeroed by appropriate stabilator deflection.

The slower dynamics, (4.40), (4.41), and (4.42), are called the "phugoid" dynamics, which describe oscillations in speed, V, flight path angle, γ, and altitude, h. These dynamics tend to oscillate in aircraft at much slower rates. When an aircraft slows down, its flight path angle decreases which causes gravity to increase its speed and decrease its altitude. This, in turn, causes the flight path angle to increase, and the aircraft to slows down. Phugoid dynamics are different for each aircraft but generally are easily corrected by a pilot or by an aircraft with automatic control.

Using the δ_{htrim}, we can eliminate the $\dot{q}$ equation and assume that any commands from the guidance system will be steady commands, which assume $q = 0$. Figure 4.13 graphs the input of the trim stabilator schedule versus the moment equations

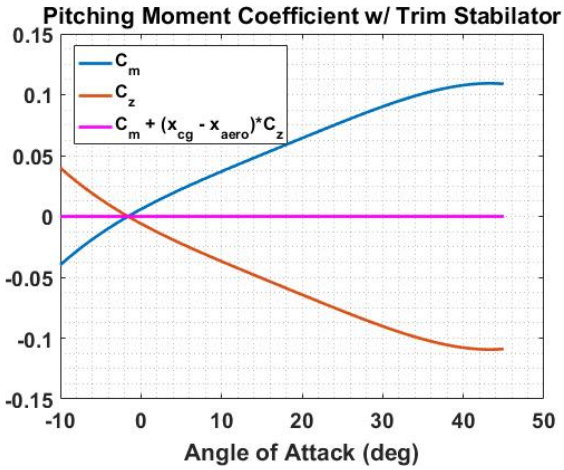

Figure 4.13: With pitch rate assumed to be zero, the trim stabilator zeroes the pitch acceleration equation

This natural split in dynamics is exploited by control systems. A guidance system or a pilot will control the phugoid state variables. An autopilot or an automatic control system will control the short period state variables. A diagram of the situation is given in figure 4.13.

In order to reduce the dynamics, we will use the trim angle of attack, α_{trim}, as a control to design trajectory. The α_{trim} will be presumed to pass into some autopilot control system which will automatically determine the deviations from the trim stab or δ_{htrim} to control the system.

With the assumption that $q = 0$ and that δ_{trim} is always chosen to solve $\dot{q} = 0$, we arrive at a simplified version of the dynamics:

$$\dot{h} = V \sin\gamma, \tag{4.45}$$

$$\dot{V} = -\sum F_D\left(\alpha_{trim}\right) - mg\sin\gamma, \tag{4.46}$$

$$mV\dot{\gamma} = \sum F_L\left(\alpha_{trim}\right) - mg\cos\gamma. \tag{4.47}$$

In this new version of the dynamics, the control is given by the choice of the trim angle of attack:

$$u = \alpha_{trim}. \tag{4.48}$$

The states for the problem are:

- $h(t)$, altitude,
- $V(t)$, the airspeed,
- $\gamma(t)$, the flight path angle.

Because the $\dot{q}$ equation as the $\dot{\alpha}$ equations is now simplified, an autopilot controls the ancillary dynamics:

$$q = \dot{u} + \dot{\gamma}, \tag{4.49}$$

$$I\dot{q} = M(u, \delta_h, \hat{q}). \tag{4.50}$$

The autopilot determines the correct value of δ_h to achieve any commanded α_{trim}.

Feedback information entering the autopilot are q_s and α_s, the sensed pitch rate and the senses angle of attack. The feedback information entering the guidance scheme are V_s, γ_s, and h_s the sensed airspeed, the sensed flight path angle, and the sensed altitude. Detailed discussion of how these states are controlled in practice are found in [39].

Chapter 5

Perturbation Feedback Control

In this chapter, we present an application of perturbation feedback control (PFC) to an F-16 ground collision avoidance system. A ground collision avoidance system (GCAS) automatically returns both pilot and aircraft to a safe flight path when a pilot inadvertently steers towards the ground or another obstacle. A PFC guidance algorithm determines neighboring extremal trajectories to a nominal aircraft trajectory. The PFC guidance algorithm derives from reentry guidance examples presented in [34].

We discuss the control theory to optimally calculate a trajectory which attains a safe flight path using the minimum energy. We detail the calculations for an optimal recovery trajectory from a dangerous flight path angle to a safe flight condition. Combined with the nominal trajectory, the PFC guidance changes the aircraft's angle of attack command when aircraft states deviate from the pre-calculated optimal trajectory. The commands feed into an autopilot that changes the aircraft control surfaces.

Throughout the chapter, we comment on how optimal control aids the engineering design process. We present graphs and practical discussion of the simulation results.

5.1 Problem Formulation

Consider an F-16 aircraft in a steep dive. A recovery signal initiated either by the pilot or a computer activates a GCAS to save both pilot and aircraft. Once a recovery command initiates, the GCAS must transfer the initial state of the aircraft x_0 to the terminal condition x_T by transmitting recovery angle of attack commands into an autopilot. The commands cause the aircraft stabilator deflections to change, and they are selected to maximize the terminal velocity during the recovery. This ensures that the aircraft does not stall.

First, we derive a numerical procedure to calculate an optimal angle of attack command schedule. Second, we derive the perturbation feedback control along the nominal schedule. Finally, we combine the nominal trajectory and perturbation feedback control in a guidance scheme.

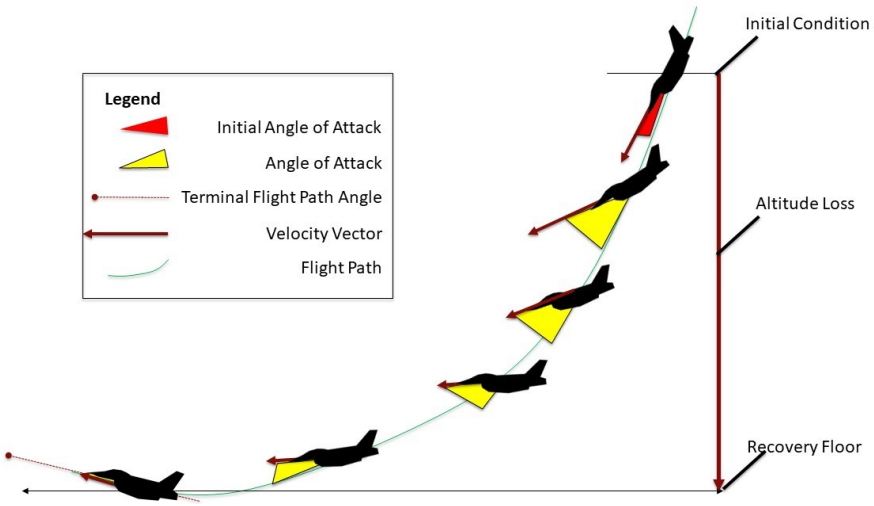

Figure 5.1: A sketch of the problem **OC**

The diagram in figure 5.1 depicts some of the basic features of the problem. A designer, a priori, selects a desired terminal condition and recovery altitude. The control system determines the optimal continuum of angle of attack commands, depicted in yellow starting from the initial condition in red. The velocity vector increases in magnitude, as the aircraft falls, and decreases in magnitude, as the angle of attack changes. This causes the drag and lift on the aircraft to increase. The flight path along the maneuver changes from a steep and dangerous angle to a nearly level angle due to the changes in lift. The objective of

the problem is to maximize the magnitude of the velocity vector when aircraft reaches the desired terminal flight path angle and recovery floor.

We make the following assumptions.

1. The aircraft measurements are pure. Noise or disturbances do not affect the states.
2. The aircraft actuation and sensation dynamics are neglected in our calculations.
3. The dynamics of air density for the recovery distances is negligible, and throughout the trajectory we assume a standard day air density based on the initial condition.
4. We assume no capability to control the power level of the engines, and choose the power setting for the engine to be idle. The value of thrust is assumed to be constant in the short recovery period. The values chosen for the thrust are based on a table lookup for the initial conditions taken from [55].
5. Initially, we will assume that the angle of attack command remains within the interior of the control set. We will relax the assumption later in the next chapter.
6. We avoid more complicated state-space structures and neglect path constraints. We will relax the assumption in the next chapter.

5.1.1 Mathematical Control System

Utilizing the notation from Chapter 2, the 4 tuple, $\Sigma = (M, U, f, \mathcal{U})$, represents the control system of the F-16 aircraft.

The state-space, M, is the open subset of $\mathbb{R}^3$, defined by

$$M := \left\{(h, V, \gamma) \mid h \in \mathbb{R}, V \in \mathbb{R}^+, \quad \gamma \in (-\pi, \pi), \quad h > 0, \quad V > 0\right\}. \tag{5.1}$$

The states and controls, $x \in M$ and $u \in U$, parameterize the dynamics $\dot{x} = f(x, u)$,

$$f : M \times U \to \mathbb{R}^3, \quad (x, u) \mapsto \begin{pmatrix} f_h(x, u) \\ f_V(x, u) \\ f_\gamma(x, u) \end{pmatrix}. \tag{5.2}$$

The components of f are f_h, f_V, f_γ, as follows:

$$f_h = \dot{h} = V \sin\gamma, \tag{5.3}$$

$$f_V = \dot{V} = \frac{1}{m}\left(-\mathbb{D}\left(V, \alpha\right) - mg\sin\gamma\right), \tag{5.4}$$

$$f_\gamma = \dot{\gamma} = \frac{1}{mV}\left(\mathbb{L}\left(V, \alpha\right) - mg\cos\gamma\right). \tag{5.5}$$

The three states, corresponding to (5.3), (5.4), and (5.5), are altitude, h, velocity, V, and flight path angle, γ, respectively.

The symbols, $\mathbb{D}$ and $\mathbb{L}$, are short-hand for the sum of all forces in drag and lift axes:

$$\begin{bmatrix} \mathbb{D} \\ \mathbb{L} \end{bmatrix} = \begin{bmatrix} -\cos\alpha & -\sin\alpha \\ \sin\alpha & -\cos\alpha \end{bmatrix} \begin{bmatrix} \frac{1}{2}\rho S V^2 C_x(\alpha) + T \\ \frac{1}{2}\rho S V^2 C_z(\alpha) \end{bmatrix} \tag{5.6}$$

The purpose of the short-hand is to concisely write the external forces on the body of the aircraft. The aerodynamic external forces in the X and Z axis are $\frac{1}{2}\rho S V^2 C_x(\alpha)$ and $\frac{1}{2}\rho S V^2 C_z(\alpha)$. The propulsive force in the X axis is the thrust, T.

The control u is the angle of attack command as a function of time, and we abide by the standard notation in aerospace literature by referring to the angle of attack command as $\alpha(t)$. We choose the class of admissible controls, $\mathcal{U}$, to be continuously differentiable functions, *i.e.*, the set of all C^1 angle of attack command functions of time.

The control set, U, is the set of available values of angle of attack, α, for the recovery profile at each instant in time. The full range of the angle of attack is -10 to 45 degrees; however, above 29 degrees, the F-16 is prone to spin departure. As a result, we choose the control set to span up to 28 degrees,

$$U := \{\alpha \mid \alpha \in [-10, 28]\}. \tag{5.7}$$

5.1.2 Terminal Constraint

Since we chose to neglect the effect of altitude on air density, the terminal altitude for the recovery maneuver is arbitrary. The altitude loss between recovery initiation and termination is the more practical variable of interest for trajectory design. Thus, we arbitrarily set the desired recovery position to be an altitude of 30,000 feet.

The recovery flight path angle is 0 degrees, which corresponds to horizontal flight. In a practical recovery system, 0 degrees would likely be a lower bound on terminal flight path angles.

The terminal constraint, ψ, captures the desired altitude and flight path angle terminal condition:

$$\psi(h, \gamma) = \begin{bmatrix} h - 30k \\ \gamma \end{bmatrix}. \tag{5.8}$$

5.1.3 Objective Function

The objective function, J, maximizes the terminal speed. The optimization convention used throughout this dissertation solves minimization problems. To use the convention, J takes minimization form as:

$$J = -V(T). \tag{5.9}$$

The optimal control problem is in Mayer form with a terminal penalty, $\phi = -V$, and a Lagrangian, $L \equiv 0$.

5.1.4 Statement of the GCAS Optimal Control Problem

We seek functions $\alpha(t)$ in the time interval $I = [t_0, T]$,

$$\alpha : [t_0, T] \to U, t \mapsto \alpha(t), \tag{5.10}$$

which solve the corresponding initial value problem,

$$\dot{x}(t) = f(x(t), \alpha(t)), \quad x(t_0) = x_0, \tag{5.11}$$

with a solution to the initial value problem that exists over I. We call x the trajectory corresponding to the control α and refer to the pair (x, α) as a controlled trajectory.

The precise statement of the optimal control problem will be referred to as **[OC]**:

[OC] Minimize the objective $J(T) = -V$ over all admissible controlled trajectories (x, u) that satisfy the terminal constraint $\psi(h, V) = 0$ for the control system Σ.

5.2 First Order Necessary Conditions for Optimality

An extremal is a triple $\Gamma = (x, u, \lambda)$, which satisfies the first order necessary conditions specified in the Pontryagin maximum principle. The adjoint vector λ solves the adjoint equation with the initial condition determined by unknown control parameters ν given by the transversality condition. Additionally, the control must satisfy the instantaneous minimizer condition.

Knowledge of the control parameters at the terminal time garners the extremal which solves **[OC]**. The extremal can be calculated by integrating the state and adjoint equations backwards from the terminal conditions, while holding the minimizer condition true. Alternatively, guessing a value of the adjoint vector at the intimal time and then integrating with state equations under the minimization condition can also yield the optimal trajectory, if the transversality condition is satisfied. This fact serves as the basis for a shooting method presented later.

5.2.1 The Adjoint Equation

From the maximum principle, the Hamiltonian is

$$H = \lambda f. \tag{5.12}$$

We only consider normal extremals and let $\lambda_0 = 1$. Let the components of λ be λ_h, λ_V, and λ_γ, which correspond to f_h, f_V, and f_γ, respectively.

The Hamiltonian takes the form:

$$H = \lambda_h \left[V \sin\gamma\right] + \lambda_V \left[\frac{1}{m}\left(-\mathbb{D}\left(V,\alpha\right) - mg\sin\gamma\right)\right] + \lambda_\gamma \left[\frac{1}{mV}\left(\mathbb{L}\left(V,\alpha\right) - mg\cos\gamma\right)\right]. \tag{5.13}$$

The adjoint equation,

$$\dot{\lambda} = -\frac{\partial H}{\partial x}, \tag{5.14}$$

is calculated using the derivatives of the Hamiltonian with respect to the state:

$$\frac{\partial H}{\partial h} = 0, \tag{5.15}$$

$$\begin{aligned}\frac{\partial H}{\partial V} &= \lambda_h \sin\gamma + \lambda_V \left[-\frac{1}{m}\left(\frac{\partial \mathbb{D}}{\partial V}\left(V,\alpha\right)\right)\right], \\ &\quad + \lambda_\gamma \left[\frac{1}{mV}\left(\frac{\partial \mathbb{L}}{\partial V}\left(V,\alpha\right)\right) - \frac{1}{mV^2}\left(\mathbb{L}\left(V,\alpha\right) - mg\cos\gamma\right)\right],\end{aligned} \tag{5.16}$$

$$\frac{\partial H}{\partial \gamma} = \lambda_h \left[V\cos\gamma\right] + \lambda_V \left[-g\cos\gamma\right] + \lambda_\gamma \left[\frac{1}{V}\left(g\sin\gamma\right)\right]. \tag{5.17}$$

The component adjoint equations combine into a single row vector,

$$\begin{bmatrix} \dot{\lambda}_h & \dot{\lambda}_V & \dot{\lambda}_\gamma \end{bmatrix} = -\begin{bmatrix} \frac{\partial H}{\partial h} & \frac{\partial H}{\partial V} & \frac{\partial H}{\partial \gamma} \end{bmatrix} = -\lambda \frac{\partial f}{\partial x}, \tag{5.18}$$

which succinctly captures the adjoint equations using the following Jacobian matrix:

$$\frac{\partial f}{\partial x} = \begin{bmatrix} 0 & \sin\gamma & V\cos\gamma \\ 0 & -\frac{1}{m}\left(\frac{\partial \mathbb{D}}{\partial V}(V,\alpha)\right) & -g\cos\gamma \\ 0 & \frac{1}{mV}\left(\frac{\partial \mathbb{L}}{\partial V}(V,\alpha)\right) - \frac{1}{mV^2}\left(\mathbb{L}(V,\alpha) - mg\cos\gamma\right) & \frac{g}{V}\sin\gamma \end{bmatrix}. \tag{5.19}$$

5.2.2 Instantaneous Minimization Condition

The instantaneous minimization condition is

$$\frac{\partial H}{\partial u} = 0 \tag{5.20}$$

since we made the assumptions that the minimizing control lies in the interior of the control set.

The instantaneous minimization condition yields:

$$\begin{aligned} \frac{\partial H}{\partial \alpha} =& \lambda_V \left[-\frac{1}{m}\frac{\partial \mathbb{D}}{\partial \alpha}(V,\alpha)\right] + \lambda_\gamma \left[\frac{1}{mV}\left(\frac{\partial \mathbb{L}}{\partial \alpha}(V,\alpha)\right)\right] \\ =& -\frac{\lambda_V}{m}\left(-\frac{1}{2}\rho V^2 S\frac{\partial C_D}{\partial \alpha} + T\sin\alpha\right) + \frac{\lambda_\gamma}{mV}\left(\frac{1}{2}\rho V^2 S\frac{\partial C_L}{\partial \alpha} + T\cos\alpha\right) = 0. \end{aligned} \tag{5.21}$$

Rearranging equation (5.21) implicitly determines the control, α, in terms of λ and V.

5.2.3 Transversality Conditions

The transversality conditions yield the terminal multiplier, ν, and the equation for the final time, Ω. The transversality equation is repeated from before, and we assume that $\lambda_0 = 1$.

$$H + \lambda_0\frac{\partial \phi}{\partial t} + \nu\frac{\partial \Psi}{\partial t} = 0, \qquad \lambda = \lambda_0\frac{\partial \phi}{\partial x} + \nu\frac{\partial \Psi}{\partial x} \qquad \text{at } (T, x_*(T)). \tag{5.22}$$

The value of the adjoint is given in terms of the unspecified multiplier, ν, which has two components, ν_h and ν_V, corresponding to the two constraint equations:

$$\lambda_T = \begin{bmatrix} \nu_h & -1 & \nu_\gamma \end{bmatrix}. \tag{5.23}$$

The clock constraint determines the final time, T, as follows:

$$\Omega = \nu_h \left(V \sin\gamma\right) - \frac{1}{m}\left(-\mathbb{D}\left(V,\alpha\right) - mg\sin\gamma\right) + \nu_\gamma \left(\frac{1}{mV}\left(\mathbb{L}\left(V,\alpha\right) - mg\cos\gamma\right)\right) = 0. \tag{5.24}$$

5.3 Numerical Procedure

The procedure that was used to determine a trajectory which satisfies the necessary conditions is given by the shooting method. This approach is adapted from the method described by [37]. We use the superscript notation, $(\cdot)^i$, to denote the number of the iteration i.

We aim to determine the control history α, the adjoint vector λ, the final time T, and the terminal condition x_T that satisfy all of the conditions. To be precise, we present a table of known and unknown quantities in Table 5.1.

Component	**Known**	**Unknown**
Initial Conditions	h_0, V_0, γ_0	$\lambda_h(0), \lambda_V(0), \lambda_\gamma(0)$
Terminal Conditions	h_T, γ_T	$V_T, \lambda_h(T), \lambda_V(T), \lambda_\gamma(T)$
Terminal Time		T
Control Parameters	ν_v	ν_h, ν_γ
Control		$\alpha(t)$
Trajectory		$x(t)$
Adjoint		$\lambda(t)$

Table 5.1: Parameters sorted by whether they are specified or unspecified

The method iterates on values of the initial conditions for the adjoint equations and the final time for the clock constraint. If the initial conditions to the adjoint equation are known, then the condition, $\frac{\partial H}{\partial u} = 0$, yields a candidate control. The candidate control substitutes into the adjoint equations and the state equations. Both the adjoint and state equations are integrated forward in time–continually updating the instantaneous minimization condition. Integration stops at the final time.

If the terminal time and terminal conditions satisfy the clock constraint, terminal constraint, and the transversality condition, then the procedure successfully generated a candidate extremal. Second order conditions verify the local optimality of the candidate extremal.

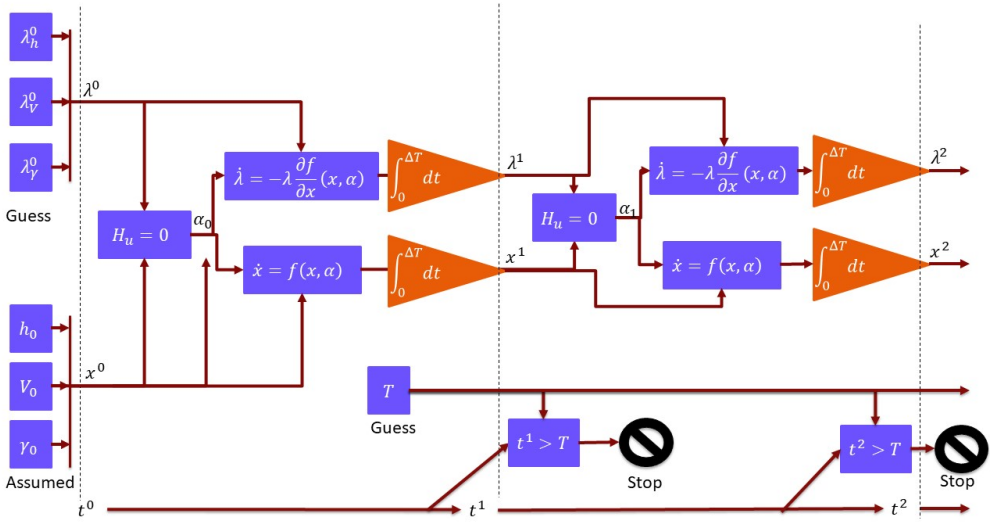

Figure 5.2: A signal flow graph illustrating two steps of the reduced equations of motion.

To explain the procedure in detail:

1. Start with the initial conditions in formulation of **[OC]**. Guess a value of the adjoint equations for the initial time:

$$h_0, \gamma_0, V_0 \text{ are fixed.}$$
$$\lambda_h{}^1(0), \lambda_V{}^1(0), \lambda_\gamma{}^1(0) \text{ need to be guessed.}$$

   (a) Solve the "reduced equations of motion" by combining the adjoint equations and dynamics into a set of differential equations to be integrated forward with time. With this approach, the equation (5.21) can be solved for $\alpha(t)$. The initial conditions are:

$$x_0 = (h_0, V_0, \gamma_0) \text{ and } \lambda_0^i(T) = \left(\lambda_h^i(T), \lambda_V^i(T), \lambda_\gamma^i(T)\right). \tag{5.25}$$

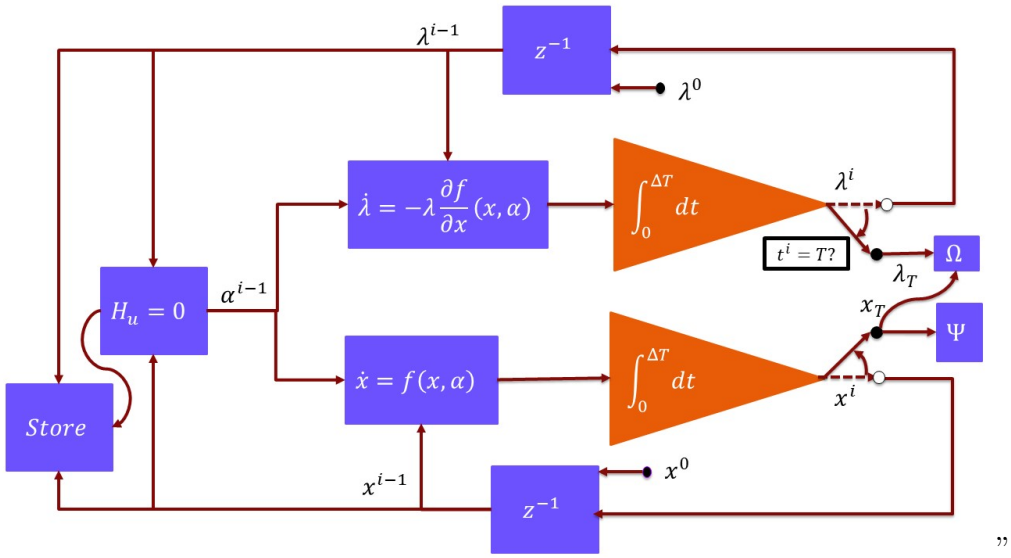

Figure 5.3: A signal flow graph to represent the difference equation for solving the reduced equations of motion.

(b) Integrate the equations,

$$\dot{x} = f(x, \alpha), \tag{5.26}$$

$$\dot{\lambda} = -\lambda \frac{\partial f}{\partial x}(x, \alpha), \tag{5.27}$$

for an initial guess in the terminal time, T. Choosing a time which is reasonably long enough is helpful.

2. Calculate $\Omega^i(T)$, $\psi^i(T) - \begin{bmatrix} 30k \\ 0 \end{bmatrix}$, and $\lambda_V^i(T) = -1$.

3. Perturb each of the following variables, $\lambda_h^i(t_0)$, $\lambda_V^i(t_0)$, $\lambda_\gamma^i(t_0)$, and T, by a small percentage of their value. Make perturbations one at a time. For each perturbation, Δ, solve the "reduced equations of motion" by combining the adjoint equations and dynamics into a set of differential equations to be integrated forward with time.

(a) Integrate using "reduced equations of motion" from $[t_0, T]$,

$$\dot{x} = f(x, \alpha), \tag{5.28}$$

$$\dot{\lambda}^T = -\frac{\partial f}{\partial x}^T (x, \alpha)\lambda^T, \tag{5.29}$$

starting from $x_0 = (h_0, V_0, \gamma_0)$ and $\lambda_0^i = \left(\lambda_h^i(0) + \Delta, \lambda_V^i(0), \lambda_\gamma^i(0)\right)$.

(b) Integrate using "reduced equations of motion" from $[t_0, T]$:

$$\dot{x} = f(x, \alpha), \tag{5.30}$$

$$\dot{\lambda}^T = -\frac{\partial f}{\partial x}^T (x, \alpha)\lambda^T, \tag{5.31}$$

starting from $x_0 = (h_0, V_0, \gamma_0)$ and $\lambda_0^i = \left(\lambda_h^i(0), \lambda_V^i(0) + \Delta, \lambda_\gamma^i(0)\right)$.

(c) Integrate using "reduced equations of motion" from $[t_0, T]$:

$$\dot{x} = f(x, \alpha), \tag{5.32}$$

$$\dot{\lambda}^T = -\frac{\partial f}{\partial x}^T (x, \alpha)\lambda^T, \tag{5.33}$$

starting from $x_0 = (h_0, V_0, \gamma_0)$ and $\lambda_0^i = \left(\lambda_h^i(0), \lambda_V^i(0), \lambda_\gamma^i(0) + \Delta\right)$.

(d) Integrate using "reduced equations of motion" from $[t_0, T + \Delta]$

$$\dot{x} = f(x, \alpha), \tag{5.34}$$

$$\dot{\lambda}^T = -\frac{\partial f}{\partial x}^T (x, \alpha)\lambda^T, \tag{5.35}$$

starting from $x_0 = (h_0, V_0, \gamma_0,)$ and $\lambda_0^i = \left(\lambda_h^i(0), \lambda_V^i(0), \lambda_\gamma^i(0)\right)$.

4. Using calculations in (2), compute the sensitivity matrix J to the perturbations,

$$J = \begin{bmatrix} \frac{\partial \Omega^i}{\partial \lambda_h^i(0)} & \frac{\partial \Omega^i}{\partial \lambda_V^i(0)} & \frac{\partial \Omega^i}{\partial \lambda_\gamma^i(0)} & \frac{\partial \Omega^i}{\partial T} \\ \frac{\partial \lambda_V(T)^i}{\partial \lambda_h^i(0)} & \frac{\partial \lambda_V(T)^i}{\partial \lambda_V^i(0)} & \frac{\partial \lambda_V(T)^i}{\partial \lambda_\gamma^i(0)} & \frac{\partial \lambda_V(T)^i}{\partial T} \\ \frac{\partial h(T)^i}{\partial \lambda_h^i(0)} & \frac{\partial h(T)^i}{\partial \lambda_V^i(0)} & \frac{\partial h(T)^i}{\partial \lambda_\gamma^i(0)} & \frac{\partial h(T)^i}{\partial T} \\ \frac{\partial V(T)^i}{\partial \lambda_h^i(0)} & \frac{\partial V(T)^i}{\partial \lambda_V^i(0)} & \frac{\partial V(T)^i}{\partial \lambda_\gamma^i(0)} & \frac{\partial V(T)^i}{\partial T} \end{bmatrix}. \tag{5.36}$$

5. Choose a step size τ. In this dissertation, we selected a step size of 20%. Replace the starting conditions $\lambda_h^1(0)$, $\lambda_V^1(0)$, $\lambda_\gamma^1(0)$ and T^1 with $\lambda_h^i(0)$, $\lambda_V^i(0)$, $\lambda_\gamma^i(0)$ and T^i where

$$\begin{bmatrix} \lambda_h^{i+1}(0) \\ \lambda_V^{i+1}(0) \\ \lambda_\gamma^{i+1}(0) \\ T^{i+1} \end{bmatrix} = -\tau J^{-1} \begin{bmatrix} \Omega(T) \\ \gamma(T) \\ h(T) - 30k \\ \lambda_V + 1 \end{bmatrix}. \tag{5.37}$$

6. Repeat the procedure until all of the constraints for Ω, ψ, and λ_V are zero. Ten is a reasonable maximum for repetitions of the procedure.

7. Refer to Figure 5.2, which shows the initialization, and Figure 5.3, which shows the recursive procedure, for steps 1 and step 2. Refer to Figure 5.4 for steps 3 and 4.

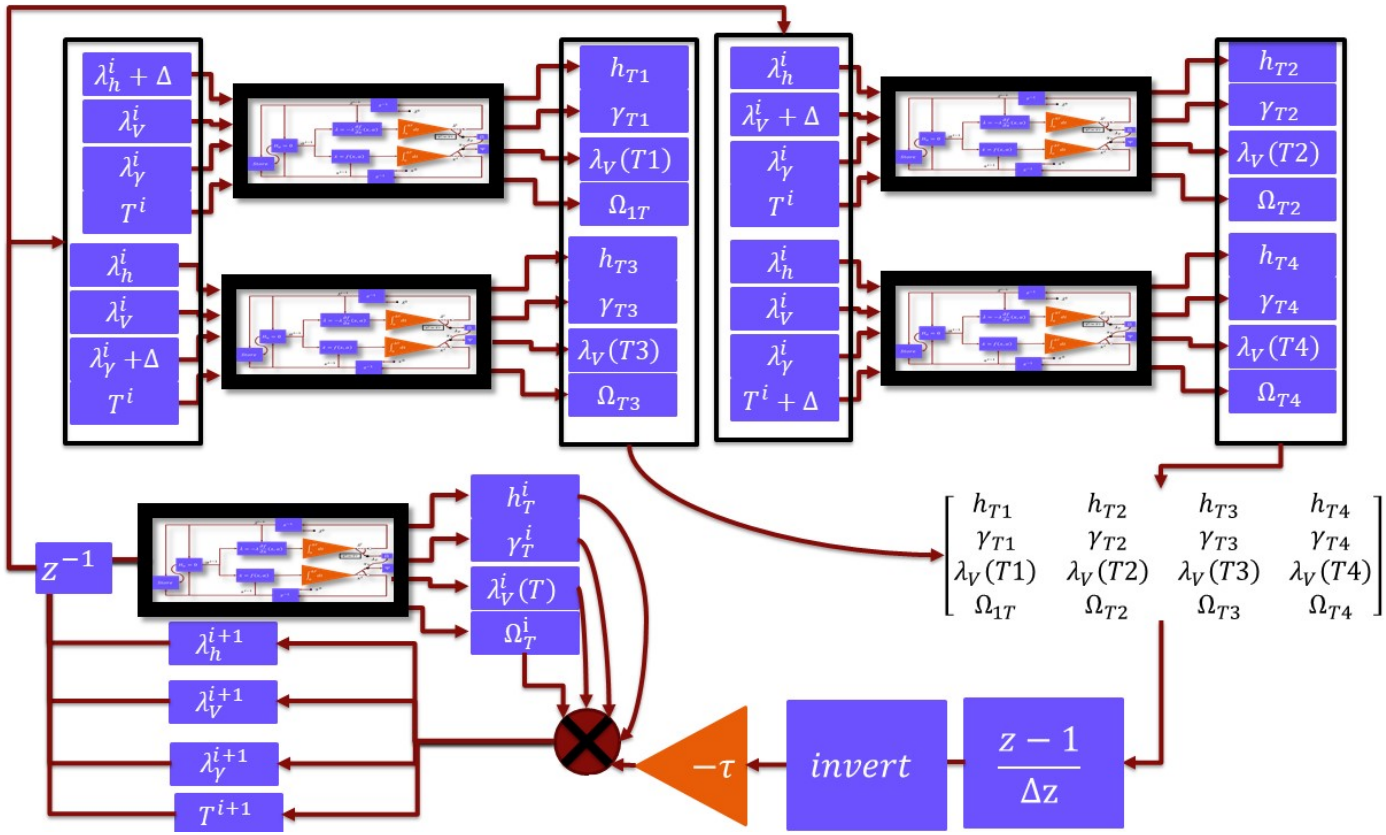

Figure 5.4: A signal flow graph for the numerical method to calculate an extremal. Newton's method generates guesses for adjoint initial conditions.

5.4 Second Order Conditions

Though second order conditions are not required to generate extremal trajectories, perturbation feedback control uses second order information to construct neighboring optimum solutions. The second order conditions develop from the sensitivity equations.

For any flight control system, the sensitivity equations are the primary basis for deriving feedback controls. The second order conditions are easily calculated. They provide an engineer with essential checks on the validity of candidate extremals.

This section explains how to complete the remaining calculations to construct a perturbation feedback control. It assumes that the numerical procedure for calculating an extremal successfully yielded a candidate that satisfies the necessary conditions for optimality.

We need to solve the coupled differential equations which follow:

$$\frac{\mathrm{d}}{\mathrm{d}t}\left(\frac{\partial x}{\partial p}\right) = A(t)\left(\frac{\partial x}{\partial p}\right) - B(t)\left(\frac{\partial \lambda}{\partial p}\right), \tag{5.38}$$

$$\frac{\mathrm{d}}{\mathrm{d}t}\left(\frac{\partial \lambda^T}{\partial p}\right) = C(t)\left(\frac{\partial x}{\partial p}\right) - A^T(t)\left(\frac{\partial \lambda^T}{\partial p}\right). \tag{5.39}$$

The matrices A, B, C are defined as:

$$A = \left(\frac{\partial f}{\partial x}\right) - \left(\frac{\partial f}{\partial u}\right)\left(\frac{\partial^2 H}{\partial u^2}\right)^{-1}\left(\frac{\partial^2 H}{\partial u \partial x}\right), \tag{5.40}$$

$$B = \left(\frac{\partial f}{\partial u}\right)\left(\frac{\partial^2 H}{\partial u^2}\right)^{-1}\left(\frac{\partial f}{\partial u}^T\right), \tag{5.41}$$

$$C = \left(\frac{\partial^2 H}{\partial x^2}\right) - \left(\frac{\partial^2 H}{\partial x \partial u}\right)\left(\frac{\partial^2 H}{\partial u^2}\right)^{-1}\left(\frac{\partial^2 H}{\partial u \partial x}\right). \tag{5.42}$$

All of these equations are evaluated along the reference extremal controlled trajectory computed earlier. We assume that the reference extremal is non-singular. This assumption is easily verified on the computed extremal.

5.4.1 Variational Equation of the Dynamics

The variational equations result from derivatives of the Hamiltonian for the state x and control u. In aerospace, these parameters have particular significance and are studied in depth by aerodynamic stability and control engineers.

Variational equations depend on the linearization of the trajectory, and, depending on which coefficients are considered independent, dimensionless coefficients take separate forms. For the system under consideration here, we obtain:

$$\begin{bmatrix} \frac{\mathrm{d}}{\mathrm{d}t}\left(\frac{\partial h}{\partial p}\right) \\ \frac{\mathrm{d}}{\mathrm{d}t}\left(\frac{\partial V}{\partial p}\right) \\ \frac{\mathrm{d}}{\mathrm{d}t}\left(\frac{\partial \gamma}{\partial p}\right) \end{bmatrix} = \begin{bmatrix} 0 & \sin\gamma & V\cos\gamma \\ 0 & -\frac{1}{m}\left(\frac{\partial \mathbb{D}}{\partial V}(V,\alpha)\right) & -g\cos\gamma \\ 0 & \frac{1}{mV}\left(\frac{\partial \mathbb{L}}{\partial V}(V,\alpha)\right) - \frac{1}{mV^2}\left(\mathbb{L}(V,\alpha) - mg\cos\gamma\right) & \frac{g}{V}\sin\gamma \end{bmatrix} \begin{bmatrix} \frac{\partial h}{\partial p} \\ \frac{\partial V}{\partial p} \\ \frac{\partial \gamma}{\partial p} \end{bmatrix} + \begin{bmatrix} 0 \\ -\frac{1}{m}\frac{\partial \mathbb{D}}{\partial \alpha}(V,\alpha) \\ \frac{1}{mV}\left(\frac{\partial \mathbb{L}}{\partial \alpha}(V,\alpha)\right) \end{bmatrix} \left(\frac{\partial \alpha}{\partial p}\right). \quad (5.43)$$

We will illustrate how the variational equations are the linear plant dynamics in aerospace. Like the static coefficients and dynamic coefficients, which were discussed in the previous chapter, engineers use "stability derivatives" which capture the sensitivity to state variables non-dimensionally.

For example, using the convention in [55], the term $\frac{\partial \mathbb{D}}{\partial V}$ can be rewritten in terms of force dimensional derivative sand stability derivatives. Utilizing the definition of C_D and C_L from the previous chapter, we can convert from body axis coefficients, C_x, C_z, to stability axis coefficients, C_D, C_L

$$\begin{aligned} \begin{bmatrix} \mathbb{D} \\ \mathbb{L} \end{bmatrix} &= \begin{bmatrix} -\cos\alpha & -\sin\alpha \\ \sin\alpha & -\cos\alpha \end{bmatrix} \begin{bmatrix} \bar{q}SC_x \\ \bar{q}SC_z \end{bmatrix} + T \begin{bmatrix} -\cos\alpha \\ \sin\alpha \end{bmatrix} \\ &= \begin{bmatrix} \frac{1}{2}\rho V^2 S C_D \\ \frac{1}{2}\rho V^2 S C_L \end{bmatrix} + T \begin{bmatrix} -\cos\alpha \\ \sin\alpha \end{bmatrix} \quad (5.44) \\ \frac{\partial \mathbb{D}}{\partial V} &= \rho V S C_d + \frac{1}{2}\rho V^2 S \frac{\partial C_d}{\partial V} = \frac{\frac{1}{2}\rho V^2 S}{V}\left(2C_d + V\frac{\partial C_d}{\partial V}\right). \quad (5.45) \end{aligned}$$

Since the drag coefficient C_D is non-dimensional, then $V\frac{\partial C_D}{\partial V}$ is non-dimensional and is called the speed damping derivative, C_{D_V},

$$C_{D_V} = V\frac{\partial C_D}{\partial V}.$$

The dimensional force is called D_V, and is defined as follows:

$$D_V = \frac{\frac{1}{2}\rho V^2 S}{V}\left(C_{D_V} + 2C_D\right). \tag{5.46}$$

Force dimensional derivatives are dimensionless accelerations. Since body X-axis acceleration is opposite to drag axis acceleration, we write this as:

$$X_V = -\frac{\frac{1}{2}\rho V^2}{mV} S\left(C_{D_V} + 2C_D\right). \tag{5.47}$$

Similarly, we can define for the lift terms:

$$C_{L_V} = V\frac{\partial C_L}{\partial V}, \qquad L_V = \frac{\frac{1}{2}\rho V^2}{V} S\left(C_{L_V} + 2C_L\right), \qquad Z_V = -\frac{1}{2}\frac{\rho V^2}{mV} S\left(C_{L_V} + 2C_L\right). \tag{5.48}$$

For the control derivatives:

$$\frac{\partial \mathbb{L}}{\partial \alpha} = \frac{1}{2}\rho V^2 S\frac{\partial C_L}{\partial \alpha} + T\cos\alpha, \tag{5.49}$$

$$\frac{\partial \mathbb{D}}{\partial \alpha} = \frac{1}{2}\rho V^2 S\frac{\partial C_D}{\partial \alpha} + T\sin\alpha. \tag{5.50}$$

We call C_{L_α} the lift curve slope, and we call C_{D_α} the drag curve slope:

$$C_{L_\alpha} = \frac{\partial C_L}{\partial \alpha}, \qquad C_{D_\alpha} = \frac{\partial C_D}{\partial \alpha}, \qquad L_\alpha = \frac{1}{2}\rho V^2 S\frac{\partial C_L}{\partial \alpha}, \qquad D_\alpha = \frac{1}{2}\rho V^2 S\frac{\partial C_D}{\partial \alpha}. \tag{5.51}$$

The force dimensionless coefficients are:

$$Z_\alpha = -\frac{1}{2}\frac{\rho V^2 S}{m}\frac{\partial C_L}{\partial \alpha}, \qquad X_\alpha = -\frac{1}{2}\frac{\rho V^2 S}{m}\frac{\partial C_D}{\partial \alpha}. \tag{5.52}$$

We substitute into the original equations (5.49) and (5.50) to yield:

$$\frac{1}{m}\frac{\partial \mathbb{L}}{\partial \alpha} = -Z_\alpha + \frac{T}{m}\cos\alpha \qquad \frac{1}{m}\frac{\partial \mathbb{D}}{\partial \alpha} = -X_\alpha + \frac{T}{m}\sin\alpha. \tag{5.53}$$

Thus, the exact variational equation of the dynamics is:

$$\begin{bmatrix} \frac{\mathrm{d}}{\mathrm{d}t}\left(\frac{\partial h}{\partial p}\right) \\ \frac{\mathrm{d}}{\mathrm{d}t}\left(\frac{\partial V}{\partial p}\right) \\ \frac{\mathrm{d}}{\mathrm{d}t}\left(\frac{\partial \gamma}{\partial p}\right) \end{bmatrix} = \begin{bmatrix} 0 & \sin\gamma & V\cos\gamma \\ 0 & X_V & -g\cos\gamma \\ 0 & -\frac{Z_V}{V} - \frac{1}{mV^2}\left(L + T\sin\alpha - mg\cos\gamma\right) & \frac{g}{V}\sin\gamma \end{bmatrix} \begin{bmatrix} \frac{\partial h}{\partial p} \\ \frac{\partial V}{\partial p} \\ \frac{\partial \gamma}{\partial p} \end{bmatrix} + \begin{bmatrix} 0 \\ X_\alpha - \frac{T}{m}\sin\alpha \\ -\frac{Z_\alpha}{V} + \frac{T}{mV}\cos\alpha \end{bmatrix} \frac{\partial \alpha}{\partial p}. \tag{5.54}$$

Typical linear flight control design simplifies the variational equation of the dynamics. Generally, unless at very low speed, the V^2 in the denominator will shrink terms. We can assume small flight path angles, $\gamma \simeq 0$. If desired, we can also assume small angle approximations for α. What results is a linear dynamical representation of the aircraft in terms of standard force dimensional derivatives,

$$\frac{\mathrm{d}}{\mathrm{d}t}\left(\frac{\partial x}{\partial p}\right) = \begin{bmatrix} 0 & \gamma & V \\ 0 & X_V & -g \\ 0 & -\frac{Z_V}{V} & \frac{g}{V}\gamma \end{bmatrix} \left(\frac{\partial x}{\partial p}\right) + \begin{bmatrix} 0 \\ X_\alpha + \frac{T}{m}\alpha \\ -\frac{Z_\alpha}{V} - \frac{T}{mV} \end{bmatrix} \frac{\partial \alpha}{\partial p}. \tag{5.55}$$

We use the true variational equation of the dynamics, (5.54), for perturbation feedback control.

5.4.2 The Variational Equation of the Adjoint Equations

The variational equation of the adjoint equations requires the calculation of

$$\frac{\partial^2 H}{\partial x^2}, \frac{\partial^2 H}{\partial x \partial u}, \frac{\partial^2 H}{\partial u^2}.$$

The matrix, $\frac{\partial^2 H}{\partial x^2}$, simplifies, because all partial derivatives with respect to h are zero:

$$\frac{\partial^2 H}{\partial h^2} = \frac{\partial^2 H}{\partial h \partial V} = \frac{\partial^2 H}{\partial \gamma \partial h} = \frac{\partial^2 H}{\partial \gamma \partial h} = \frac{\partial^2 H}{\partial V \partial h} = 0. \tag{5.56}$$

The remaining terms require calculation of the second derivatives of forces in lift and drag axes. For convenience, we write all terms here:

$$\frac{\partial^2 \mathbb{L}}{\partial V^2} = \rho S C_L + 2\rho S V \frac{\partial C_L}{\partial V} + \frac{1}{2}\rho V^2 S \frac{\partial C_L^2}{\partial V^2}, \tag{5.57}$$

$$\frac{\partial^2 \mathbb{D}}{\partial V^2} = \rho S C_D + 2\rho S V \frac{\partial C_D}{\partial V} + \frac{1}{2}\rho V^2 S \frac{\partial C_D^2}{\partial V^2}. \tag{5.58}$$

We define the dimensionless quantities $C_{L_{VV}}$ and $C_{D_{VV}}$:

$$C_{L_{VV}} = V^2 \frac{\partial^2 C_L}{\partial V^2}, \qquad C_{D_{VV}} = V^2 \frac{\partial^2 C_D}{\partial V^2}. \tag{5.59}$$

We define the second derivatives as D_{VV} and L_{VV} :

$$L_{VV} = \frac{\partial^2 \mathbb{L}}{\partial V^2} = \frac{\frac{1}{2}\rho V^2 S}{V^2}\left(2C_L + 4C_{L_V} + C_{L_{VV}}\right), \tag{5.60}$$

$$D_{VV} = \frac{\partial^2 \mathbb{D}}{\partial V^2} = \frac{\frac{1}{2}\rho V^2 S}{V^2}\left(2C_D + 4C_{D_V} + C_{D_{VV}}\right). \tag{5.61}$$

We define force dimensional 2nd derivatives as follows:

$$Z_{VV} = -\frac{\frac{1}{2}\rho V^2 S}{mV^2}\left(2C_L + 4C_{L_V} + C_{L_{VV}}\right), \tag{5.62}$$

$$X_{VV} = -\frac{\frac{1}{2}\rho V^2 S}{mV^2}\left(2C_D + 4C_{D_V} + C_{D_{VV}}\right). \tag{5.63}$$

Similarly, we define the following terms:

$$\frac{\partial^2 \mathbb{L}}{\partial \alpha^2} = \frac{1}{2}\rho V^2 S \frac{\partial^2 C_L}{\partial \alpha^2} - T\sin\alpha, \qquad \frac{\partial^2 \mathbb{D}}{\partial \alpha^2} = \frac{1}{2}\rho V^2 S \frac{\partial^2 C_D}{\partial \alpha^2} - T\cos\alpha, \tag{5.64}$$

$$C_{L_{\alpha\alpha}} = \frac{\partial^2 C_L}{\partial \alpha^2}, \qquad C_{D_{\alpha\alpha}} = \frac{\partial^2 C_D}{\partial \alpha^2}, \tag{5.65}$$

$$L_{\alpha\alpha} = \frac{1}{2}\rho V^2 S \frac{\partial^2 C_L}{\partial \alpha^2}, \qquad D_{\alpha\alpha} = \frac{1}{2}\rho V^2 S \frac{\partial^2 C_L}{\partial \alpha^2}, \tag{5.66}$$

$$Z_{\alpha\alpha} = -\frac{1}{2}\frac{\rho V^2 S}{m}\frac{\partial^2 C_L}{\partial \alpha^2}, \qquad X_{\alpha\alpha} = -\frac{1}{2}\frac{\rho V^2 S}{m}\frac{\partial^2 C_L}{\partial \alpha^2}, \tag{5.67}$$

$$\frac{1}{m}\frac{\partial^2 \mathbb{L}}{\partial \alpha^2} = -Z_{\alpha\alpha} - T\sin\alpha, \qquad \frac{1}{m}\frac{\partial^2 \mathbb{D}}{\partial \alpha^2} = -X_{\alpha\alpha} - T\cos\alpha. \tag{5.68}$$

For the mixed derivatives, define the dimensionless coefficients:

$$C_{D_{V\alpha}} = V\frac{\partial^2 C_D}{\partial V \partial \alpha}, \qquad C_{L_{V\alpha}} = V\frac{\partial^2 C_L}{\partial V \partial \alpha}. \tag{5.69}$$

With these coefficients, the subsequent terms are similar to the other second partial derivatives:

$$\frac{\partial^2 \mathbb{L}}{\partial \alpha \partial V} = \frac{\frac{1}{2}\rho V^2 S}{V}\left(2C_{L_\alpha} + C_{L_{V\alpha}}\right), \qquad \frac{\partial^2 \mathbb{D}}{\partial \alpha \partial V} = \frac{\frac{1}{2}\rho V^2 S}{V}\left(2C_{D_\alpha} + C_{D_{V\alpha}}\right), \tag{5.70}$$

$$L_{V\alpha} = \frac{\frac{1}{2}\rho V^2 S}{V}\left(2C_{L_\alpha} + C_{L_{V\alpha}}\right), \qquad D_{V\alpha} = \frac{\frac{1}{2}\rho V^2 S}{V}\left(2C_{D_\alpha} + C_{D_{V\alpha}}\right), \tag{5.71}$$

$$Z_{V\alpha} = -\frac{\frac{1}{2}\rho V^2 S}{mV}\left(2C_{L_\alpha} + C_{L_{V\alpha}}\right), \qquad D_{V\alpha} = -\frac{\frac{1}{2}\rho V^2 S}{mV}\left(2C_{D_\alpha} + C_{D_{V\alpha}}\right). \tag{5.72}$$

These calculations can be substituted into the second derivatives of the Hamiltonian:

$$\begin{aligned}\frac{\partial^2 H}{\partial V^2} &= \lambda_V\left[-\frac{1}{m}\left(\frac{\partial^2 \mathbb{D}}{\partial V^2}(V,\alpha)\right)\right] \\ &\quad + \lambda_\gamma\left[\frac{1}{mV}\frac{\partial^2 \mathbb{L}(V,\alpha)}{\partial V^2} - \frac{1}{mV^2}\left(\frac{\partial \mathbb{L}(V,\alpha)}{\partial V}\right) + \frac{2}{mV^3}\left(\mathbb{L}(V,\alpha) - mg\cos\gamma\right)\right],\end{aligned} \tag{5.73}$$

$$\frac{\partial^2 H}{\partial \gamma \partial V} = \frac{\partial^2 H}{\partial V \partial \gamma} = \lambda_h\left[\cos\gamma\right] + \lambda_\gamma\left[-\frac{g}{V^2}\sin\gamma\right], \tag{5.74}$$

$$\frac{\partial^2 H}{\partial \gamma^2} = \lambda_h\left[-V\sin\gamma\right] + \lambda_V\left[g\sin\gamma\right] + \lambda_\gamma\left[\frac{1}{V}\left(g\cos\gamma\right)\right]. \tag{5.75}$$

The equations are combined in (5.76),

$$H_{xx} = \begin{bmatrix} 0 & 0 & 0 \\ 0 & H_{VV} & H_{V\gamma} \\ 0 & H_{\gamma V} & H_{\gamma\gamma} \end{bmatrix}. \tag{5.76}$$

We assume that H_{xu} and H_{ux} are both at least C^1. As a result, we can take advantage of their symmetry. Accordingly, the terms, $\frac{\partial^2 H}{\partial h \partial \alpha}$ and $\frac{\partial^2 H}{\partial \gamma \partial \alpha}$, vanish, and combining the three equations yields the mixed second derivative of the Hamiltonian:

$$\frac{\partial^2 H}{\partial x \partial \alpha} = \begin{bmatrix} \\ \lambda_V \left[-\frac{1}{m} \left(\frac{\partial^2 \mathbb{D}}{\partial \alpha \partial V} (V, \alpha) \right) \right] + \lambda_\gamma \left[\frac{1}{mV} \left(\frac{\partial^2 \mathbb{L}(V,\alpha)}{\partial \alpha \partial V} \right) - \frac{1}{mV^2} \left(\frac{\partial \mathbb{L}(V,\alpha)}{\partial \alpha} \right) \right] \\ \\ \end{bmatrix}. \begin{matrix} 0 \\ \\ 0 \end{matrix}$$

5.4.3 Variational Equation of the Minimizer Condition

We calculate the second variation of the Hamiltonian with respect to the control, H_{uu} :

$$H_{uu} = \lambda_V \left[-\frac{1}{m} \frac{\partial^2 \mathbb{D}(V, \alpha)}{\partial \alpha^2} \right] + \lambda_\gamma \left[\frac{1}{mV} \left(\frac{\partial^2 \mathbb{L}(V, \alpha)}{\partial \alpha^2} \right) \right]. \tag{5.77}$$

5.4.4 The Riccati Equations

Differentiating the terminal constraint and clock constraint yields additional variational equations for the transversality condition. The variational equations, as previously stated, yield not only sufficient conditions, but also Riccati matrices for perturbation feedback control.

At the terminal constraint, the variational equations assume that perturbations in the state, control parameters, and terminal time relate linearly to perturbations in the adjoint, terminal

constraint, and clock constraint (see 3.5.2):

$$\begin{bmatrix} \frac{\partial \lambda}{\partial p} \\ \frac{\partial \psi}{\partial p} \\ 0 \end{bmatrix} = \begin{bmatrix} \frac{\partial^2 \Upsilon}{\partial x^2} & \left(\frac{\partial \psi}{\partial x}\right)^T & \frac{\partial \Omega}{\partial x} \\ \frac{\partial \psi}{\partial x} & 0 & \frac{\mathrm{d}\psi}{\mathrm{d}t} \\ \frac{\partial \Omega}{\partial x} & \left(\frac{\mathrm{d}\psi}{\mathrm{d}t}\right)^T & \frac{\mathrm{d}\Omega}{\mathrm{d}t} \end{bmatrix} \begin{bmatrix} \frac{\partial x}{\partial p} \\ \frac{\partial \nu}{\partial p} \\ \frac{\partial T}{\partial p} \end{bmatrix}. \tag{5.78}$$

From the terminal condition, with the clock constraint satisfied, the Riccati matrices evolve backwards to the current time. This integration occurs along the reference extremal, Γ_0, which is produced by the numerical procedure for calculating a candidate extremal. The grouping of the matrices defined above yields the following feedback implementation:

$$\dot{S} = -SA - A^T S - SBS + C, \tag{5.79}$$

$$\dot{\mathcal{R}} = \mathcal{R}(-A + BS), \tag{5.80}$$

$$\dot{\mathcal{Q}} = \mathcal{R}B\mathcal{R}^T. \tag{5.81}$$

As before, we have the following differential equations

$$\dot{R} = R(-A + BS), \qquad \dot{r} = r(-A + BS), \tag{5.82}$$

$$\dot{Q} = RBR^T, \qquad \dot{q} = RBr^T \tag{5.83}$$

$$\dot{a} = rBr^T, \tag{5.84}$$

and these matrices are grouped into $\mathcal{Q}$ and $\mathcal{R}$ as follows:

$$\mathcal{Q}(t,p) = \begin{bmatrix} Q(t,p) & q(t,p) \\ q^T(t,p) & a(t,p) \end{bmatrix}, \qquad \mathcal{R}(t,p) = \begin{bmatrix} R(t,p) \\ r(t,p) \end{bmatrix}. \tag{5.85}$$

5.5 Perturbation Feedback Control

From the perturbation equations to second order, we have the matrices, which are by now known quantities. We will refer to the matrix command perturbations as $\delta\psi, \delta\Omega$, which

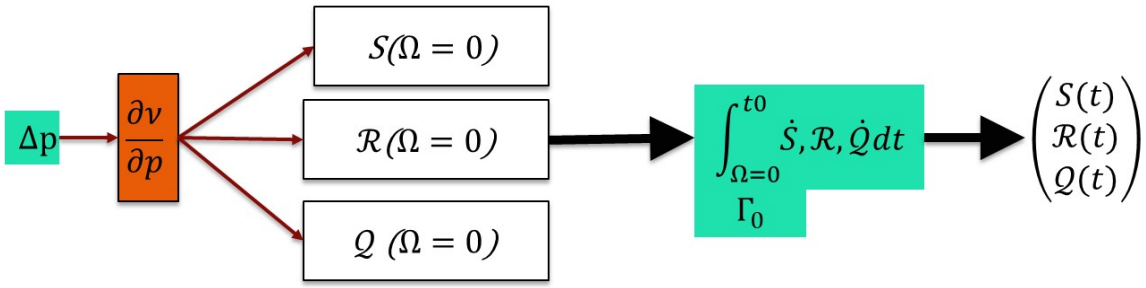

Figure 5.5: The calculation of Riccati matrices

represent the changes in the constraints with respect to the reference trajectory.

$$\begin{bmatrix} \frac{\partial \lambda}{\partial p} \\ \delta\psi \\ \delta\Omega \end{bmatrix} = \begin{bmatrix} \mathcal{S} & \mathcal{R}^T \\ \mathcal{R} & \mathcal{Q} \end{bmatrix} \begin{bmatrix} \frac{\partial x}{\partial p} \\ \frac{\partial \nu}{\partial p} \\ \frac{\partial T}{\partial p} \end{bmatrix} \tag{5.86}$$

Using this notation, we can calculate the time-varying feedback control gains:

$$\begin{bmatrix} \frac{\partial \nu}{\partial p} \\ \frac{\partial T}{\partial p} \end{bmatrix} = \mathcal{Q}^{-1} \left(\begin{bmatrix} \delta\psi \\ \delta\Omega \end{bmatrix} - \mathcal{R} \frac{\partial x}{\partial p} \right). \tag{5.87}$$

This allows for an explicit formula for the variations in terms of the shadow prices:

$$\frac{\partial \lambda}{\partial p} = \mathcal{S} - \mathcal{R}\mathcal{Q}^{-1} \left(\begin{bmatrix} \delta\psi \\ \delta\Omega \end{bmatrix} - \mathcal{R} \frac{\partial x}{\partial p} \right). \tag{5.88}$$

Substituting this allows us to directly implement it in the reduced variational equations, as follows:

$$\frac{\partial u}{\partial p} = \frac{\partial^2 H}{\partial u^2}^{-1} \frac{\partial f}{\partial u}^T \left(\mathcal{S} - \mathcal{R}\mathcal{Q}^{-1} \left(\begin{bmatrix} \delta\psi \\ \delta\Omega \end{bmatrix} - \mathcal{R} \frac{\partial x}{\partial p} \right) \right). \tag{5.89}$$

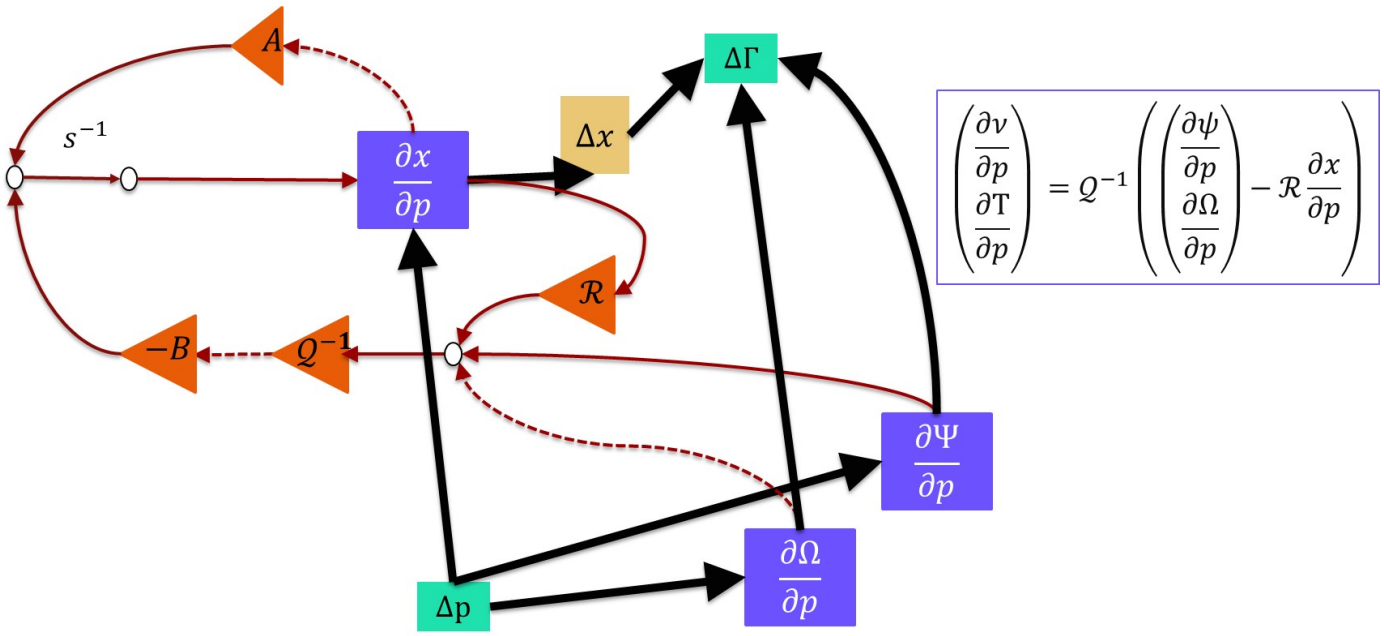

Figure 5.6: The feedback control with Riccati gain matrices demonstrates flow of information to generate neighboring optimum solutions. Black arrows show path from a perturbation to a new reference extremal.

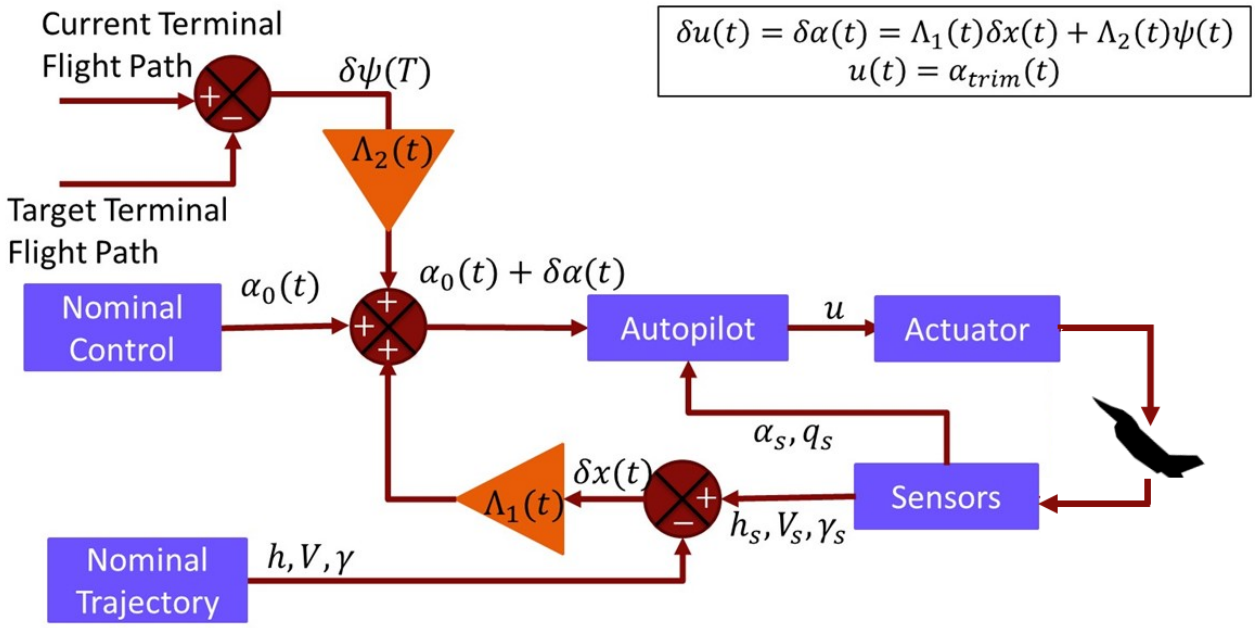

Figure 5.7: The control system divides the dynamics into fast and slow dynamics. The fast dynamics, which are the angle of attack and pitch rate signals, are handled by an autopilot. The slow dynamics, which are the altitude, fight path angle, and speed, are handled by the perturbation feedback guidance control law.

5.6 Results

5.6.1 Solver Performance During Calculation of Nominal Trajectories

Figures 5.8 and 5.9 present graphs of the solver progress as it constructs an extremal, to demonstrate how the solver progresses with each iteration, the maximum number of allowable guesses was increased to 50 guesses for each of the four unknown parameters, $T, \lambda_h(0)$, $\lambda_\gamma(0)$, and $\lambda_V(0)$. The trajectories evolve from dark blue (indicating the initial extremal) to gold (indicating the final extremal).

By guessing the initial parameters, the solver initially iterates towards an optimal solution without difficulty. This convergence rapidly approaches the steady-state nominal trajectory, as is visualized in the altitude graphs, in Figure 5.8, where hardly more than two blue trajectories are visible.

For these effective initial guesses, the solver rapidly converges. However, when the initial conditions are perturbed significantly from these initial values, the solver struggles to find an optimum solution.

Like other shooting algorithms, the solver suffers from a tendency to overshoot the solution. For example, it is clear from the first graph in Figure 5.9 that the constant value is extremely sensitive. This can be inferred from the orange blurring near the bottom of the graph, which indicates many iterations. The step size needs to be reduced to ensure that the trajectory converges and that solutions will not iterate to excessively large values in the adjoint variables.

After considerable effort, one key observation facilitates solver convergence. Guesses on the adjoint variables should be restricted to a range of reasonable values. The adjoint variables are restricted to remain negative and a limit that is one order of magnitude larger than what was observed during iterations is placed on each. If the solver remains stuck at a limit, the limits are expanded. Generally, if any of the unknown variables saturated at a limit, it indicates no hope of convergence, and the solver will need to be restarted.

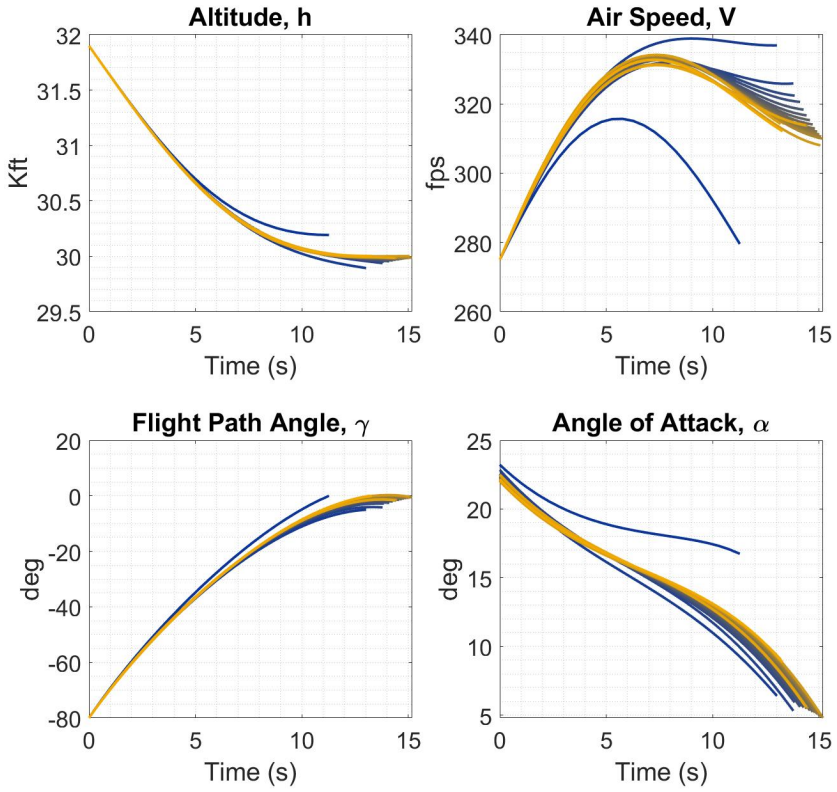

Figure 5.8: The solver iterates to an optimum solution in 10 steps. It starts from blue trajectories and transitions to orange ones. The solver nearly converges in the first 4 steps.

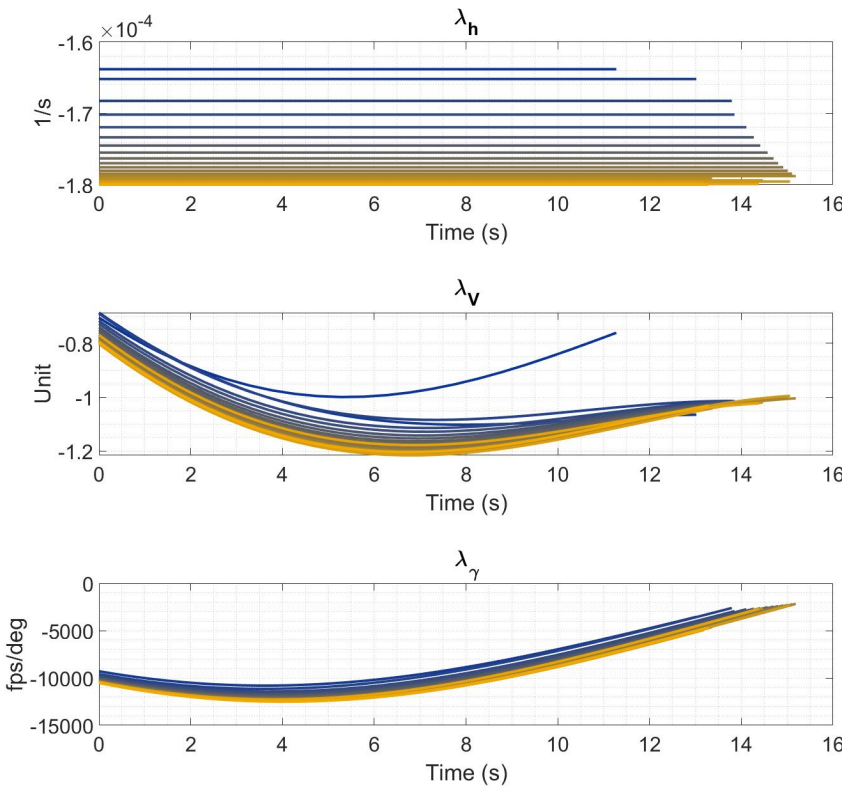

Figure 5.9: The adjoint time histories show the starting guesses, and the terminal times can be observed by comparing the lengths of blue and orange guesses.

Evolutions in the final times are visible in the lengths of the plot traces. The solver initially increases the time required towards 15s and then decreases settling on a value near 14s in Figure 5.9. The final time variable needed a restriction to exclude unreasonably small or unreasonably long final times.

A final issue afflicting solver progress can be observed in Figure 5.9 by examining the y-axis of each graph. The scales of each adjoint variable differ in orders of magnitude; the same is true for the state variables. One improvement that could be made to the solver would be to remove the dimension from the equations by scaling all the variables to unit dimension. Determining an appropriate step size that works for each variables perturbations proves challenging.

5.6.2 An Example of Failure to Find a Locally Optimal Solution

Even when the solver converged on an extremal solution, there was no guarantee that the solution was a local minimum. The algorithm developed in this dissertation allows us to determine if this occurs.

Here, we give an example which shows that much can go wrong. If the block matrix, $\mathcal{Q}$, loses rank earlier than the final time, the computed reference trajectory has a conjugate point. In this case, the trajectory is not locally optimal.

In spite of this, if one attempts to use PFC guidance, then the feedback control oscillates abruptly. Figure 5.14 demonstrates an example of oscillation where the extremal satisfies the necessary conditions, but the matrix $\mathcal{Q}$ changes signs twice before the final time.

The figure depicts two suboptimal extremal trajectories. "OC" is the original reference trajectory. "POC" is another extremal trajectory starting from perturbed initial condition to a perturbed terminal condition. Another trajectory, labelled "PFC," starts with the reference angle of attack profile of "OC" and the initial conditions of "POC." The "PFC" trajectory dynamically corrects it's flight path to maximize terminal speed using PFC guidance.

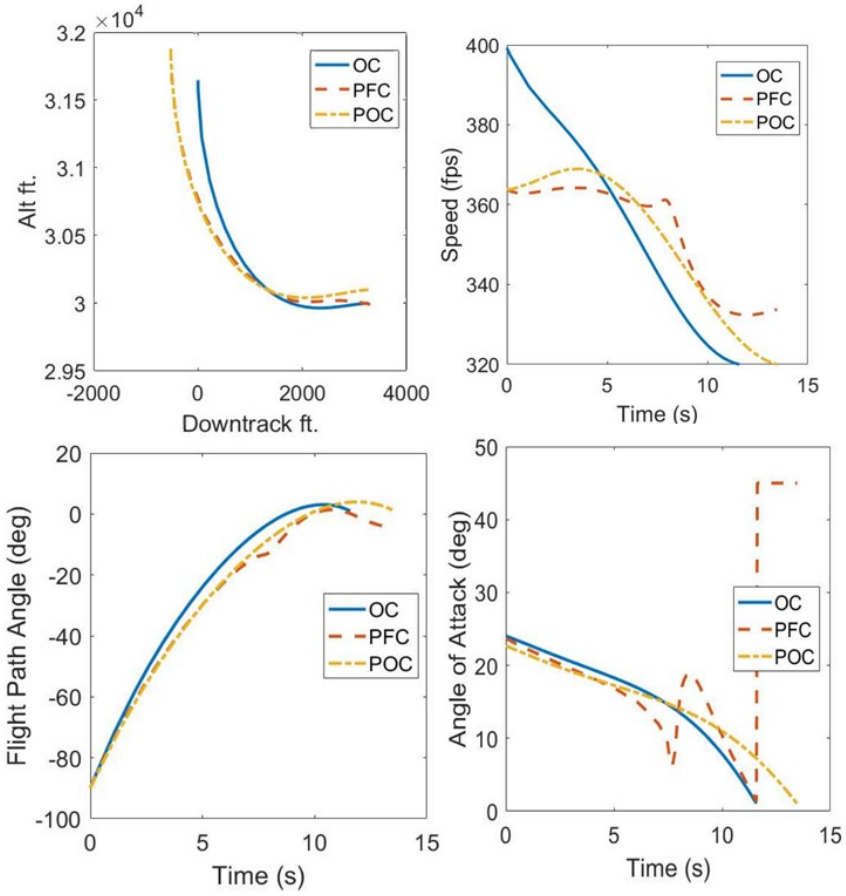

Figure 5.10: The states for a optimization procedure when the extremal is not locally optimal.

Since the reference trajectory "OC" passes through a conjugate point, the control oscillates, and eventually saturates at the maximum available angle of attack command. The abrupt changes occur when $\mathcal{Q}$ loses rank.

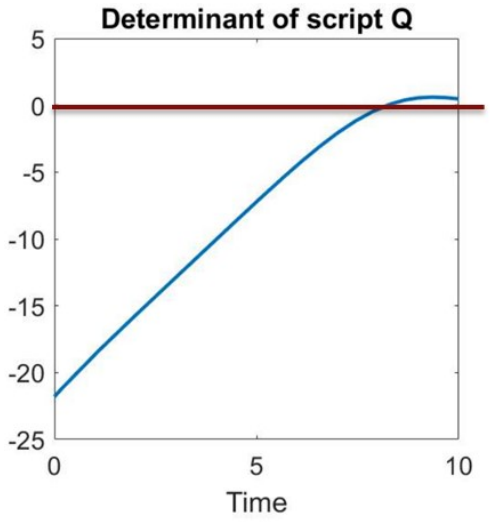

Figure 5.11: The determinant of the block matrix $\mathcal{Q}$ crosses zero before the final time for the reference extremal in this example.

Figure 5.11 reveals that the first 10s of the nominal extremal time history could not be optimal. This is because of the conjugate point. *The failure highlights the importance of not only computing an extremal, but also verifying satisfaction of second order conditions of local optimality.* The practical value of the sufficiency conditions can serve as diagnostic checks for the quality of a solution, even if one does not seek to use perturbation feedback control.

5.6.3 Application of Perturbation Feedback Control

Figure 5.12 compares a perturbation feedback guidance scheme against two trajectories which are not aided by the guidance scheme. Similar to the example in the previous discussion, two reference optimal trajectories starting from different initial conditions, labeled optimal control (OC) and perturbed optimal control (POC), use two separate optimal angle of attack schedules to maneuver to separate terminal conditions. Another trajectory uses the OC angle of attack schedule, starting from the POC initial condition, to maneuver to the POC terminal condition.

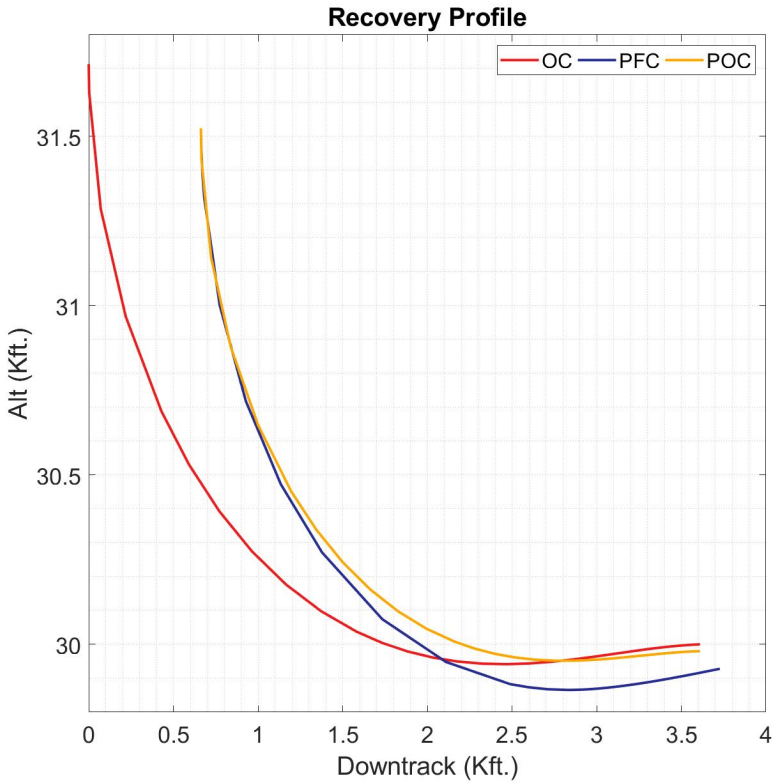

Figure 5.12: Three recovery profiles. OC is the reference optimum trajectory. The POC trajectory is another optimum trajectory with a perturbed initial condition that flies a perturbed terminal condition. The PFC trajectory uses the reference angle of attack profile starting from the POC trajectory. The PFC uses perturbation feedback control to become a neighboring extremal.

The purpose of the simulations depicted in Figure 5.12 is to evaluate whether the PFC feedback control scheme can transition the aircraft from one locally optimal extremal to a nearby locally optimal extremal. The PFC trajectory corrects towards an extremal that terminates near the perturbed terminal condition starting using the suboptimal reference command. In the figure, one can see that the the PFC trajectory does not satisfy the POC terminal constraint exactly.

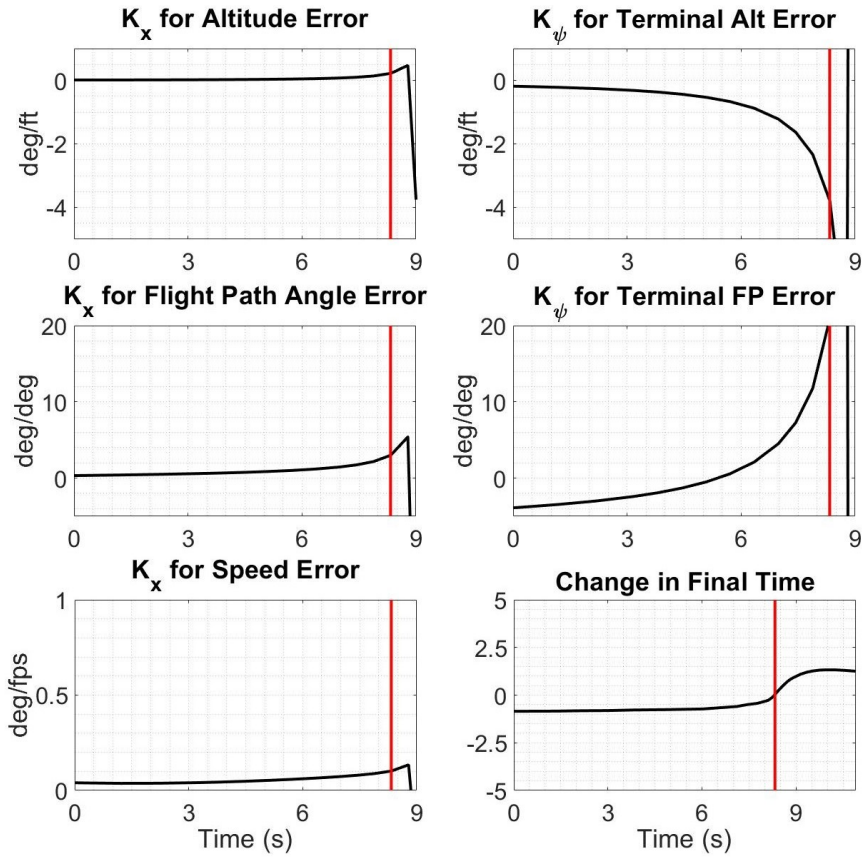

Figure 5.13: The gain schedules evolve with time along the trajectory. The red lines show the point where gains were frozen, corresponding to when the estimated change in the final time changes signs. After that time, the frozen gains prevent information from singular Riccati matrices from corrupting the angle of attack commands.

The OC and POC simulations terminate when they reach the optimal stopping times determined by the numerical procedure which determines the nominal trajectory. The PFC trajectory terminates at the minimum of the OC and POC simulations. The reason for this

is that the aircraft "runs out of gains" as observed in [34]. The control scheme employs the error between the reference trajectory and the optimal trajectory as a feedback.

Practically, at the point where the aircraft runs out of gains in an empirical implementation, the control scheme either needs to hold the terminal value of the reference trajectory, extrapolate from it to continue the maneuver, or switch to a FPAH autopilot or similar automatic function. Switching to another autopilot control system would indicate that aggressive maneuvering is no longer required to save the aircraft and pilot.

Figure 5.13 plots the time-varying feedback gains for the PFC trajectory. A red line in each graphs depicts the moment when the gain schedule gains grow too large for a practical implementation. The threshold to determine this point was selected to be the instant that the estimated change in the final time (the 6th subplot) changes sign.

As discussed in the example of the minimum energy control in Chapter 2, singularities at the terminal time occur for linear optimal control laws near the terminal time. Singularities are essentially guaranteed at the final time, when the matrix $\mathcal{Q}$ becomes singular. Since the gains are pre-scheduled along the trajectory, all of the gains grow as time approaches the terminal time.

Another observation from Figure 5.13 is that the feedback gains related to the terminal condition grow far larger than those from the feedback control. This indicates that, as the terminal condition approaches, large corrections are required to satisfy the terminal constraint. As a result, the feedback gains in the γ and h terminal errors are an order of magnitude larger than the feedback gains for these errors in the nominal trajectory.

Figure 5.14 plots the state variables and the control in time-histories. The altitude traces demonstrate that the PFC trajectory overshoots the desired altitude floor for the POC trajectory, and also overshoots the desired terminal flight path angles. While it does not achieve the constraints starting from an off-nominal condition, it does maximize the terminal speed relative to the other trajectories.

The figure shows that all trajectories fall approximately 1500 feet before reaching the terminal condition, and the flight path angle levels out in all cases. The flight path angle almost linearly increases for the majority of the trajectory, and the angle of attack curves all feature

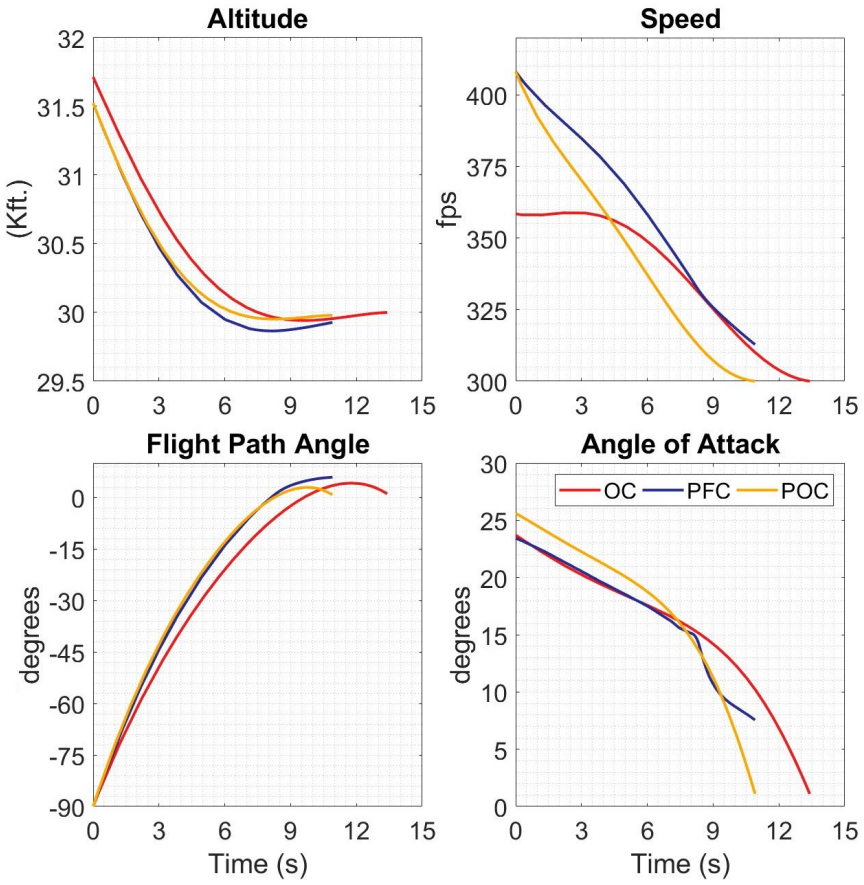

Figure 5.14: The reference optimum (OC), the perturbed optimum (POC), and the perturbation feedback control (PFC) trajectories plotted against time. The POC trajectory changes its angle of attack to match the POC, starting with the reference commands from the OC trajectory.

an “elbow” in the curve. The speed curves all appear smooth, and the PFC trajectory minimizes the OC trajectory throughout its flight. In essence, the state variables, the control, and the performance criterion all demonstrate desirable behavior through the trajectory.

These results indicate that the algorithm can be an effective design tool for time-varying maneuvers. As stated earlier, we must be careful to ensure that second order conditions are satisfied and that we take reasonable precautions to ensure that gains do not grow too large.

One can schedule the maneuvers as a function of flight condition and approximate the nominal trajectories by polynomials to save memory in a practical implementation. The PFC guidance scheme can then patch the holes in the gain schedule. The algorithm could then create control for the aircraft along trajectories that would be too expensive to store or compute.

Chapter 6

Conclusions and Future Directions

In this chapter, we consider the extension of perturbation feedback control to optimal control problems with constraints on the control and state variables. We seek to extend the procedure discussed in prior chapters to path-constrained extremal trajectories. We use formulas for the variational equations found in [45], [46], and [47]. We present a simple example of perturbation feedback control applied to the F-16's ground-collision system. We discuss practical improvements to the shooting method that calculate the reference trajectory.

6.1 An Informal Summary of Optimal Control with State-Variable Inequality Constraints

An optimal control problem's necessary conditions change significantly with the inclusion of control constraints and state constraints. Constraints dictate the evolution of the dynamics, requiring admissible trajectories to remain tangent to the constraint. Resultantly, trajectories may separate into intervals where constraints are active or inactive.

The control of a constrained trajectory often switches. As a result, corners, which are a discontinuities in the control that results from the joining of extremal segments, often arise in these trajectories. Multipliers can jump to new values at these corners, requiring modification of the maximum principle provided in this dissertation. These jumps satisfy the transversality conditions occurring at interior-points of trajectories (in contrast to terminal

points of trajectories). Locally optimal segments of trajectories glue together, in concatenations, to construct optimal trajectories. For example, [44] extends sufficient conditions to families of broken extremals.

Here, we discuss two types of constraints. One is a pure-state constraint, which is a function of only the time and state, t and x, *i.e.*:

$$S(t,x) \leq 0. \tag{6.1}$$

The other is a mixed control-state constraint, $C(t,x,u) \leq 0$, which is a function of the state, the control, and the time, t, x, and u,

A pure-state constraint imposes a mixed control-state constraint. This is because we employ a process of repeated total differentiation to derive a mixed-state constraint,

$$C(t,x,u) = S^q(t,x,u) \leq 0, \tag{6.2}$$

where q refers to the number of total differentiations.

From [28], this procedure follows:

$$\mathbb{S}(t,x) = \begin{bmatrix} \frac{\mathrm{d}}{\mathrm{d}t}^0 S(t,x) \\ \frac{\mathrm{d}}{\mathrm{d}t}^1 S(t,x) \\ \vdots \end{bmatrix},$$

where we continue to differentiate using the chain rule and the dynamics, $\dot{x} = f(t,x,u)$. This procedure terminates when the control appears explicitly, for the first time, in one of the differential algebraic relations, referred to as a qth order state-constraint. The set of constraints, $\mathbb{S}(t,x)$, are the tangency conditions [34]. Tangency conditions $\mathbb{S}(t,x)$ need to be satisfied to remain admissible, yielding interior-point transversality conditions.

We will only consider first order constraints in this discussion. As a result,

$$S(t,x) = \mathbb{S}(t,x),$$

and we can refer to the state constraint and tangency constraints as $S(t,x)$. We can refer to the imposed mixed state-control constraint as $C(t,x,u)$.

A concise statement of the optimal control problem with state-variable inequality constraints follows:

[OCVIC] Minimize the objective, $J = J(u)$, $J = \min \int_{t_0}^{T} L(t,x,u)\mathrm{d}t + \phi(x(T),T)$, over all admissible, controlled trajectories (x,u), subject to the constraints $(T,x(T)) \in N$ and $S(t,x) \leq 0$, during the interval $[t_0,T]$.

A survey of necessary and sufficient conditions for a problem of this type appears in [28], where the informal maximum principle gives the necessary conditions for optimal control problems with path constraints.

6.2 An Example of Constrained Feedback Control

We include an example of an explicit, nonlinear feedback law in the presence of path constraints to motivate an implicit, nonlinear feedback law. The Bounded Brachistochrone problem (**BB**) modifies the original Brachistochrone problem to include a state constraint. The **BB** problem used in this dissertation emerges from [52], [24], and [49]. Its nonlinear feedback laws is from [52]. Also, [54] describes procedure to calculate the constrained arc in the problem.

We wish to transfer the system defined by

$$\dot{E} = V\cos\gamma, \qquad \dot{U} = V\sin\gamma, \qquad \dot{V} = g\sin\gamma. \tag{6.3}$$

from the initial condition, $x_0 = (E_0, U_0, V_0)$ to the line $E(T) - \ell$. The path this system takes depends on the following state constraint:

$$S(t,x) = y - x\tan\theta - h \leq 0. \tag{6.4}$$

We seek the flight path angles, γ, which accomplish this transfer in the minimum time. That is, we seek to minimize the final time, T.

If the trajectory enters the state-constraint, the control takes the value

$$\gamma(t) = \theta, \quad t \in [t_1, t_2],$$

where the times of entry and exit into the constraint are t_1 and t_2 respectively, because

$$\dot{S} = V \sin\gamma - V \cos\gamma \tan\theta = \frac{V \sin\gamma \cos\theta - V \cos\gamma \sin\theta}{\cos\theta} = V \sec\theta \sin(\gamma - \theta). \tag{6.5}$$

From [52], an explicit nonlinear feedback solution for the unconstrained problem depends on the dimensionless state, α_1,

$$\alpha_1(t_0) = g\frac{(\ell - x(t_0))}{v(t_0)^2}, \tag{6.6}$$

that is used in the following relation:

$$\alpha_1(t_0) = \frac{\gamma(t_0)\left(\sec\gamma(t_0)\right)^2 + \tan\gamma(t_0)}{2}. \tag{6.7}$$

From [52], an explicit nonlinear feedback solution for the constrained problem additionally includes a dimensionless state, α_2,

$$\alpha_2(t_0) = g\frac{(y(t_0) - h - x(t_0)\tan\theta)}{V(t_0)^2}, \tag{6.8}$$

that is used in the following relation:

$$\alpha_2(t_0) = \frac{(\gamma(t_0) - \theta)\tan\theta \sec\gamma(t_0)^2 + \tan\theta\tan\gamma(t_0) - (\tan\gamma(t_0))^2}{2}. \tag{6.9}$$

The control law switches from (6.8) to (6.9) depending on the location in a reduced state space of (α_1, α_2).

While these formulas give an analytical and exact answer, they are transcendental. Their computation online would be difficult. In the future, we would like to derive formulas that accomplish the same control implicitly, using linear feedback control. We postulate what

this linear constrained feedback law would look like by modifying the sweep method in the next section.

6.3 Path Constrained Perturbation Feedback Control

As before, we wish to rewrite the multipliers in the formulas in terms of the terminal constraints. This constructs a feedback law described purely in terms of the current state and current values of the constraints, which dynamically varies with the trajectories.

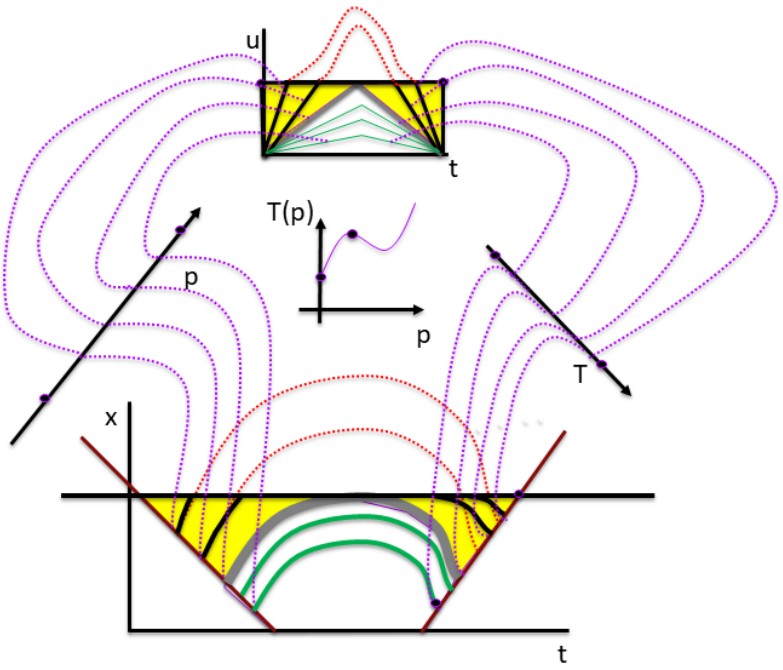

Figure 6.1: A hypothetical parameterization for **OCSVIC**

We imagine Figure 6.1, where trajectories transition from path-unconstrained to path-constrained depending on their location in (t, x) space. The above diagram illustrates this feature hypothetically. In the fixed terminal time constraint, trajectories collapse to a single point; in an active path constraint, trajectories collapse to a single path. Everywhere in (t, x) space, except on the path constraint, each trajectory can be uniquely defined by the final time. In the yellow area with the boundary of a gray trajectory, trajectories with active

path constraints touch the boundary at exactly 1 point. The red lines represent the path-unconstrained trajectory, which starts with initial conditions in the constrained region. One set of variational equations holds in the yellow region, and a distinct set holds elsewhere. Their parameterization is only valid between the black dots. With this picture in mind, we can proceed to formulas.

The variational equations describing the trajectories starting and finishing in the yellow region of 6.1 are found in [46]. They differ from the trajectories starting and finishing in the white region, because for a trajectory to remain on a state constraint, which explicitly determines the control:

$$C(x(t;p),u(t;p)) = 0. \tag{6.10}$$

However, if we seek to determine the control *implicitly*, we differentiate the mixed-state constraint,

$$\frac{\partial C}{\partial x}(x,u)\left(\frac{\partial x}{\partial p}\right) + \frac{\partial C}{\partial x}(x,u)\left(\frac{\partial u}{\partial p}\right) = 0, \tag{6.11}$$

and solve for the variations in the control:

$$\left(\frac{\partial u}{\partial p}\right) = -\left(\frac{\partial C}{\partial u}(x,u)\right)^{-1}\left(\frac{\partial C}{\partial x}(x,u)\right)\left(\frac{\partial x}{\partial p}\right). \tag{6.12}$$

From [46], we can use the procedure described earlier in the dissertation. This procedure gives:

$$\frac{\mathrm{d}}{\mathrm{d}t}\left(\frac{\partial x}{\partial p}\right) = \frac{\partial f}{\partial x}\left(\frac{\partial x}{\partial p}\right) + \frac{\partial f}{\partial u}\left(\frac{\partial u}{\partial p}\right), \tag{6.13}$$

$$\frac{\mathrm{d}}{\mathrm{d}t}\left(\frac{\partial \lambda}{\partial p}\right) = -\frac{\partial^2 H}{\partial x^2}\left(\frac{\partial x}{\partial p}\right) - \frac{\partial^2 H}{\partial x \partial u}\left(\frac{\partial u}{\partial p}\right) - \frac{\partial f^T}{\partial x}\left(\frac{\partial \lambda}{\partial p}\right) - \frac{\partial C^T}{\partial x}\left(\frac{\partial \mu}{\partial p}\right). \tag{6.14}$$

Differentiation with respect to the control gives variational equations which describe how changes in the control should occur with changes in the parameter,

$$0 = \frac{\partial^2 H}{\partial u \partial x}\left(\frac{\partial x}{\partial p}\right) + \frac{\partial^2 H}{\partial u^2}\left(\frac{\partial u}{\partial p}\right) + \frac{\partial f^T}{\partial u}\left(\frac{\partial \lambda}{\partial p}\right) + \frac{\partial C}{\partial u}\left(\frac{\partial \mu}{\partial p}\right). \tag{6.15}$$

This can be solved for variations in the Lagrange multiplier, μ :

$$\frac{\partial \mu}{\partial p} = -\left(\frac{\partial C}{\partial u}\right)^{-1}\left(\frac{\partial^2 H}{\partial u \partial x}\frac{\partial x}{\partial p} + \frac{\partial^2 H}{\partial u^2}\frac{\partial u}{\partial p} + \frac{\partial f^T}{\partial u}\frac{\partial \lambda}{\partial p}\right). \tag{6.16}$$

We can eliminate variations in the control and variations in the state

$$\frac{\mathrm{d}}{\mathrm{d}t}\left(\frac{\partial x}{\partial p}\right) = \left(\frac{\partial f}{\partial x} - \frac{\partial f}{\partial u}\left(\frac{\partial C}{\partial u}\right)^{-1}\frac{\partial C}{\partial x}\right)\left(\frac{\partial x}{\partial p}\right), \tag{6.17}$$

$$\begin{aligned}\frac{\mathrm{d}}{\mathrm{d}t}\left(\frac{\partial \lambda}{\partial p}\right) =& \left(-\frac{\partial^2 H}{\partial x^2} + \frac{\partial^2 H}{\partial x \partial u}\left(\frac{\partial C}{\partial u}\right)^{-1}\left(\frac{\partial C}{\partial x}\right) + \frac{\partial C^T}{\partial x}\left(\frac{\partial C}{\partial u}\right)^{-1}\frac{\partial^2 H}{\partial u \partial x},\right. \\ &- \frac{\partial C^T}{\partial x}\left(\frac{\partial C}{\partial u}\right)^{-1}\frac{\partial^2 H}{\partial u^2}\left(\frac{\partial C}{\partial u}\right)^{-1}\frac{\partial C}{\partial x}\left.\right)\left(\frac{\partial x}{\partial p}\right), \\ &+ \frac{\partial C^T}{\partial x}\left(\frac{\partial C}{\partial u}\right)^{-1}\frac{\partial f^T}{\partial u}\frac{\partial \lambda}{\partial p} - \frac{\partial f^T}{\partial x}\left(\frac{\partial \lambda}{\partial p}\right).\end{aligned} \tag{6.18}$$

If we define

$$A \equiv f_x f_u S_u^{-1} C_x, \qquad B \equiv -H_{xx} + H_{xu}C_u^{-1}C_x + C_x^T S_u^{-1} H_{ux} - C_x^T S_u^{-1} H_{uu} C_u^{-1} C_x, \tag{6.19}$$

then we arrive at a set of reduced variational equations. These equations are purely in terms of the adjoint λ and the state x:

$$\frac{\mathrm{d}}{\mathrm{d}t}\begin{pmatrix}\frac{\partial x}{\partial p} \\ \frac{\partial \lambda}{\partial p}\end{pmatrix} = \begin{pmatrix} A & 0 \\ -B & A^T \end{pmatrix}\begin{pmatrix}\frac{\partial x}{\partial p} \\ \frac{\partial \lambda}{\partial p}\end{pmatrix}. \tag{6.20}$$

Also, there are additional boundary conditions. The following interior point constraints apply at entry into the path constraint [34],

$$\lambda(t_1^-) = \lambda(t_1^+) + \pi^T \frac{\partial S}{\partial x}, \tag{6.21}$$

$$H(t_1^-) = H(t_1^+) - \pi^T \frac{\partial S}{\partial t}, \tag{6.22}$$

$$H_u(t_1^-) = H_u(t_1^+). \tag{6.23}$$

Here, we have chosen for the constrained arc that travels between t_1 and t_2 to take jump conditions at the entry point. The trajectory conditions are preserved along the boundary arc, and thus, we would have at the exit time t_2.

$$\lambda(t_2^-) = \lambda(t_2^+), \tag{6.24}$$

$$H(t_2^-) = H(t_2^+), \tag{6.25}$$

$$H_u(t_2^-) = H_u(t_2^+). \tag{6.26}$$

The first of these two conditions (6.21) and (6.22) are similar to the two constraints for the terminally constrained case, ψ and Ω. They provide the basis for a new backward sweep procedure, as discussed below.

In 6.1 we list the equations for the backward sweep at various times, and we note that $\Upsilon = \frac{\partial \phi}{\partial x} + \nu \frac{\partial \psi}{\partial x}$ and $\Omega = H + \frac{\partial \Upsilon}{\partial t}$.

Time	t_0	t_1-	t_1^+	t_2^-	t_2^+	T
Clock Condition		$H(t^+) - \pi \frac{\partial S}{\partial t}$	$H(t^+)$			$\Omega(T, x(T)) = 0$
Adjoint		$\lambda(t_1^+) + \pi \frac{\partial S}{\partial x}$	$\lambda(t_1^+)$			$\Upsilon(T, x(T))$
Lagrange Multiplier		π				ν
Variational Equations	(3.63)	(3.63)	(6.20)	(6.20)	(3.63)	(3.63)

Table 6.1: Equations for Backward Sweep for Path Constrained Optimal Control

We construct a time varying matrix M, where we assume that $\frac{\partial \lambda}{\partial p}$, $\frac{\partial \psi}{\partial p}$, and $\frac{\partial \Omega}{\partial p}$ are a linear function of $\frac{\partial \nu}{\partial p}, \frac{\partial x}{\partial p}, \frac{\partial T}{\partial p}$ that satisfies terminal conditions. We differentiate to yield matrix differential identities and eliminate $\frac{\partial \lambda}{\partial p}$ in terms of $\frac{\partial x}{\partial p}$, $\frac{\partial \nu}{\partial p}$, and $\frac{\partial T}{\partial p}$. The differential constraints on M starting from the terminal time T to t_2 are the Riccati differential equations. Thus, we have the usual backward sweep from T to t_2.

After transition from t_2^+ to t_2^-, the variational equations and control switch from the terminally constrained set, (3.63), to the path-constrained set, (6.20). Therefore, the dynamics for Riccati differential equations change to use the formulas 6.20. The new constrained Riccati differential equations will hold until t_1^+.

From t_1^+ to the entry time t_1^-, we start a new backward sweep procedure to derive more Riccati differential equations. We repeat the same backward sweep procedure from the terminal condition, except we substitute the terminal condition for the entry condition, and replace ψ with $\lambda(t_1^+) + \pi\frac{\partial S}{\partial x}$, ν with π, T with t_1^-, and Ω with $H(t^+) - \pi\frac{\partial S}{\partial t}$. We list these substitutions in Table 6.2.

Terminal Constraint Symbol	Corner Condition Symbol
T	t_1^-
Υ	$\lambda(t_1^+) + \frac{\partial S}{\partial x}$
ν	π
Ω	$H(t_1^+) - \pi\frac{\partial S}{\partial t}$

Table 6.2: Notation to change from Transversality Condition to Corner Condition

Based on this, we speculate that there are two sets of Riccati Matrices. One which we integrate from the intimal time all the way to the entry time, and another which we integrate from the entry time to the terminal time. The latter set changes its dynamics as it crosses the exit time. Sufficient conditions could possibly be derived in terms of these matrix differential equations, and would provide checks on the validity of the solution in terms of these matrices at every time between the initial and final time.

If these Riccati matrices were solved off-line and scheduled, they would provide a feedback control resembling 5.78. The feedback control would switch between the first and second set of Riccati matrices at the entry time.

Lastly, we note that in a general case, with high-order path constraints and with multiple constrained arcs, the number of sets of Riccati equations likely increases with the increasing number of corners.

6.4 Application of Constrained Case to a Flight Control Law

To demonstrate constrained perturbation feedback control, we include an example of a constrained reference trajectory and a constrained perturbed trajectory for the F-16 model, as described in the previous two chapters. Examining the trajectories in Figures 6.2 and 6.3 reveals that even with a simple constraint, in this case $\alpha \leq 20$, the perturbed trajectory (orange) has an altered switching time from the true trajectory (purple). The control variable constraint is a practical constraint, which restricts the aircraft's guidance from commanding a high-angle of attack, where aerodynamics are generally nonlinear and poorly modeled.

Ideally, we would extend the constrained optimization cases to path constraints. Doing sons for references extremals, proved to be more challenging. Practically, these cases represent load limits on the speed and angle of attack and position constraints for the aircraft's trajectory, for example to avoid a mountain. These more challenging constraints were not implemented numerically because of the optimization algorithm's sensitivity to even minor perturbations in the initial conditions.

The transition from terminally constrained optimization to path-constrained optimization transforms the optimization problems from two-point boundary value problems to multiple-point boundary value problems. Solving constrained optimization problems with the simple shooting method suffered from extreme sensitivity. The sensitivity in these problems can be greatly improved by incorporating multiple shooting methods [56]. To improve the radius of convergence of the algorithm, one can also use the variational equations required for perturbation feedback control for calculation of partial derivatives to replace partial differences.

In the future, we would like to compare an explicit and implicit feedback control, using a reference trajectory calculated from a solver with these improvements.

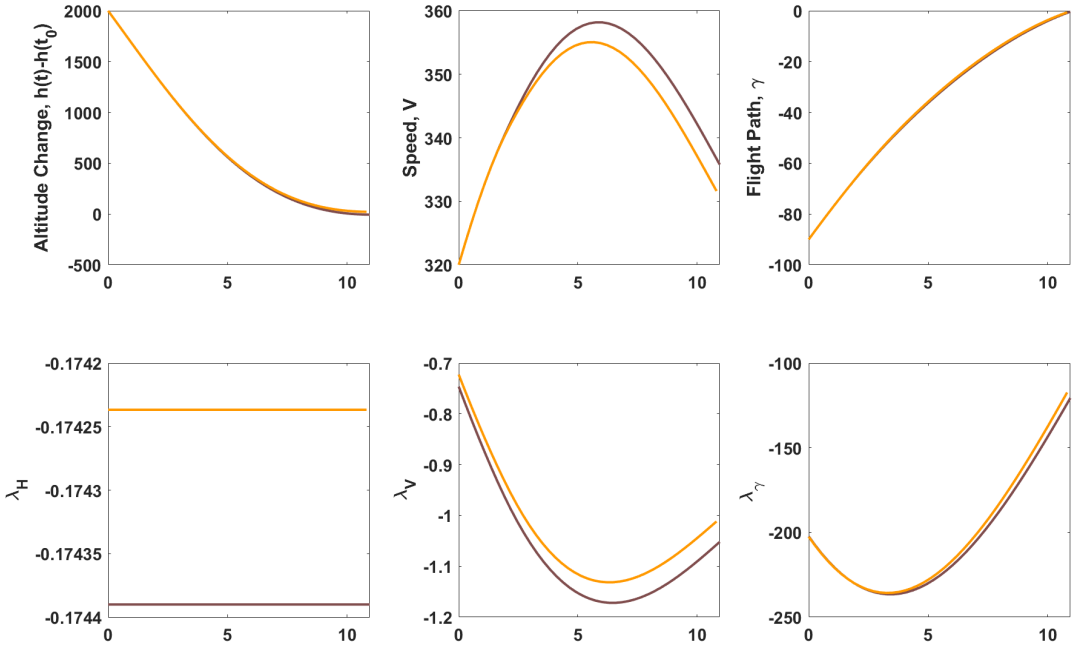

Figure 6.2: The states for a optimal perturbation feedback control trajectory (orange) compared to a true optimal trajectory (purple)

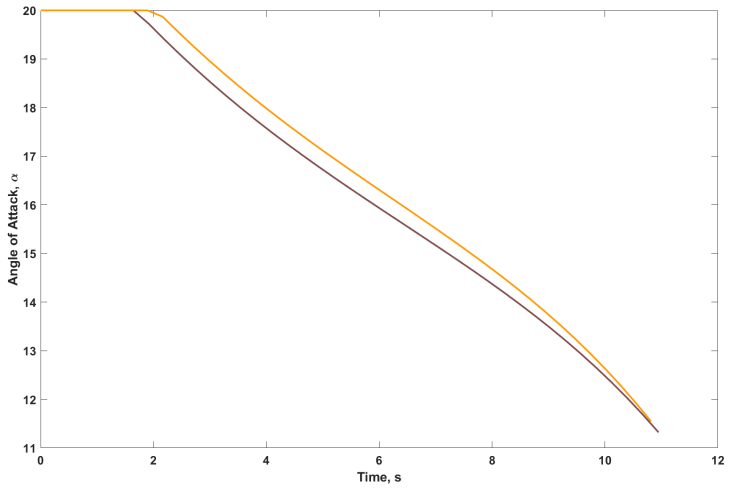

Figure 6.3: The control for a optimal perturbation feedback control trajectory (orange) compared to a true optimal trajectory (purple)

References

[1] Federal Aviation Administration. Ac 61-134 - general aviation controlled flight into terrain awareness document information, 2003.

[2] L. Bailey Et al. Controlled flight into terrain: A study of pilot perspectives in alaska. Technical Report DOT/FAA/AM-00/28, U.S. Department of Transportation Federal Aviation Administration, Washington, D.C. 20591, August 2000.

[3] J.D. Anderson. *Fundamentals of Aerodynamics*. McGraw-Hill Education, 2010.

[4] M. Athans and P. L. Falb. *Optimal Control: An Introduction to the Theory and Its Applications*. Dover Books on Engineering. Dover Publications, 2013.

[5] R.J. Atkin and N. Fox. *An Introduction to the Theory of Elasticity*. Dover Books on Physics. Dover Publications, 2013.

[6] R. E. Bellman. The theory of dynamic programming. *RAND Corporation*, 1:1–13, September 1954.

[7] L.D. Berkovitz. *Optimal Control Theory*. Applied Mathematical Sciences. Springer New York, 2013.

[8] S. Bhan and H. Schättler. A variational approach to perturbation feedback control for optimal control problems with terminal constraints and free terminal time. *Set-Valued and Variational Analysis*, Jun 2018.

[9] G.W. Bice and M.A. Skoog. Aircraft ground collision avoidance and autorecovery system device. *US*, 4,924,401, May 1990.

[10] B. Bonnard and M. Chyba. *Singular Trajectories and their Role in Control Theory*. Mathématiques et Applications. Springer Berlin Heidelberg, 2003.

[11] R.C. Le Borne. Ground collision avoidance system. US, Aug 1992.

[12] J. Bosworth and D. Enns. Success stories for control: Nonlinear multivariable flight control. *IEEE CSS*.

[13] M. Braithwaite, S. Groh, and E. Alvarez. Spatial disorientation in u.s. army helicopter accidents: An update of the 1987-92 survey to include 1993-95. page 29, 03 1997.

[14] J.V. Breakwell and Y.C. Ho. On the conjugate point condition for the control problem. *Int. J. Of Engineering Science*, 2:595–, 1965.

[15] J.V. Breakwell, J.L. Speyer, and jr. A.E. Bryson. Optimization and control of nonlinear systems using the second variation. *SIAM J. Control*, 1:193–, 1963.

[16] B.C. Breen. Controlled flight into terrain and the enhanced ground proximity warning system. *IEEE Aerospace and Electronic Systems Magazine*, 14(1):19–24, Jan 1999.

[17] A. Bressan and B. Piccoli. *Introduction to the Mathematical Theory of Control*. American Institute of Mathematical Sciences, 2007.

[18] R.W. Brockett. *Finite Dimensional Linear Systems*. Classics in Applied Mathematics. Society for Industrial and Applied Mathematics, 2015.

[19] W.L. Brogan. *Modern Control Theory*. Prentice Hall, 1991.

[20] A. Burns, D. Harper, A.F. Barfield, S. Whitcomb, and B. Jurusik. Auto gcas for analog flight control system. 10 2011.

[21] NASA Glenn Research Center. Navier stokes equations: 3-dimensional unsteady. https://www.grc.nasa.gov/www/k-12/airplane/nseqs.html. Accessed: 2010-09-30.

[22] R. Darby. Commercial jet hull losses, fatalities rose sharply in 2005. *Aviation Safety World*, pages 51–53, August 2006.

[23] X. Denoize and F. Faivre. Collision-avoidance device for aircraft, notably for avoiding collisions with the ground. *US*, 5,414,631, May 1995.

[24] S.E. Dreyfus. The numerical solution of variational problems. *Journal of Mathematical Analysis and Applications*, 5:3045, 08 1962.

[25] F. Faivre and X. Denoize. Aircraft collision-avoidance device, notably ground collision, by control of angle of descent. *US*, 5,608,392, March 1997.

[26] I.M. Gelfand and S.V. Fomin. *Calculus of Variations*. Prentice Hall, Englewood Cliffs, NJ, 1963.

[27] R. Gibb, B. Ercolin, and L. Scharff. Spatial disorientation: Decades of pilot fatalities. *Aerospace Medical Association*, 82(7):17–24.

[28] R. Hartl, R. Vickson, and S. Sethi. A survey of the maximum principles for optimal control problems with state constraints. *SIAM Review*, 37, 02 2008.

[29] M.R. Hestenes. *Calculus of Variations and Optimal Control Theory*. Krieger Publishing Co., Huntington, New York, 1980.

[30] L. Hoffman. A longitudinal field study of auto-gcas acceptance and trust: First year results and implications. *Journal of Cognitive Engineering and Decision Making*, 11, 03 2017.

[31] A. Isidori. *Nonlinear Control Systems*. Communications and Control Engineering. Springer London, 2013.

[32] F. John. *Partial Differential Equations*. Applied Mathematical Sciences. Springer New York, 1991.

[33] A.E. Bryson Jr. Optimal control-1950 to 1985. *Control Systems, IEEE*, 16:26 – 33, 07 1996.

[34] A.E. Bryson Jr and Y.C. Ho. *Applied Optimal Control: Optimization, Estimation and Control*. CRC Press, 2018.

[35] T. Kailath. *Linear Systems*. Prentice Hall, Englewood Cliffs, NJ, 1980.

[36] H.K. Khalil. *Nonlinear Systems*. Pearson Education. Prentice Hall, 2002.

[37] D.E. Kirk. *Optimal Control Theory: An Introduction*. Dover Books on Electrical Engineering. Dover Publications, 2012.

[38] H.W. Knobloch and H. Kwakernaak. *Lineare Kontrolltheorie*. Springer-Verlag, Berlin, 1985.

[39] E. Lavretsky and K. Wise. *Robust and Adaptive Control: With Aerospace Applications*. Advanced Textbooks in Control and Signal Processing. Springer London, 2012.

[40] D. Liberzon. *Calculus of Variations and Optimal Control*. Princeton University Press, New Jersey, 2012.

[41] S.R. McReynolds. A successive sweep method for solving optimal programming problems. *Proc. JACC*, 01 1965.

[42] E. Morelli and V. Klein. *Aircraft System Identification: Theory and Practice*. Sunflyte Enterprises, 2016.

[43] E.A. Morelli. Global nonlinear parametric modelling with application to f-16 aerodynamics. volume 2, pages 997 – 1001 vol.2, 07 1998.

[44] J. Noble and H. Schättler. Sufficient conditions for relative minima of broken extremals in optimal control theory. *Journal of Mathematical Analysis and Applications*, 269:98–128, 05 2002.

[45] H.J. Pesch. Numerical computation of neighboring optimum feedback control schemes in real-time. *Appl. Math. Optim.*, 5:231–252, 03 1979.

[46] H.J. Pesch. Computation of feedback controls for constrained optimal control problems, part 1: Neighboring extremals. *Optimal Control Applications and Methods*, 10:129–145, 04 1989.

[47] H.J. Pesch. Real-time computation of feedback controls for constrained optimal control problems, part 2: A correction method based on multiple shooting. *Optimal Control Applications and Methods*, 10:147–171, 04 1989.

[48] L.S. Pontryagin. *Mathematical Theory of Optimal Processes*. Classics of Soviet Mathematics. Taylor & Francis, 1987.

[49] D.K. Scharmack. An initial value method of trajectory optimization problems. *Advances in Control System, Theory and Applications*, 5, 12 1967.

[50] H. Schättler and U. Ledzewicz. *Geometric Optimal Control: Theory, Methods and Examples*. Interdisciplinary Applied Mathematics. Springer New York, 2012.

[51] M.A. Skoog, K. Prosser, and L. Hook. Ground collision avoidance system (igcas). *US*, 6,335,567B1, April 2017.

[52] J.L. Speyer. Nonlinear feedback solution to a bounded brachistochrone problem in a reduced state space. *IEEE Transactions on Automatic Control*, 12(1):90–94, February 1967.

[53] J.L. Speyer. A perspective on aerospace control systems. *Control Systems Magazine, IEEE*, 7:11 – 12, 05 1987.

[54] J.L. Speyer, R.K. Mehra, and A.E. Bryson Jr. The seperate computation of arcs for optimal flight paths with state variable inequality constraints. Technical Report 526, National Aeronautics and Space Administration Office of Naval Research, May 1967.

[55] B.L. Stevens and F.L. Lewis. *Aircraft Control and Simulation*. Wiley, 2003.

[56] J. Stoer, R. Bartels, R.W. Gautschi, R. Bulirsch, and C. Witzgall. *Introduction to Numerical Analysis*. Texts in Applied Mathematics. Springer New York, 2002.

[57] B. Tognazzini. Aircraft ground collision avoidance system and method. *US*, 6,118,401, September 2000.

[58] M. Tran. Adaptive ground collision avoidance system. *US*, 5892462A, April 1999.

[59] D.M. Wiberg. *State space and linear systems*. Schaum's outline of theory and problems. McGraw-Hill, 1971.

[60] E.L. Wiener. Controlled flight into terrain accidents: System-induced errors. *Human Factors*, 19(2):171–181, 1977.

Vita

Sankalp Kishan Bhan

Degrees

B.S. Biomedical Engineering, May 2012.
M.E. Control Engineering, May 2012.

Publications

S. Bhan and H. Schättler, (2018). A variational approach to perturbation feedback control for optimal control problems with terminal constraints and unspecified final time. *Journal of Set Valued and Variational Analysis* **10**(4): 323–336.

Employment

Guidance, Navigation, & Control Engineer.
The Boeing Company
July 2013 -
Process Automation, Control, & Optimization Engineer.
Shell Oil Company
June 2012 - June 2013

May 2019